รายงานวิจัยฉบับสมบูรณ์

โครงการ ฤทธิ์ต้านอนุมูลอิสระของสาร phytochemical phenolics ต่อการยับยั้งรังสีอัลตร้าไวโอเลตในการกระตุ้นการเกิดเม็ดสี และ matrix metalloproteinase-1 ในเซลล์ผิวหนัง

โดย รศ. ดร. พญ.อุไรวรรณ พานิช

กรกฎาคม ปี 2558

สัญญาเลขที่ RSA5580012

รายงานวิจัยฉบับสมบูรณ์

โครงการ ฤทธิ์ต้านอนุมูลอิสระของสาร phytochemical phenolics
ต่อการยับยั้งรังสีอัลตร้าไวโอเลตในการกระตุ้นการเกิดเม็ดสี
และ matrix metalloproteinase-1 ในเซลล์ผิวหนัง

รศ. ดร. พญ.อุไรวรรณ พานิช
คณะแพทยศาสตร์ศิริราชพยาบาล มหาวิทยาลัยมหิดล

สนับสนุนโดยสำนักงานกองทุนสนับสนุนการวิจัยและมหาวิทยาลัยมหิดล

Abstract

Project Code: RSA5580012

Project Title: ฤทธิ์ต้านอนุมูลอิสระของสาร phytochemical phenolics ต่อการยับยั้งรังสีอัลตร้าไวโอเลตในการกระตุ้นการเกิดเม็ดสีและ matrix metalloproteinase-1 ในเซลล์ผิวหนัง

Investigator: รศ. ดร. พญ.อุไรวรรณ พานิช ภาควิชาเภสัชวิทยา คณะแพทยศาสตร์ศิริราชพยาบาล มหาวิทยาลัยมหิดล

E-mail Address: uraiwan.pan@mahidol.ac.th

Project Period: 3 years

Ultraviolet (UV) has been recognized to be a major factor accountable for photodamage possibly through oxidative damage of skin cells including melanoyctes and keratinocytes. Responses of skin cells to oxidative stress include stimulation of melanogenesis in melanocytes and of matrix metalloproteinase-1 (MMP-1) responsible for collagen destruction, a hallmark of photoaged skin. Glutathione (GSH), GSH-related enzymes including γ-glutamate cysteine ligase (γ-GCL), glutathione S-transferase (GST) and glutathione peroxidase (GPx) and catalase (CAT) are important antioxidant defenses accountable for maintaining cellular redox balance. Improving antioxidant defense capacity to cope with oxidative insults would thus represent a promising strategy for inhibition of photoaged skin. Natural products including phytochemical phenolics have gained remarkable attention as potential photoprotective agents due to their antioxidant properties. Antioxidant phenolics, in particular, caffeic acid (CA), ferulic acid (FA) and gallic acid (GA), have been identified as common active ingredients in several medicinal herbs including Ayurved Siriraj Brand Wattana formula (AVS073) and Ayurved Siriraj Harak formula (AVS022), which have traditionally been used for health promotion and prevention of age-related problems. In order to develop natural products possessing antioxidant properties as effective photoprotective agents against skin aging, we therefore explored antioxidant mechanisms by which herbal extracts and the phytochemicals inhibited UVA-mediated melanogenesis in B16 melanoma cells and MMP-1 upregulation in keratinocyte HaCaT cells. Our findings showed that all test phenolics inhibited UVA-induced melanogenesis and MMP-1 in association with promotion of antioxidant defenses including GSH antioxidant system at cellular and molecular levels. Our study suggests that upregulation of endogenous antioxidants could be the mechanisms by which the herbal formula studied and their possible active ingredients, CA, FA and GA, suppressed UVA-stimulated pigmentation and MMP-1. Upregulation of antioxidant defense system by natural products would thus represent a promising opportunity for development of putative photoprotective agents for inhibition of premature skin aging.

Keywords: Ultraviolet A; melanogenesis; matrix metalloproteinase-1 (MMP-1); antioxidant defenses; natural products

เนื้อหาวิจัย

1. วัตถุประสงค์ของโครงการ

1.1 To study the effects of phytochemical phenolics and promising herbal formula in the inhibition of UVA-induced skin pigmentation and MMP-1 activation through redox regulation

1.2 To establish a cultured skin model to study the efficacy and safety of natural products in order to develop promising photoprotective agents against photoaging and photocarcinogenesis

2. ระเบียบวิธีวิจัย

2.1 Cell culture and treatment

B16F10 and G361 melanoma cells and keratinocyte HaCaT cells were cultured in Dulbecco's modified Eagle medium (DMEM) supplemented with 10% fetal bovine serum (FBS) and antibiotic solution [1% penicillin (100 units/ml)-streptomycin (100 μg/ml)] and maintained at 37 $^{\circ}$C in humidified air containing 5% CO_2 (P_{CO2} = 40 Torr).

2.2 Treatment of cells with phenolics or herbal extracts and UVA irradiation

The cells were treated with test phenolics (up to 60 μM or 5 *μ*g/ml) or herbal extracts (up to 60 μg/ml) for 30 min in culture medium. Then cells were washed and medium replaced with phosphate buffered saline (PBS) to avoid production with medium-derived toxic photoproducts prior to irradiation of UVA (at physiologically relevant intensity). Cells and supernatants were then harvested for the assays following UV irradiation.

2.3 Preparation of total cell lysate

Cells were harvested, pelleted by centrifugation and lysed in ice cold extracted buffer containing 50 mM Tris-HCl, 10 mM ethylene diaminetetraacetic acid (EDTA), 1% (v/v) Triton X-100, phenylmethylsulfonyl fluoride (PMSF) (100 mg/ml) and pepstatin A (1 mg/ml) in DMSO, and leupeptin (1 mg/ml) in H_2O, pH 6.8. The cells were then centrifuged at 12,000 x g for 2 min and the total cell lysate were collected, aliquoted and stored at -80 $^{\circ}$C.

2.4 Determination of cell viability by MTT reduction assay

The reduction of MTT to the purple formazan product, largely by the mitochondrial complex I and II and also involving NADH- and NADPH-dependent energetic processes in the cytosol, were measured to identify metabolically active cells. Cells were incubated with medium containing MTT (0.2 mg/ml) at 37 $^{\circ}$C for 1 h. Then DMSO was used to solubilize the purple formazan and the optical density was measured at 595 nm by a spectrophotometer.

2.5 Determination of pigmentation: melanogenesis assay

Cell tyrosinase activity assay

Tyrosinase activity in cell lysate was determined by measuring the rate of L-DOPA oxidation. Tenzymatic reaction was started by adding 20 mM L-DOPA as the substrates at 37 $^{\circ}$C. The tyrosinase activity determined as absorbance of dopachrome formation was measured spectrophotometrically at 475 nm every 10 min for 1 h at 37 $^{\circ}$C by a microplate reader. The activity was calculated by comparing with standard curves produced by the same methods using known concentrations of tyrosinase activity (2034 U/mg).

Melanin content assay

This assay correlates with uptake of ^{14}C-DOPA, an alternative evaluation of melanin synthesis. Total melanin contents were determined by solubilizing cells in 1 M NaOH. Each lysate was placed to a 96-well plate and spectrophotometrically determined at 475 nm. The melanin contents per mg of protein were determined from a standard curve derived using synthetic melanin (0-250 μg/ml).

2.6 Antioxidant assays

Measurement of intracellular GSH content

GSH content was assayed using the fluorescent reagent *o*-phthalaldehyde (OPA) reacting specifically with GSH at pH 8. Cells were lysed with 6.5% (w/v) trichloroacetic acid (TCA). Then, the TCA extracts were added to 96-well plates together with PBS and OPA (1 mg/ml). Fluorescence was measured at 350 nm excitation and 420 nm emission using a spectrofluorometer. The GSH levels were calculated by comparing with standard curves using known concentrations of GSH.

Measurement of GST activity

GST activity was assessed by following the kit protocol from Cayman chemical (Ann Arbor, MI). GS-DNB conjugate, the conjugation product between GSH with 1-chloro-2,4-dinitrobenzene (CDNB) catalyzed by the GST, was determined spectrophotometrically at 340 nm immediately and every 30 second for 10 min. 100 mM CDNB was used to generate the reaction of either sample or positive control GST with 200 mM GSH in assay buffer. The data were expressed as a percentage of the GST activity (μmol/min/mg of protein) of the unirradiated and untreated control cells (100%).

Measurement of catalase activity

Catalase activity was measured colorimetrically by following the kit protocol from Cayman chemical (Ann Arbor, MI). In principle, the enzyme reacted with methanol in the presence of H_2O_2 to produce the formaldehyde which was determined spectrophotometrically at 540 nm using 4-amino-3-hydrazino-5-mercapto-1,2,4-triazole (Purpald). The standard curve was obtained using a formaldehyde standard. One unit of

CAT activity was calculated as the amount of enzyme producing 1.0 nmol of formaldehyde per min at 25 $^{\circ}$C and represented as nmol/min/mg protein.

Measurement of glutathione peroxidase (GPx) activity

GPx activity was assessed by following manufacturer's protocol (Trevigen, Gaithersburg, MD). The activity was indirectly measured by a coupled reaction with glutathione reductase (GR) causing reduction of oxidized glutathione. The oxidation of NADPH to $NADP^+$ is accompanied by decreased absorbance at 340 nm. One unit of GPx activity was determined as the amount of enzyme converting 1 nmol of NADPH to $NADP^+$ per min at 25 $^{\circ}$C and represented as units/mg of protein.

2.7 Determination of protein content

The protein content was measured using the Bio-Rad Protein Assay Kit (Bio-Rad, Germany) with BSA as the standard.

2.8 Determination of intracellular oxidant formation

Intracellular oxidant production indicating cellular oxidative stress induced by UVA was measured using 2′, 7′-Dichlorofluorescein diacetate (DCFH-DA), a stable and non-fluorescent dye. DCFH-DA is normally hydrolyzed in the cells to DCFH, further oxidized by oxidants (e.g., H_2O_2) to fluorescent 2,7-dichlorofluorescein (DCF), and the fluorescence therefore reflected cellular oxidant formation. After treatment of cells in 24-well plate, cells were incubated with phenol red-free DMEM containing DCFHDA (5 μM) for 1 h. DCF fluorescence was monitored for 20 min at 485 nm excitation and 530 nm emission using a spectrofluorometer.

2.9 Quantitative real-time reverse transcriptase-polymerase chain reaction: determination of tyrosinase, γ-GCLC, γ-GCLM, CAT, GPx and GST mRNA expression

Cells pretreated with or without herbal extracts (7.5, 15 and 30 μg/ml) and GA (1.25, 2.5 and 5 μg/ml) were exposed to UVA (8 J/cm^2). At 2 h following UV irradiation, preparation of total RNA was carried out using the illustra RNAspin Mini RNA Isolation Kit (GE Healthcare, UK) and total RNA was reverse transcribed using the ImProm-II Reverse Transcriptase (Promega, Medison, USA) following the kit manual. 25 μl of reaction mixtures contained 5 μl cDNA template, 12.5 μl Master Mix, 10 μM forward primer (1 μl), 10 μM reversed primer (1 μl) and 5.5 μl water. Real-time PCR was carried out in triplicate for each sample on the ABI Prism 7500 Real Time PCR System (Applied Biosystems, USA). The amplification reactions were run under the following conditions: 95 °C for 10 min, 40 cycles at 95 °C for 15 s, 60 °C for 40 s, and 72 °C for 40 s. mRNA levels were determined using FastStart Universal SYBR Green Master (ROX). Primers for PCR were designed using the Primer Express software version 3.0 (Applied Biosystems, USA) (Table 1).

Amplification of a single product was verified using the melt curve analysis. The mRNA level was normalized with reference to the amount of housekeeping gene transcripts (GAPDH mRNA). The mean Ct from mRNA expression in cDNA from each sample was compared with the mean Ct from GAPDH determinations from the same cDNA samples in order to determine tyrosinase, γ-GCLC, γ-GCLM and GST mRNA. The results are expressed as fold change in gene expression calculated using the $2^{-\Delta\Delta Ct}$ method. For the control (untreated cells without UV irradiation), $\Delta\Delta C_t$ equals zero and 2^0 equals one, so that the fold change in gene expression relative to the control equals one, by definition. For the cells treated with test compounds or herb extracts, assessment of $2^{-\Delta\Delta Ct}$ determined the fold change in gene expression relative to the control.

Table 1. Sequences of PCR primer sets for tyrosinase, γ-GCLC, γ-GCLM, GST and GAPDH (in 5′-3′ direction)

Primer	Sequence (5' → 3')	Product size (bp)	GeneBank
CAT (sense) CAT (antisense)	CCT TCG ACC CAA GCA ACA TG CGA GCA CGG TAG GGA CAG TTC	148	NM_001752.3
GCLC (sense) GCLC (antisense)	GCTGTCTTGCAGGGAATGTT ACACACCTTCCTTCCCATTG	160	NM_001498.2
GCLM (sense) GCLM (antisense)	TTGGAGTTGCACAGCTGGATT TGGTTTTACCTGTGCCCACTG	200	NM_002061.2
GPx (sense) GPx (antisense)	ACG ATG TTG CCT GGA ACT TT TCG ATG TCA ATG GTC TGG AA	94	NM_201397.1
GSTP1 (sense) GSTP1 (sense)	CCTGTACCAGTCCAATACCATCCT TCCTGCTGGTCCTTCCCATA	72	NM_000852.3
TYR (sense) TYR (antisense)	CATTCTTCTCCTCTTGGCAGA CCGCTATCCCAGTAAGTGGA	267/114	NM_000372.4
GAPDH (sense) GAPDH (antisense)	CCTCCAAAATCAAGTGGGGCGATG CGAACATGGGGGCATCAGCAGA	150/124	NM_002046.3

2.10 MMP-1 activity assay by zymography

Conditioned supernatants were collected at 24 h following UVA irradiation for detecting MMP-1 activity using a zymography following the protocol previously reported. Briefly, gelatinase substrate or samples were electrophoresized on nonreducing 10% sodium dodecyl sulphate-polyacrylamide gel electrophoresis (SDS-PAGE) containing gelatin. Then, gels were washed twice with 2.5% Triton X-100 to eliminate SDS and allow MMP-1 renaturation. The gels were then incubated in the reaction buffer containing 50 mM Tris-HCl, pH 8.8, supplemented with 1% Triton X-100, 10 mM $CaCl_2$, 1 μM $ZnCl_2$ and 0.02% Na_3N for 24 h at 37° to generate MMP-1-induced degradation of gelatin. The gels were stained with 0.006% Coomassie Blue G-250 and gelatinolytic activity of MMP-1 in the gel was visualized as nonstained bands on the blue background. The gels were scanned using a CAMAG TLC scanner (Muttenz, *Switzerland*) and integrated density of each band was analyzed to determine MMP-1 activity using the ImageMaster software (Hoefer Pharmacia Biotech). Data was represented as arbitrary densitometric units of MMP-1 activity per 1,000,000 cells.

2.11 Statistical Analysis

Values are expressed as means ± standard error of the mean (SEM) calculated from data taken from at least 3 separate experiments performed on separate days. The significance of individual treatment groups in comparison to the UVA-irradiated groups was determined with one-way analysis of variance (ANOVA) or independent *t*-test (Student's; 2 populations) using Prism (GraphPad Software Inc., San Diego, CA). Values of $p < 0.05$ were considered statistically significant.

3. ผลงานวิจัยที่ได้รับ

3.1 Phytochemical antioxidants including caffeic acid (CA) and ferulic acid (FA) as well as extracts of Ayurved Siriraj Brand Wattana formula (AVS073) and gallic acid (GA) inhibited UVA-induced melanogenesis.

At first, cytotoxicity of CA and FA on melanoma B16F10 cells and the herbal formula and GA, a possible active component of AVS073, on melanoma G361 cells was assessed in order to indicate that the inhibitory effects of all test compounds on melanin synthesis were not due to reduced number of cells. MTT assay demonstrated that CA and FA up to 60 μM as well as the formula up to 60 μg/ml and GA up to 10 μg/ml did not affect cell viability (Fig. 1A and 1B).

To study anti-melanogenic effects of CA and FA on B16F10 cells, UVA irradiation led to 35 ± 6.4% (t-test; $p < 0.001$) induction in melanin content, although pretreatment of cells with CA and FA resulted in a substantial decline in melanin level induced by UVA exposure (8 J/cm^2) in a concentration-dependent manner (Fig. 2A).

In addition, the antimelanogenic effects of the herbal extracts and GA were assessed in G361 cells irradiated with UVA (16 J/cm^2). UVA irradiation caused 42.6 ± 5% (t-test; $p < 0.001$) induction in melanin production. However, UVA-mediated enhanced melanin content (Fig. 2B) was markedly inhibited by AVS073 extracts and GA in a concentration-dependent manner.

3.2 AVS073 extracts and GA inhibited UVA-induced ROS formation, GSH depletion and GST inactivation by AVS073

The redox mechanisms associated with antimelanogenic effects of AVS073 were assessed by investigating GSH-related antioxidant defenses including GSH level and GST activity. Irradiation of G361 cells with UVA (8 J/cm^2) caused a substantial elevation in intracellular oxidant production by 49.2 ± 7.2% ($p < 0.01$) in irradiated cells compared to nonirradiated cells. In contrast, pretreatment of cells with AVS073 (15-60 μg/ml) (Fig. 3A) and GA (2.5-10 μg/ml) (Fig. 3B) resulted in a substantial inhibition of UVA-induced oxidant generation. Moreover, a significant decline in GSH content by 52.5 ± 7.2% ($p < 0.001$) (Fig. 4) and GST activity by 53.5 ± 9.4% ($p < 0.001$) (Fig. 5) was observed in irradiated G361 cells compared to nonirradiated cells. Nevertheless, AVS073 extracts and GA were observed to protect against the loss of GSH (Fig. 4A and 4B) and inactivation of GST (Fig. 5A and 5B) in a concentration-dependent manner.

3.3 AVS073 extracts and GA inhibited UVA-induced upregulation of tyrosinase mRNA and downregulation of γ-GCLC, γ-GCLM and GST

The quantitative analysis of gene expression changes was carried out in order to investigate the effects of AVS073 (7.5-30 μg/ml) and GA (1.25-5 μg/ml) on increased melanogenesis at mRNA level at 2 h after irradiation. In agreement with the data observed in the study of tyrosinase activity, a rise in tyrosinase mRNA expression (2.2 ± 0.2-fold change; $p < 0.01$) was observed in response to UVA irradiation (8 J/cm^2), although AVS073 (Fig. 6A) and GA (Fig. 6B) significantly diminished tyrsoinase mRNA levels. Furthermore, while UVA exposure led to reduction of mRNA levels of γ-GCLC (0.51 ± 0.01-fold decrease; $p < 0.001$), γ-GCLM (0.59 ± 0.04-fold decrease; $p < 0.001$) and GST (0.74 ± 0.04-fold decrease; $p < 0.001$), upregulation of their mRNA was detected in the cells pretreated with AVS073 extracts (Fig. 6C and 6E) and GA (Fig. 6D and 6F).

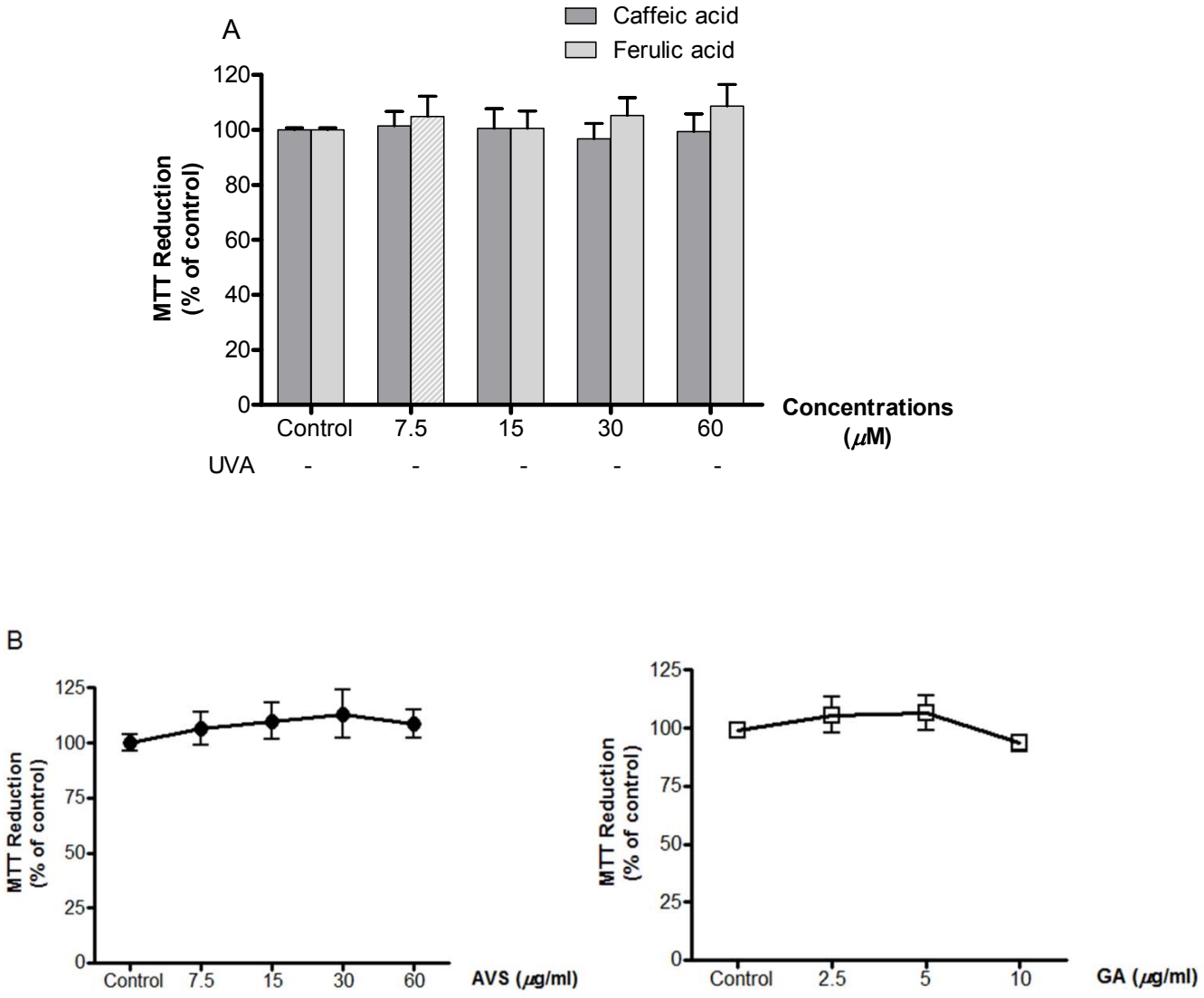

Figure 1. Determination of cell viability by using MTT reduction assay. Effects of CA and FA (A) and AVS073 extracts and GA (B) on cell viability without UVA irradiation. Cell viability was expressed as a percentage of control (100%, unirradiated and untreated cells).

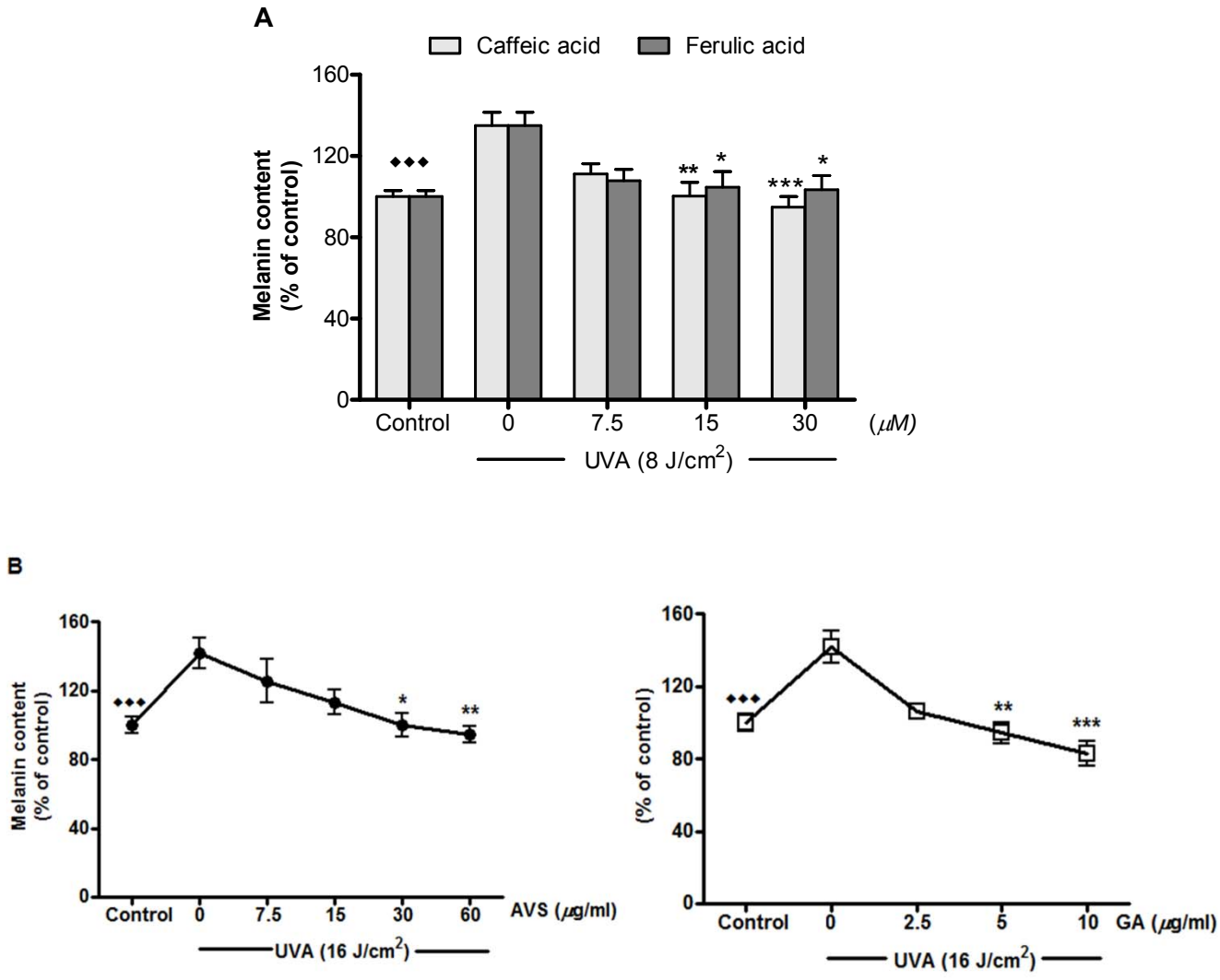

Figure 2. Determination of melanogenesis by using melanin content assay. Inhibition of UVA-induced melanin synthesis by CA and FA in melanoma B16F10 cells and by AVS073 and GA in melanoma G361 cells. The melanin production induced by a single UVA dose of 8 or 16 J/cm^2 in B16F10 and G361 cells, respectively, related to the protein concentration were expressed as a percentage of control (100%, unirradiated and untreated cells). Values given are mean ± SEM of at least 6 determinations. The statistical significance of differences between the control and UVA-irradiated cells was evaluated by Student's t test and between UVA-irradiated and compounds-treated cells by one-way ANOVA followed by Tukey's *post hoc* test. ♦♦♦ $P < 0.001$ compared with UVA-irradiated cells. * $P < 0.05$; ** $P < 0.01$; *** $P < 0.001$ compared with untreated cells exposed to UVA.

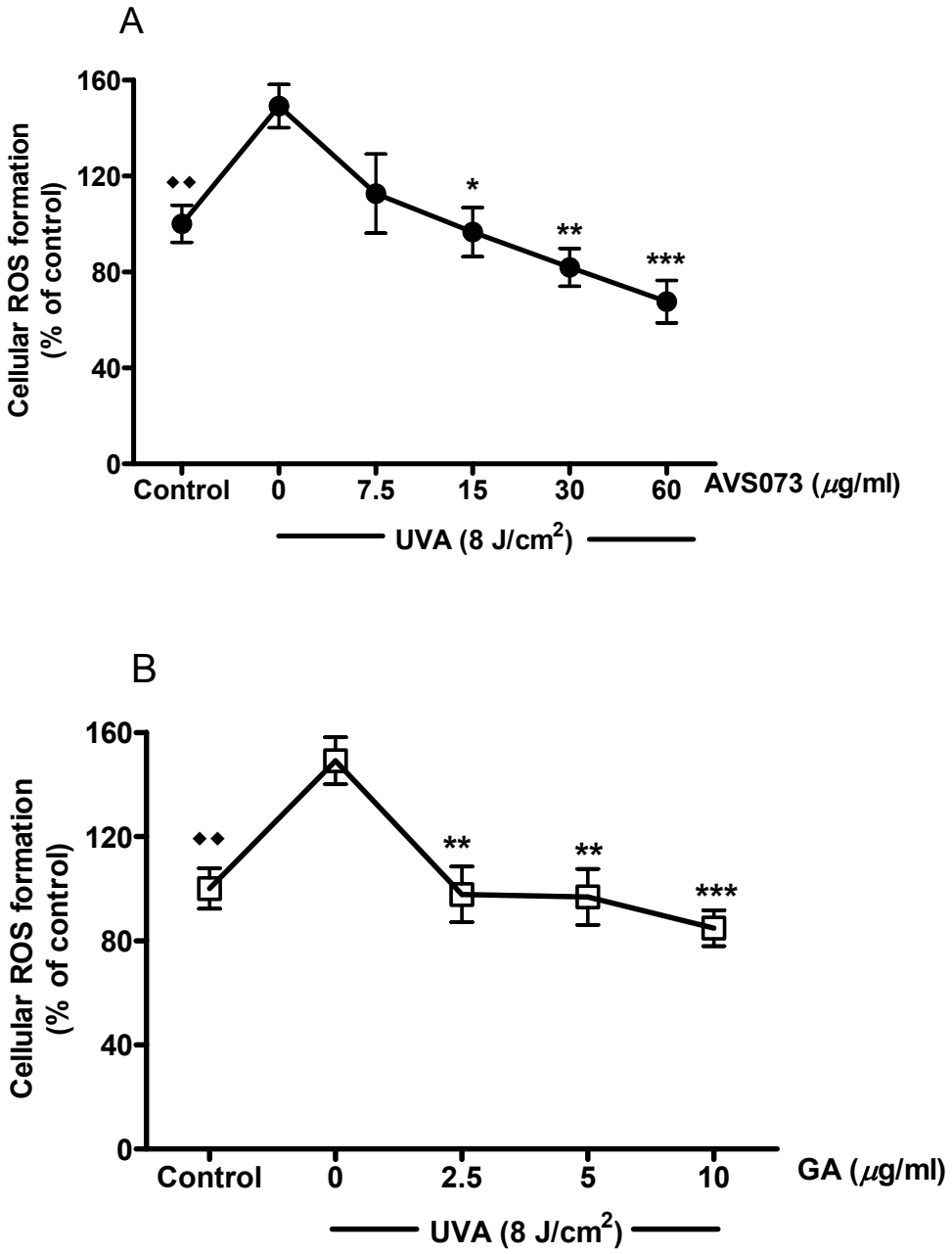

Figure 3. Inhibition of UVA (8 J/cm^2)-induced ROS formation by AVS073 (A) and GA (B). Oxidant formation was assessed by measurement of fluorescence of the DCF. Values are expressed as mean ± SEM of at least 6 determinations. The statistical significance of differences between the control and UVA-irradiated cells was evaluated by Student's t test and between UVA-irradiated and AVS073 extracts- or GA-treated cells by one-way ANOVA followed by Tukey's *post hoc* test. ◆◆$P < 0.01$ compared with UVA-irradiated cells. *$P < 0.05$; **$P < 0.01$; ***$P < 0.001$ compared with untreated cells exposed to UVA.

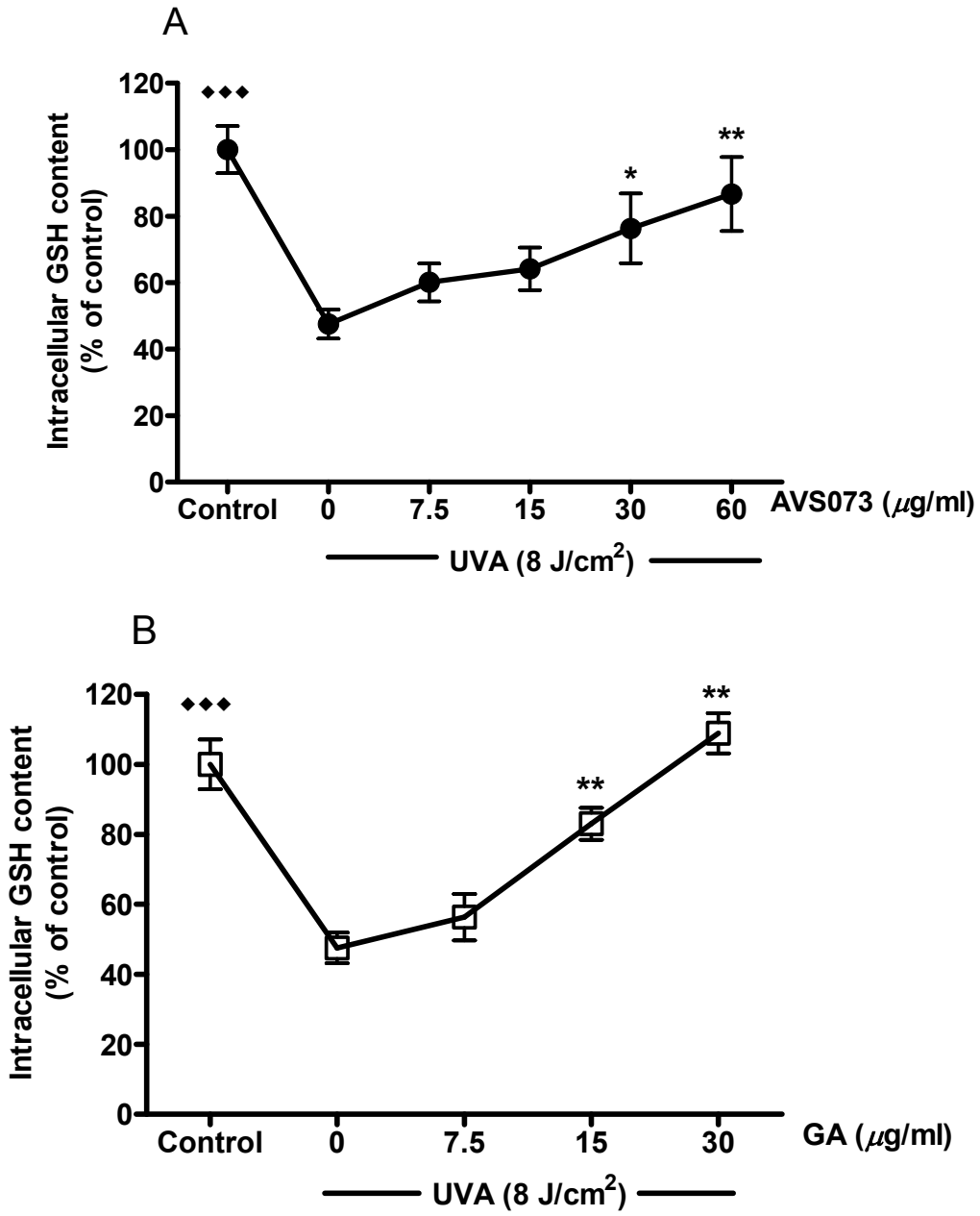

Figure 4. Inhibition of UVA (8 J/cm^2)-induced GSH depletion by AVS073 (A) and GA (B). GSH level was determined by measurement of fluorescence of the GSH-OPA adduct and the GSH content related to the protein concentrations were expressed as a percentage of control (100%, unirradiated and untreated cells). Values are expressed as mean ± SEM of at least 6 determinations. The statistical significance of differences between the control and UVA-irradiated cells was determined by Student's t test and between UVA-irradiated and AVS073 extracts- or GA-treated cells by one-way ANOVA followed by Tukey's *post hoc* test. ◆◆◆ $P < 0.001$ compared with UVA-irradiated cells. *$p < 0.05$; **$p < 0.01$; ***$p < 0.001$ compared with irradiated cells without compound treatment.

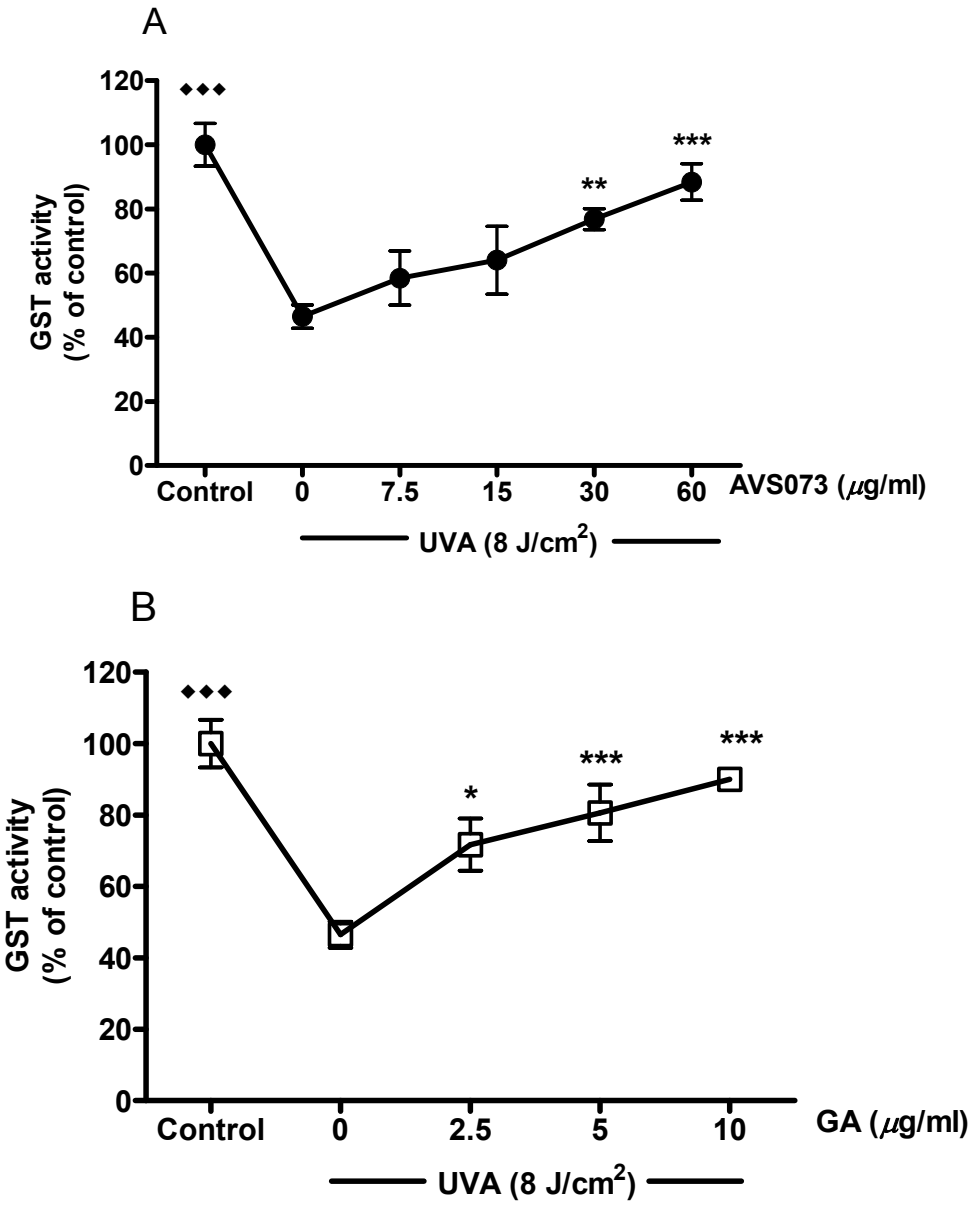

Figure 5. Inhibition of UVA (8 J/cm^2)-induced GST inactivation by AVS073 (A) and GA (B). GST activity were determined by measurement of absorbance of the GSH-CDNB and GST activity related to the protein concentrations was expressed as a percentage of control (100%, unirradiated and untreated cells). Values are expressed as mean ± SEM of at least 6 determinations. The statistical significance of differences between the control and UVA-irradiated cells was determined by Student's t test and between UVA-irradiated and AVS073 extracts- or GA-treated cells by one-way ANOVA followed by Tukey's *post hoc* test. ◆◆◆ $P < 0.001$ compared with UVA-irradiated cells. *$p < 0.05$; **$p < 0.01$; ***$p < 0.001$ compared with irradiated cells without compound treatment.

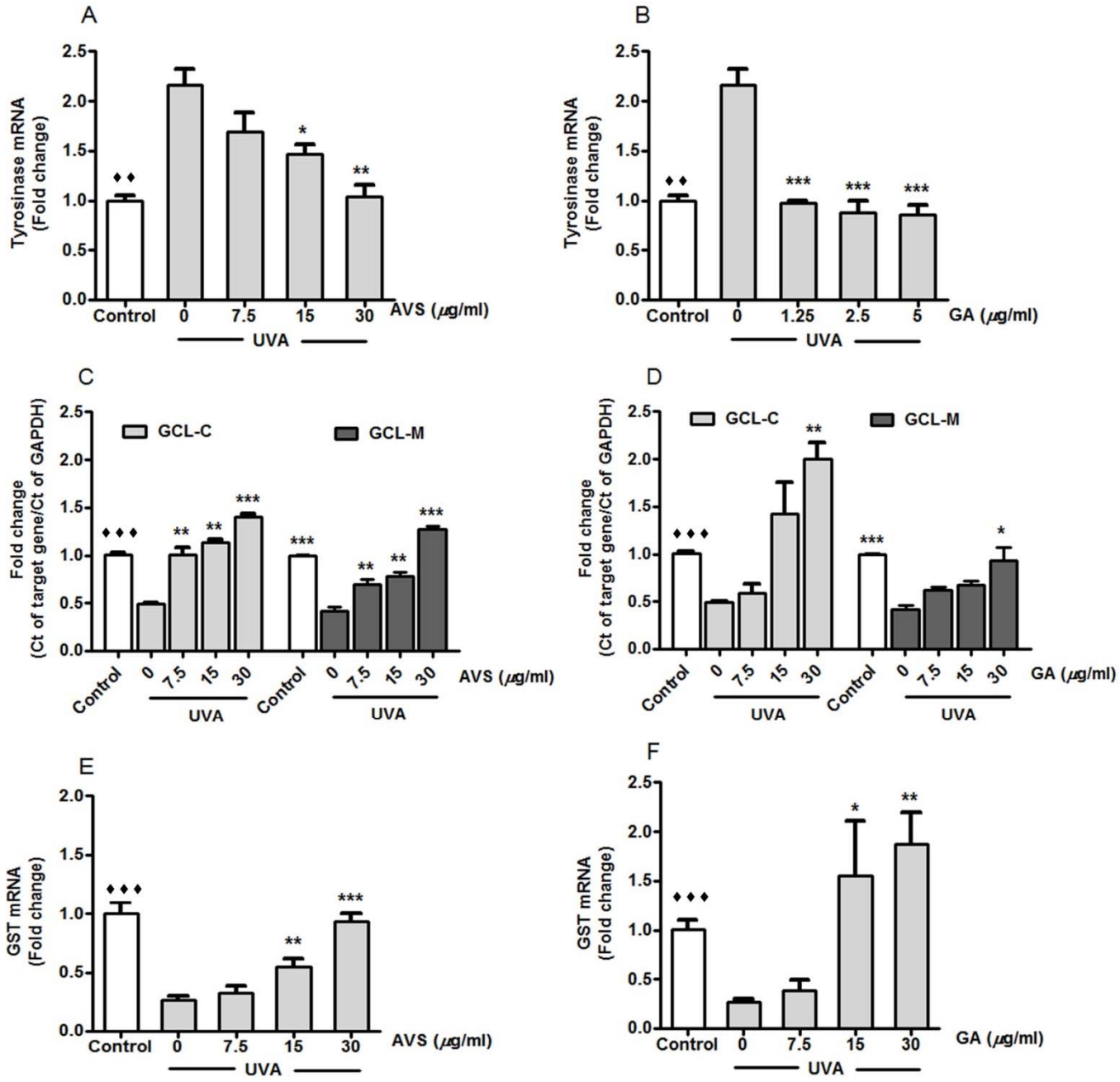

Figure 6. Inhibition of UVA-induced upregulation of tyrosinase mRNA (A and B) and downregulation of γ-GCLC and γ-GCLM (C and D) as well as GST (E and F) by AVS073 and GA. The data shown as the fold change in gene expression normalized to GAPDH and relative to the control sample. Values given are mean±SEM. The statistical significance of differences between the control and UVA-irradiated cells was determined by Student's t test and between UVA-irradiated and AVS073 extracts- or GA-treated cells by one-way ANOVA followed by Tukey's *post hoc* test. ♦♦♦$P < 0.01$; ♦♦♦$P < 0.001$ compared with UVA-irradiated cells. *$p < 0.05$; **$p < 0.01$; ***$p < 0.001$ compared with AVS073- or GA-treated cells without UV irradiation.

3.4 AVS022 and GA protected against UVA-induced HaCaT cytotoxicity

A UVA dose of 4 J/cm^2 was observed to cause a substantial decrease in keratinocyte HaCaT cell viability by 32.95 ± 2.3 % (P < 0.001) compared to non-irradiated cells. Nevertheless, pretreatment with AVS022 (Fig. 7A) and GA (Fig. 7B) was able to significantly and dose-dependently hamper cytotoxicity induced by UVA irradiation.

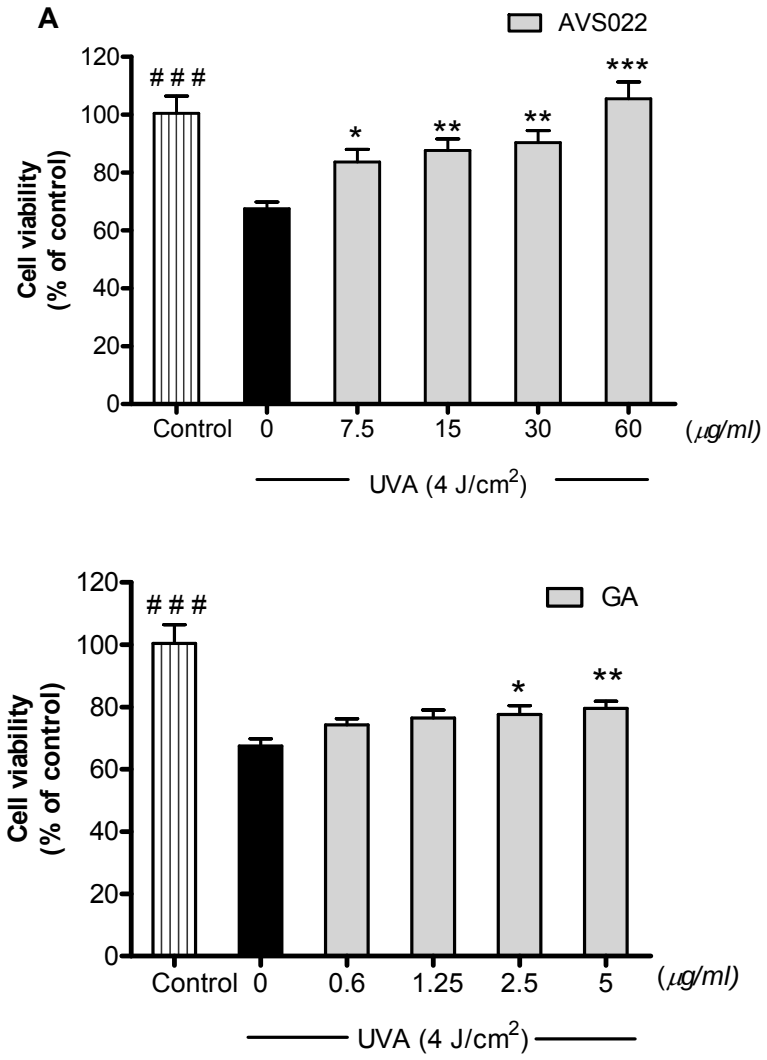

Figure 7. Inhibition of UVA (4 J/cm^2)-induced HaCaT cell toxicity by the AVS022 formula (A) and GA (B). Data was expressed as mean ± SEM. The statistical significance of differences between the control and UVA-irradiated cells was evaluated by Student's t test and between UVA-irradiated and herb extracts- or GA-treated cells by one-way ANOVA followed by Dunnett's test. ### P < 0.001 compared with UVA irradiated cells. ### P < 0.001 compared with UVA-irradiated cells. *P < 0.05; **P < 0.01; ***P < 0.001 compared with untreated cells irradiated with UVA.

3.5 AVS022 and GA protected against MMP-1 activation in irradiated HaCaT cells

We further examined inhibition of UVA-stimulated MMP-1 activity by herb extracts and GA since MMP-1 is a major metalloproteinase for collagen destruction, a hallmark of photoaging. As shown in Fig. 8, UVA (4 J/cm^2) markedly stimulated activity of MMP-1 by 206 ± 2.3 % (P < 0.001) compared to non-irradiated cells, although a significant and dose-dependent reduction of MMP-1 activity was observed in HaCaT cells pretreated with the whole formulation of AVS022 (Fig. 8A) and GA (Fig. 8B) compared with un-pretreated cells following UV irradiation.

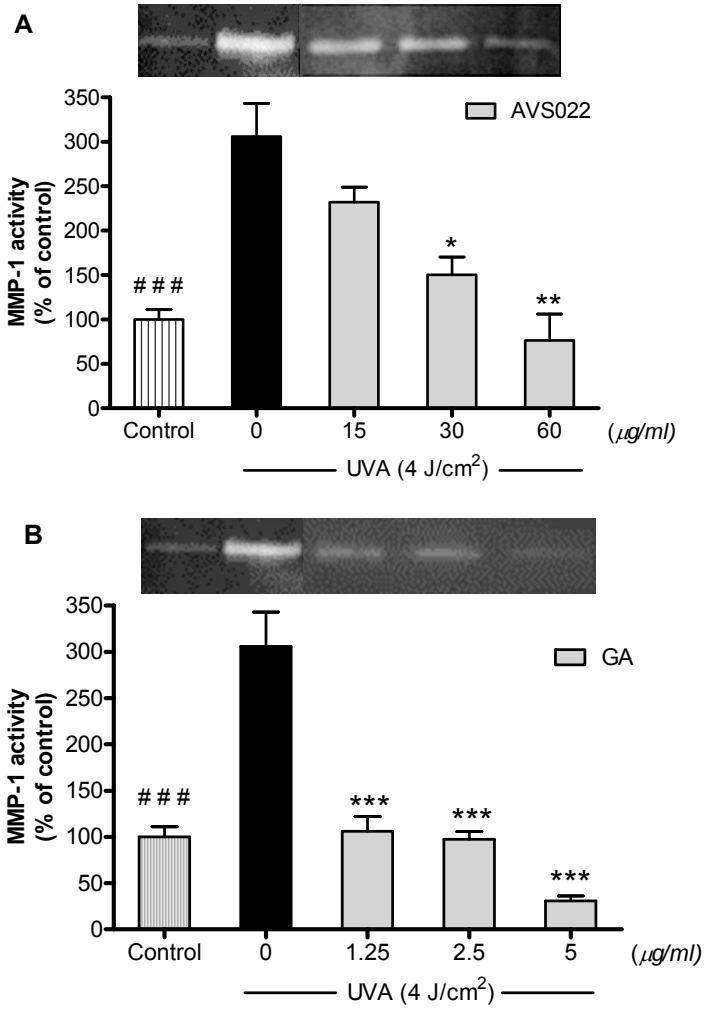

Figure 8. Inhibition of UVA-stimulated MMP-1 activity in HaCaT cells by the whole formula (A) and GA (B). Zymography analysis of secreted MMP-1 was performed as described in Materials and methods. Data was represented as mean ± SEM. The statistical significance of differences between the control and irradiated cells was evaluated by Student's t test and between UVA-irradiated and herb extracts- or GA-treated cells by one-way ANOVA followed by Dunnett's test. ### P < 0.001 compared with irradiated cells. *P < 0.05; **P < 0.01; ***P < 0.001 compared with non-treated cells exposed to UVA.

3.6 AVS022 and GA protected against melanogenesis in irradiated B16 cells

To study anti-melanogenic effects of AVS022 and GA on B16F10 cells, UVA irradiation led to 33 ± 5.26 % (t-test; $p < 0.001$) increase in melanin content, although pretreatment of cells with AVS022 extracts (Fig. 9A) and GA (Fig. 9B) resulted in a substantial reduction in melanin level induced by UVA exposure (8 J/cm^2) in a concentration-dependent manner.

Moreover, UVA irradiation caused a significant induction of tyrosinase activity by 61.98 ± 7.39% (P<0.001) compared with non-irradiated cells (Fig. 10), although pretreatment with AVS022 extracts (Fig. 10A) and GA (Fig. 10B) significantly inhibited UVA-induced tyrosinase activity.

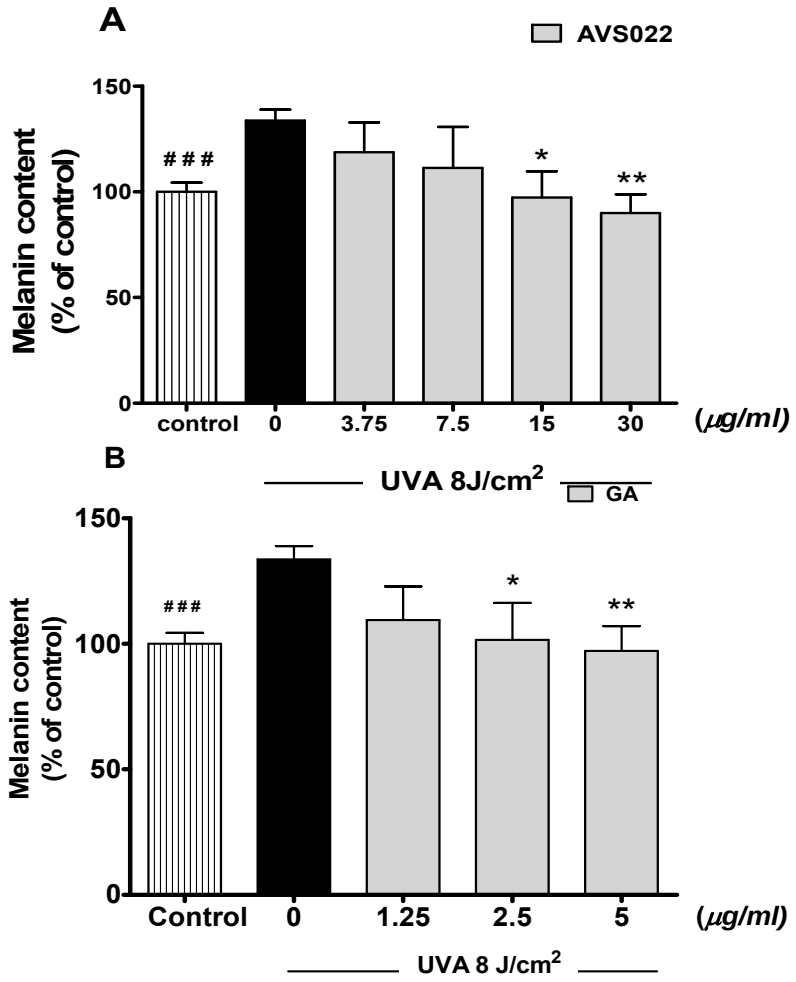

Figure 9. Inhibition of UVA-stimulated melanin production in B16F10 cells by the AVS022 formula (A) and GA (B). The melanin production induced by a single UVA dose of 8 J/cm^2 in B16F10 cells related to the protein concentration were expressed as a percentage of control (100%, unirradiated and untreated cells). Data was represented as mean ± SEM. The statistical significance of differences between the control and irradiated cells was evaluated by Student's t test and between UVA-irradiated and herb extracts- or GA-treated cells by one-way ANOVA followed by Dunnett's test. ### $P < 0.001$ compared with irradiated cells. *$P < 0.05$; **$P < 0.01$ compared with non-treated cells exposed to UVA.

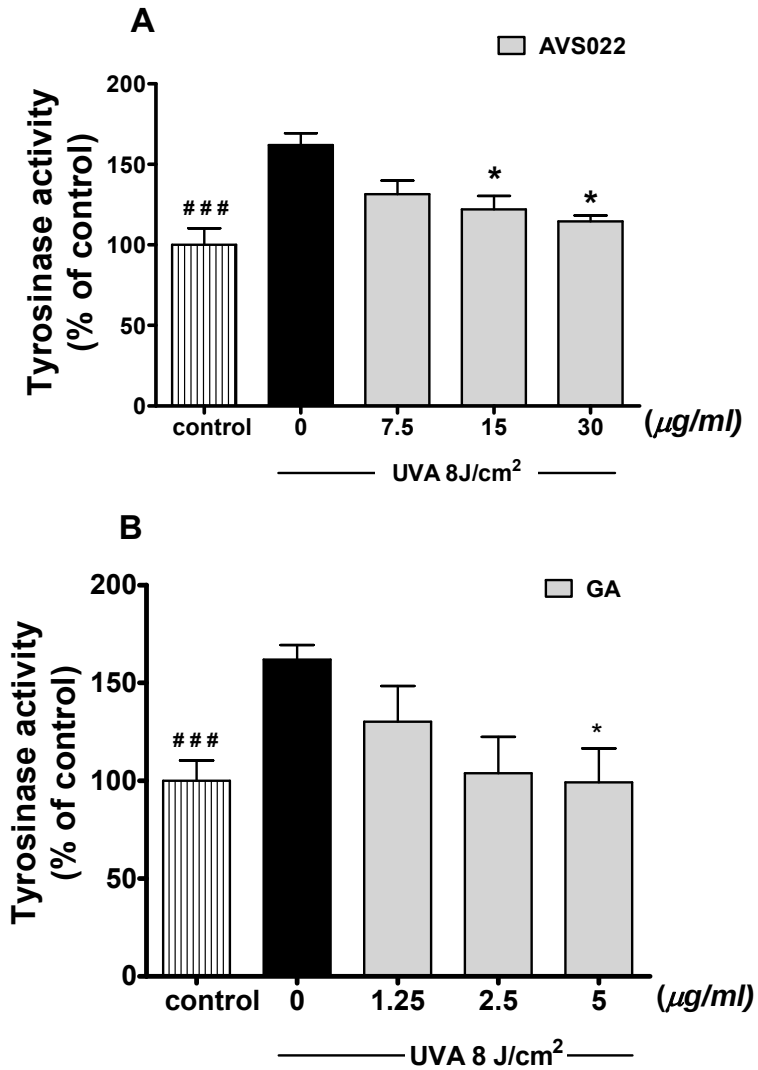

Figure 10. Inhibition of UVA-induced tyrosinase activity in B16F10 cells by the AVS022 formula (A) and GA (B). The tyrosinase activity induced by a single UVA dose of 8 J/cm^2 in B16F10 cells related to the protein concentration were expressed as a percentage of control (100%, unirradiated and untreated cells). Data was represented as mean ± SEM. The statistical significance of differences between the control and irradiated cells was evaluated by Student's t test and between UVA-irradiated and herb extracts- or GA-treated cells by one-way ANOVA followed by Dunnett's test. ### $P < 0.001$ compared with irradiated cells. *$P < 0.05$ compared with non-treated cells exposed to UVA.

3.7 AVS022 and GA protected against oxidant formation and GSH loss in irradiated HaCaT and B16 cells.

Level of cellular oxidant and GSH is an important marker to indicate cellular redox status. We assessed whether redox mechanisms were involved in the inhibitory effects of AVS022 extracts studied and GA on UVA-dependent MMP-1 upregulation and melanogenesis. Fig. 11 demonstrated that, at 1 h post-irradiation, UVA doses of 4 and 8 J/cm^2 led to a substantial increase in oxidant formation by 38.54 ± 2.1 % (P < 0.001) in HaCaT cells and 71.76 ± 5.99% (P < 0.001) in B16F10 cells compared with non-irradiated cells. A dramatic decline in GSH level by 49.3 ± 1.3 % (P < 0.001) in HaCaT and by 50.10 ± 2.30 % (P < 0.001) in B16F10 cells was also observed. In contrast, pretreatment of HaCaT and B16F10 cells with the AVS022 formula and GA caused a significant and dose-dependent inhibition of ROS formation (Fig. 11) and GSH loss (Fig. 12) as compared to un-pretreated cells following UV irradiation.

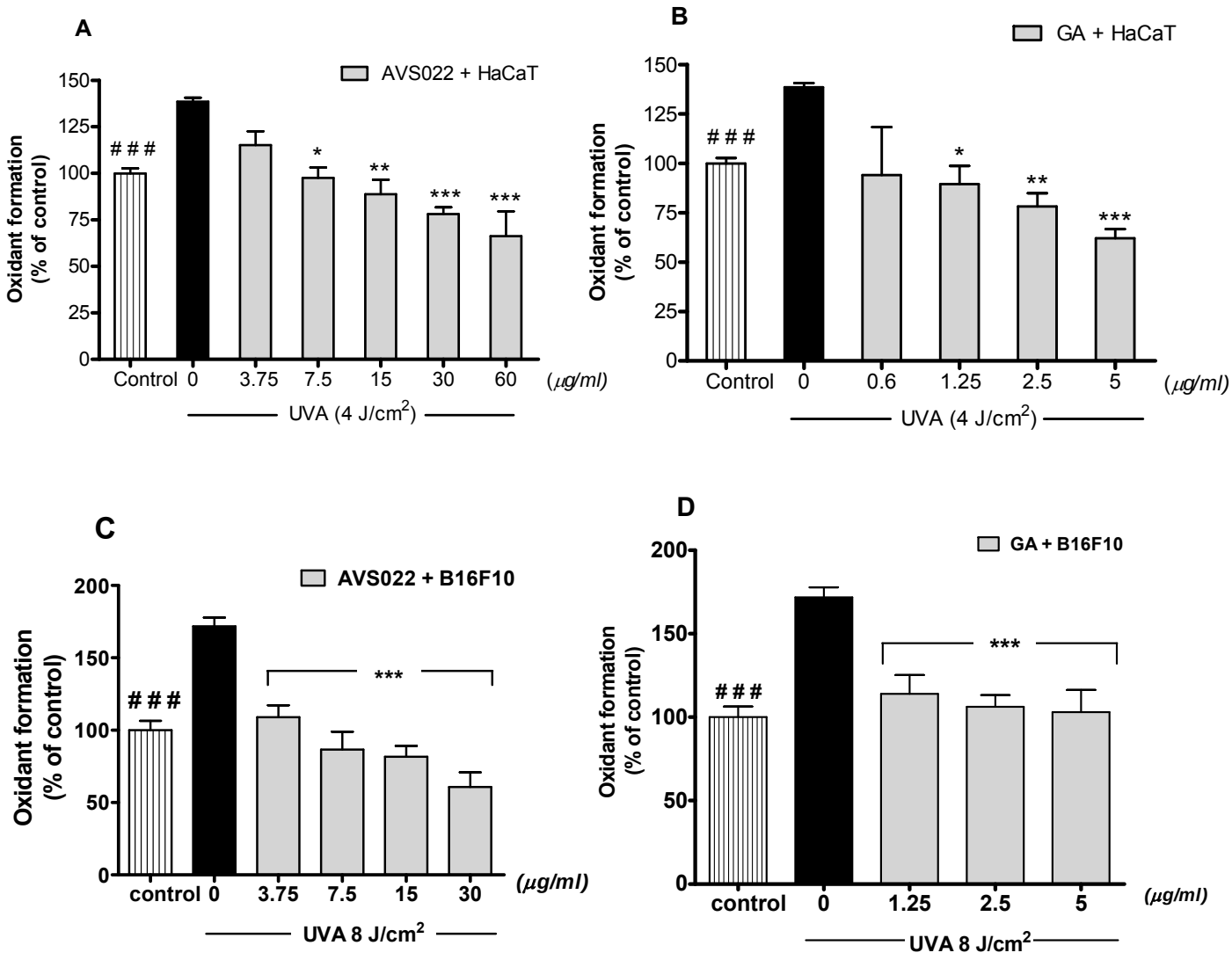

Figure 11. Inhibition of UVA-induced cellular ROS formation in HaCaT and B16F10 cells by AVS022 formula (A,C) and GA (B,D). The fluorescent DCF as an indicator of ROS formation was measured at 485 nm excitation and 530 nm emission as described in Materials and methods. Data were represented as a percentage of control (100%, non-irradiated and non-treated cells) using a microplate reader. The statistical significance of differences between the control and irradiated cells was determined by Student's t test and between UVA-irradiated and herb extracts- or GA-treated cells by one-way ANOVA followed by Dunnett's test. ### $P < 0.001$ compared with irradiated cells. *$P < 0.05$; **$P < 0.01$; ***$P < 0.001$ compared with non-treated cells exposed to UVA.

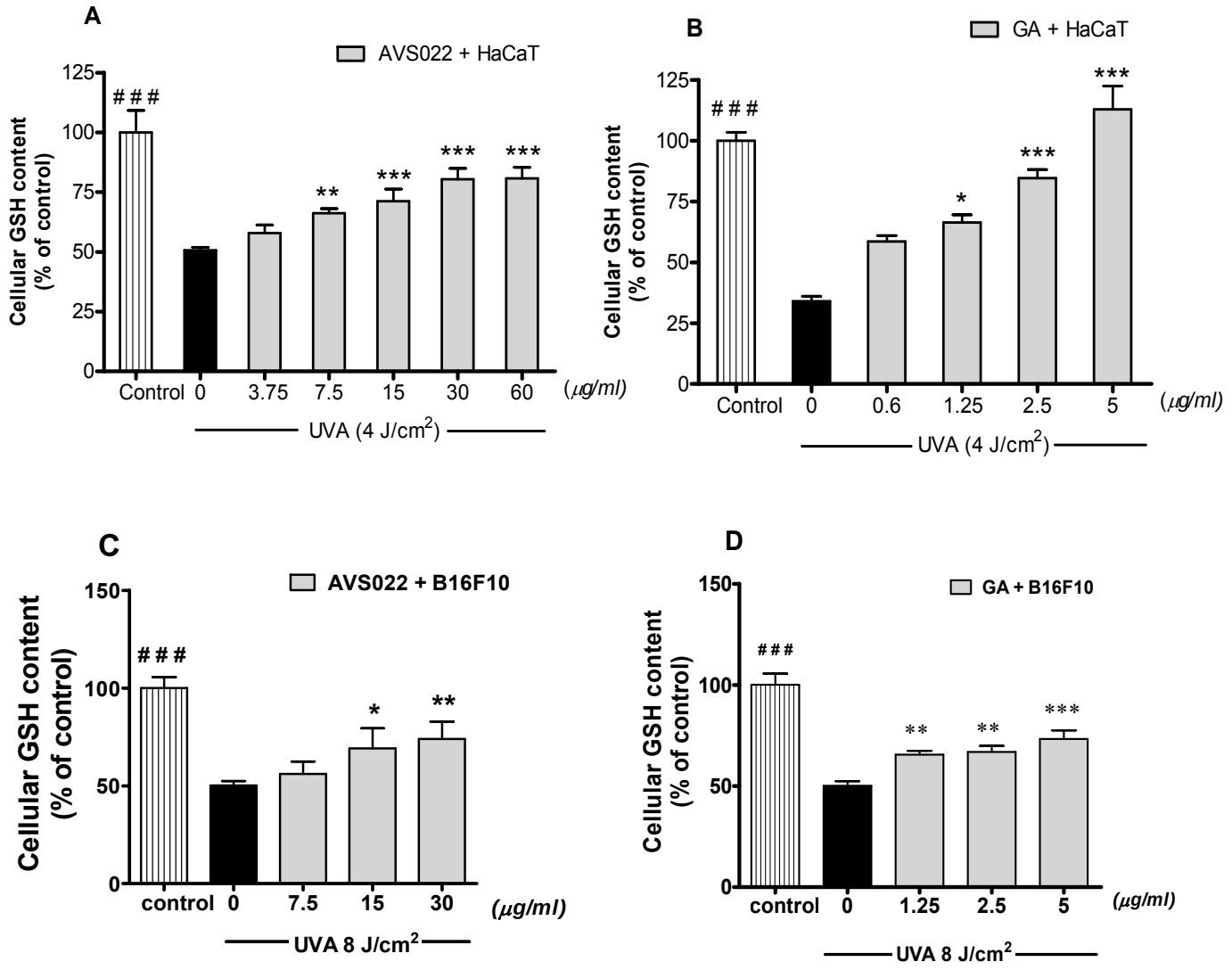

Figure 12. Inhibition of UVA-dependent GSH loss in HaCaT and B16F10 cells by the AVS022 formula (A,C) and GA (B,D). GSH level was detected by fluorescence intensity of the GSH-OPA adduct at 350 nm excitation and 420 nm emission as described in Materials and methods. The statistical significance of differences between the control and irradiated cells was evaluated by Student's t test and between UVA-irradiated and herb extracts- or GA-treated cells by one-way ANOVA followed by Dunnett's test. ### $P < 0.001$ compared with irradiated cells. *$P < 0.05$; **$P < 0.01$; ***$P < 0.001$ compared with non-treated cells exposed to UVA.

3.8 AVS022 and GA protected against catalase and glutathione peroxidase inactivation in irradiated HaCaT and B16 cells.

To further investigate redox mechanisms of AVS022 extracts studied and GA with respect to modulation of endogenous antioxidants, Fig. 13 showed that UVA doses of 4 and 8 J/cm^2 irradiation drastically reduced catalase activity by 43.53 ± 7.7 % (P < 0.001) in HaCaT cells and by 52.94 ± 3.10% (P < 0.001) in B16F10 cells, respectively, as compared with non-irradiated cells. Furthermore, Fig. 14 demonstrated a decrease in GPx activity by 66 ± 8.4 % (P < 0.001) in HaCaT cells exposed to UVA (4 J/cm^2) and by 21.44 ± 1.36% (P<0.001) in irradiated B16F10 cells exposed to UVA (8 J/cm^2) compared to non-irradiated control cells. However, pretreatment with AVS022 extracts (Fig. 13A,C and 14A,C) and GA (Fig. 13B,D and 14B,D) prior to UVA exposure was able to dose-dependently reverse inactivation of both catalase and GPx compared to both irradiated HaCaT and B16F10 cells in the absence of test compounds. In consistent with our findings for cytotoxicity and MMP-1 activity in HaCaT cells, melanogenesis in B16F10 cells as well as oxidant formation and GSH level in both HaCaT and B16F10 cells, AVS022 and GA were also shown to exert protective effects on UVA-dependent catalase and GPx inactivation in both HaCaT and B16F10 cells.

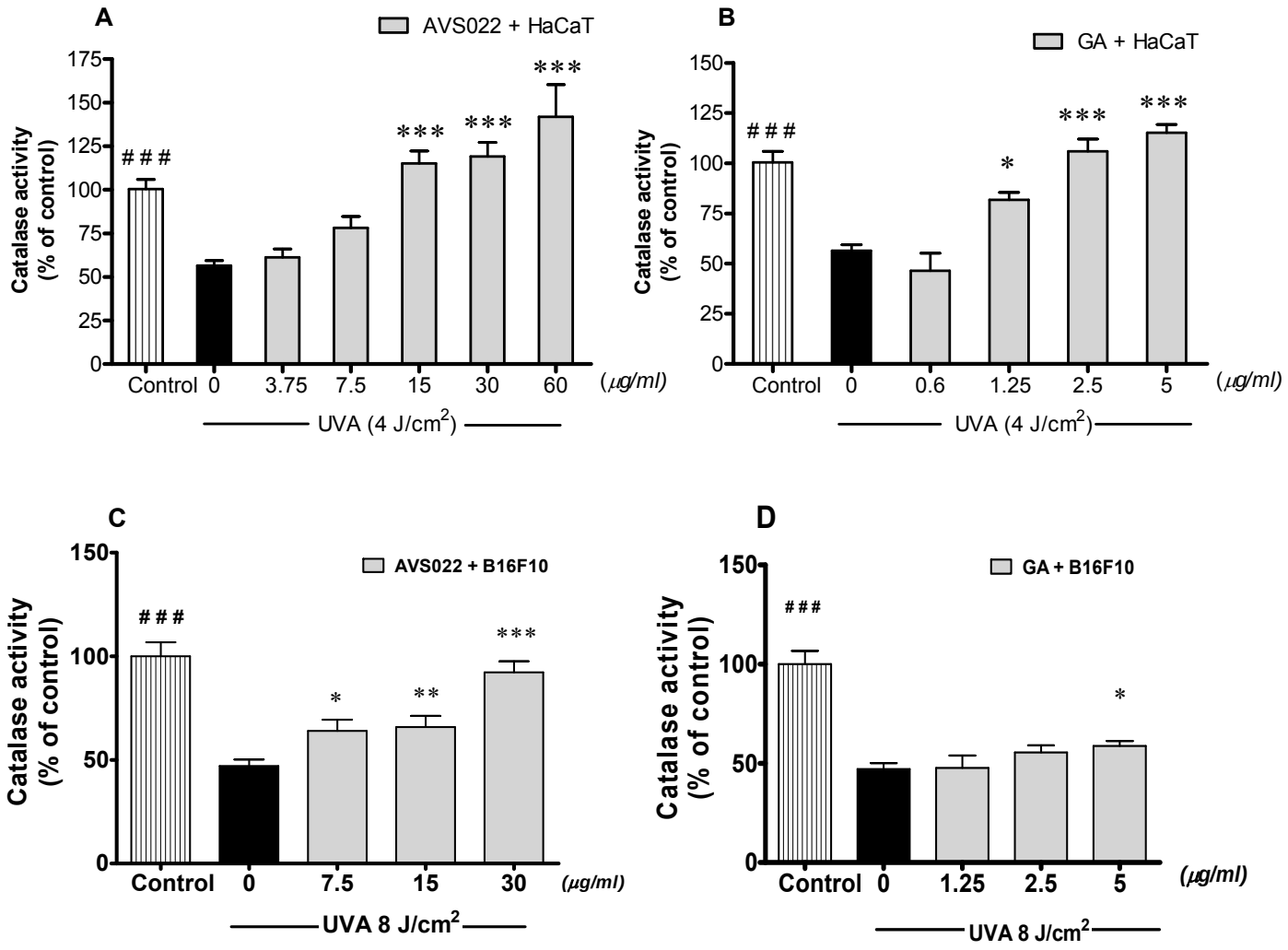

Figure 13. Inhibition of UVA-dependent catalase inactivation in HaCaT and B16F10 cells by the AVS022 formula (A,C) and GA (B,D). The formaldehyde generated was determined spectrophotometrically with Purpald as a chromogen at 540 nm as described in Materials and methods. The statistical significance of differences between the control and irradiated cells was evaluated by Student's t test and between UVA-irradiated and herb extracts- or GA-treated cells by one-way ANOVA followed by Dunnett's test. ### $P < 0.001$ compared with irradiated cells. *$P < 0.05$; ***$P < 0.001$ compared with non-treated cells exposed to UVA.

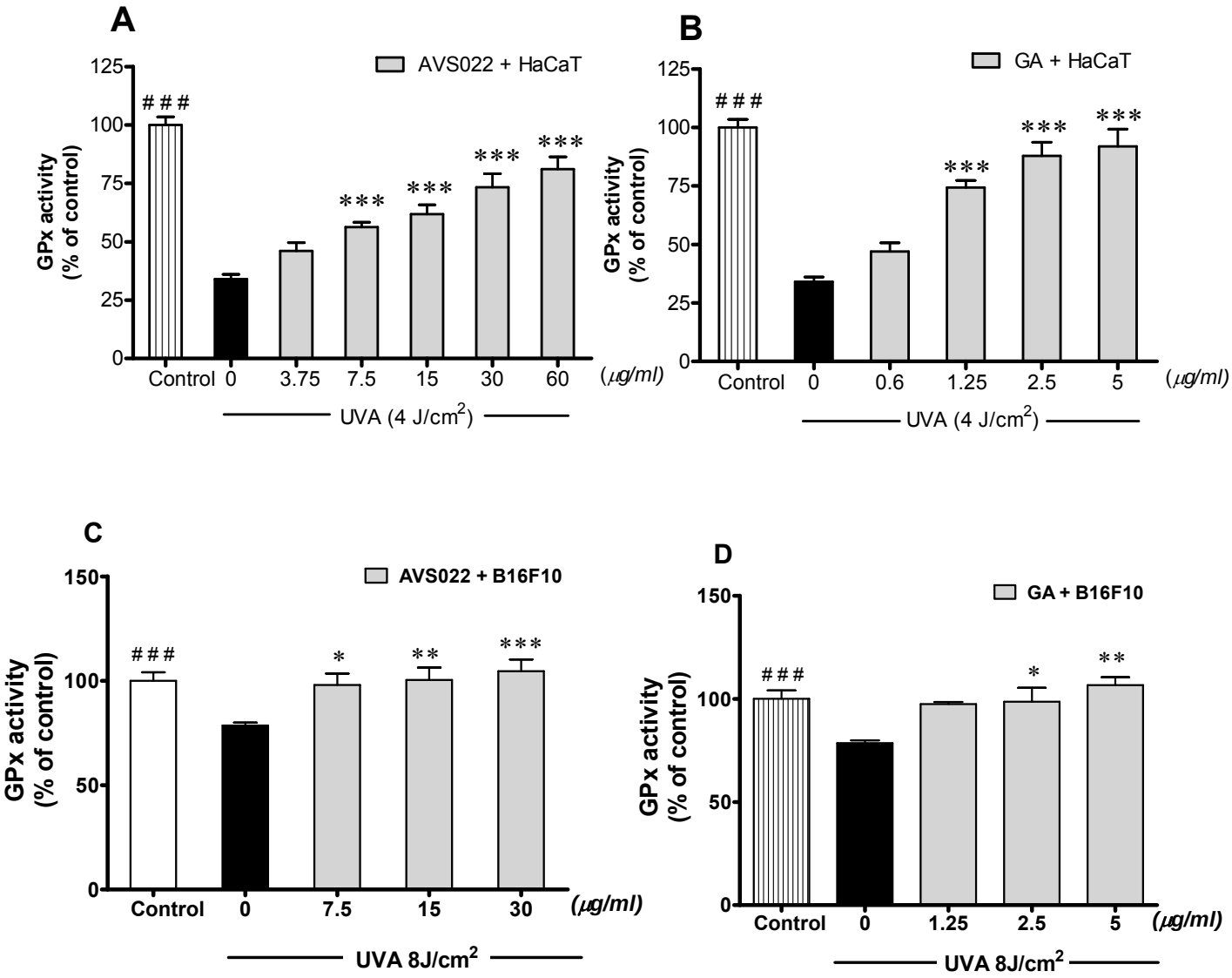

Figure 14. Inhibition of UVA-dependent GPx inactivation in HaCaT and B16F10 cells by the AVS022 formula (A,C) and GA (B,D). GPx activity was measured as described in Materials and methods. The statistical significance of differences between the control and irradiated cells was evaluated by Student's t test and between UVA-irradiated and herb extracts- or GA-treated cells by one-way ANOVA followed by Dunnett's test. ### $P < 0.001$ compared with irradiated cells. *$P < 0.05$; **$P < 0.01$; ***$P < 0.001$ compared with non-treated cells exposed to UVA.

3.9 AVS022 and GA protected against downregulation of catalase, γ-GCL and glutathione peroxidase mRNA in irradiated HaCaT and B16 cells.

To assess whether AVS022 extracts and GA modulated antioxidant defenses at transcriptional levels, exposure of HaCaT to UVA doses of 4 J/cm^2 and B16F10 of 8 J/cm^2 resulted in a pronounced decrease in mRNA levels of catalase (0.53 ± 0.1 and 0.4 ± 0.2-fold decrease) (Fig. 15), γ-GCLC (0.52 ± 0.1 and 0.75 ± 0.1-fold decrease) and γ-GCLM (0.62 ± 0.1 and 0.54 ± 0.1-fold decrease) (Fig. 16) and GPx (0.6 ± 0.03 and 0.44 ± 0.03-fold decrease) (Fig. 17) in irradiated HaCaT and B16F10 cells, respectively, compared to unirradiated cells. Nevertheless, pretreatment of both HaCaT and B16F10 cells with AVS022 extracts and GA prior to UVA challenge led to upregulation of all gene studied.

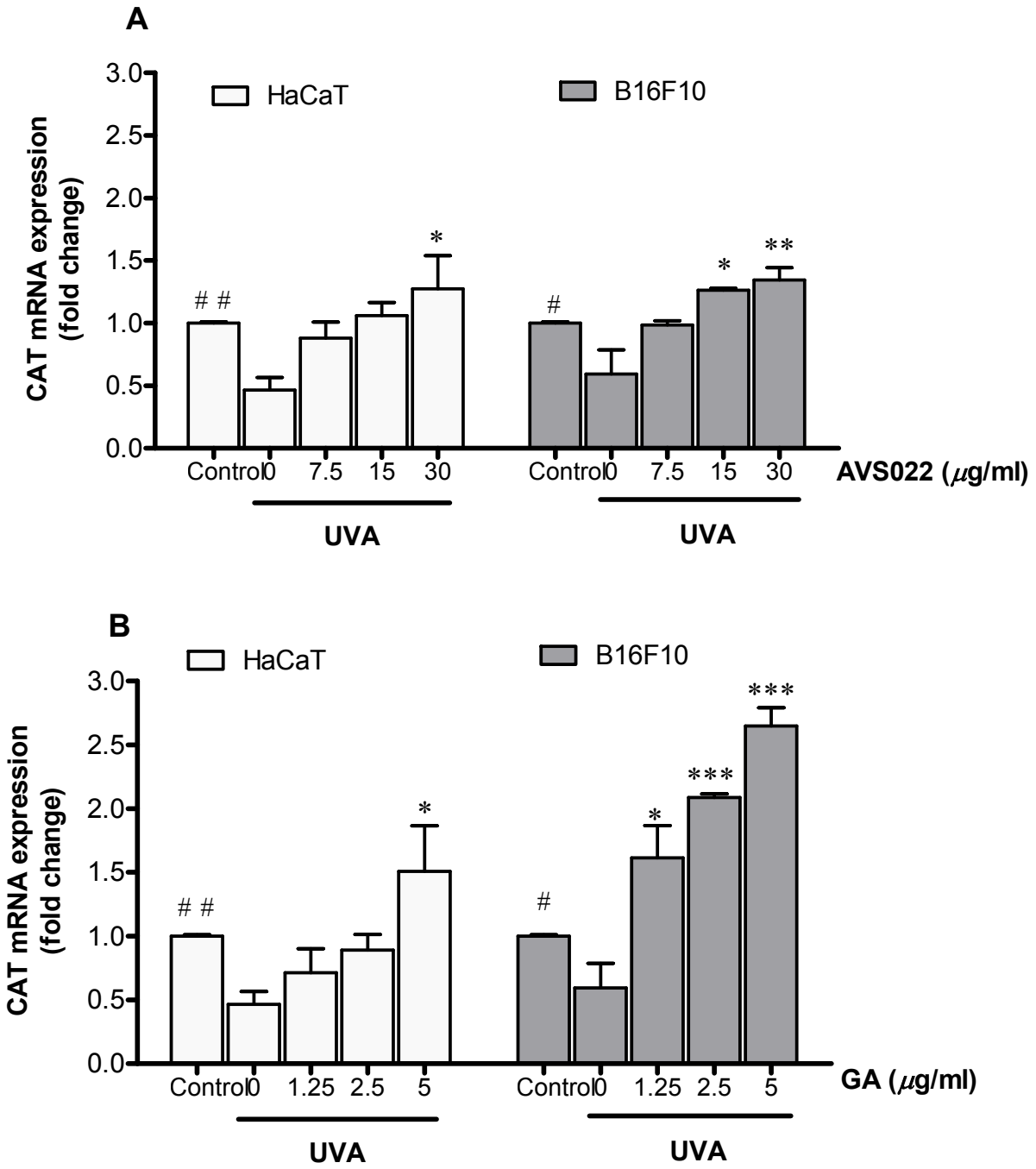

Figure 15. Inhibition of UVA-induced downregulation of catalase (CAT) mRNA by AVS022 extracts (A) and GA (B) in HaCaT and B16F10 cells. The data shown as the fold change in gene expression normalized to GAPDH and relative to the control sample. Values given are mean±SEM. The statistical significance of differences between the control and UVA-irradiated cells was determined by Student's t test and between UVA-irradiated and AVS022 extracts- or GA-treated cells by one-way ANOVA followed by Dunnett's test. #$P < 0.05$; ## $P < 0.01$ compared with irradiated cells. *$P < 0.05$; **$P < 0.01$; ***$P < 0.001$ compared with non-treated cells exposed to UVA.

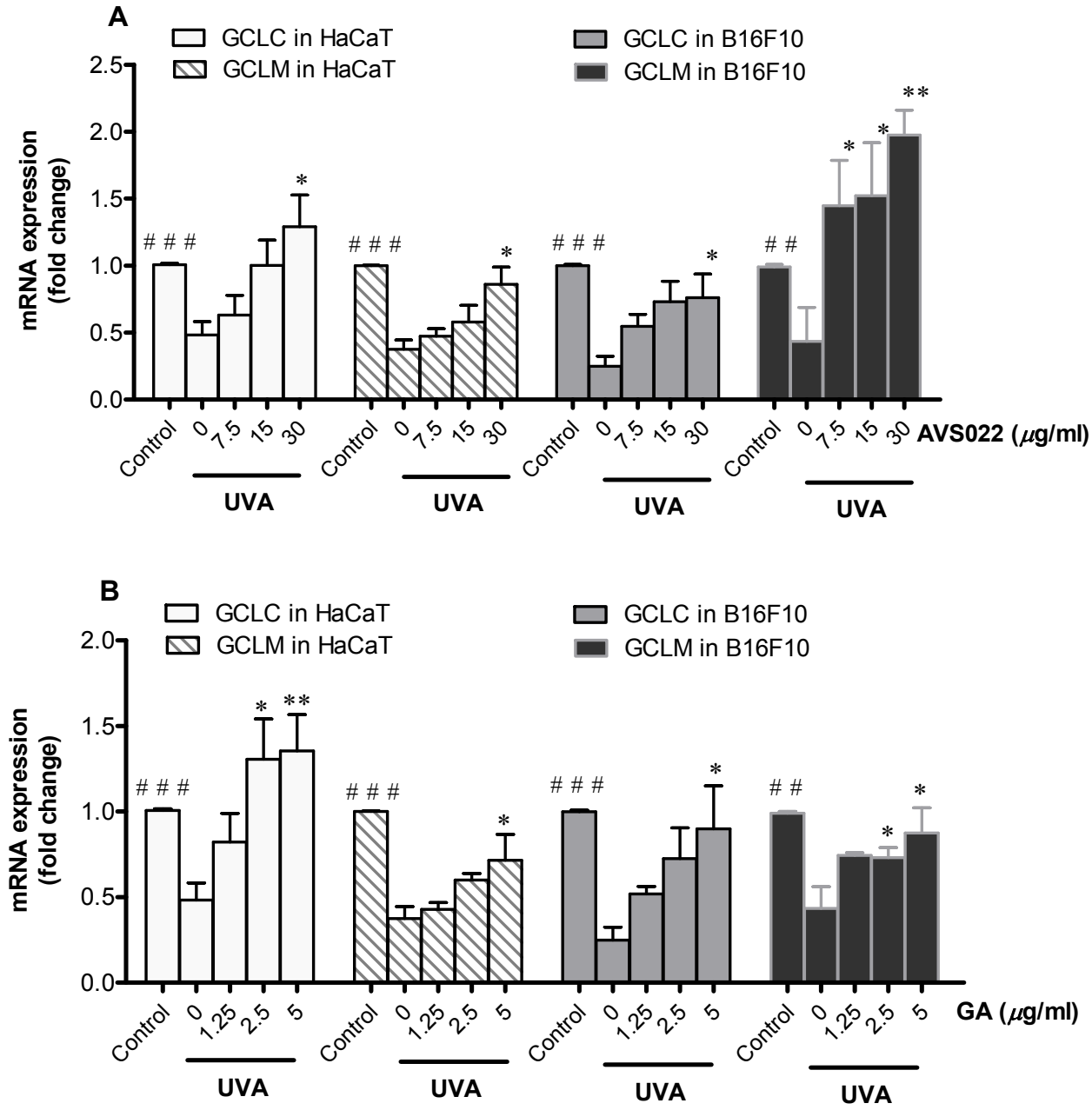

Figure 16. Inhibition of UVA-induced downregulation of GCL mRNA by AVS022 extracts (A) and GA (B) in HaCaT and B16F10 cells. The data shown as the fold change in gene expression normalized to GAPDH and relative to the control sample. Values given are mean±SEM. The statistical significance of differences between the control and UVA-irradiated cells was determined by Student's t test and between UVA-irradiated and AVS022 extracts- or GA-treated cells by one-way ANOVA followed by Dunnett's test. ## $P < 0.01$; ### $P < 0.001$ compared with irradiated cells. *$P < 0.05$; **$P < 0.01$ compared with non-treated cells exposed to UVA.

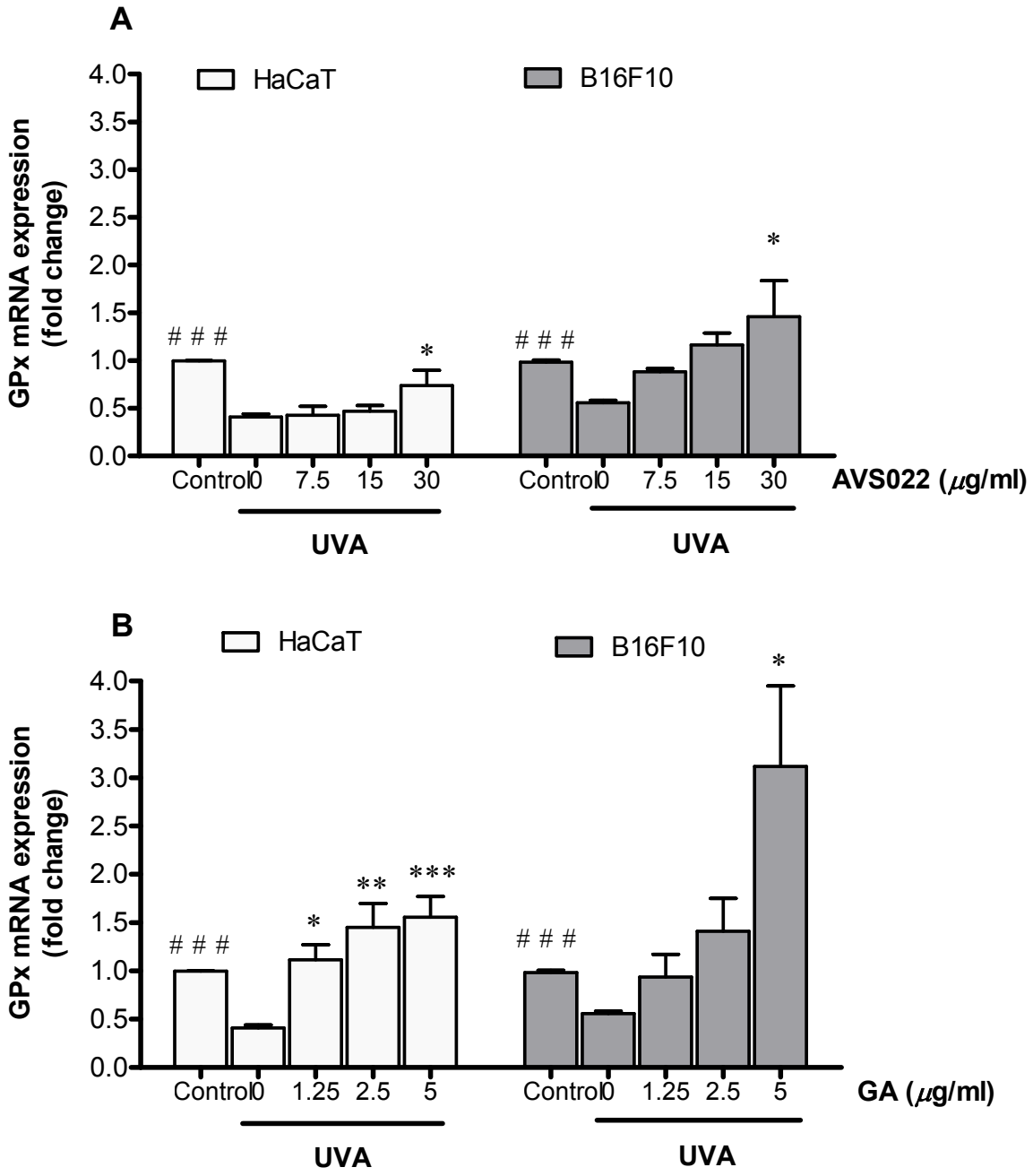

Figure 17. Inhibition of UVA-induced downregulation of glutathione peroxidase (GPx) mRNA by AVS022 extracts (A) and GA (B) in HaCaT and B16F10 cells. The data shown as the fold change in gene expression normalized to GAPDH and relative to the control sample. Values given are mean±SEM. The statistical significance of differences between the control and UVA-irradiated cells was determined by Student's t test and between UVA-irradiated and AVS022 extracts- or GA-treated cells by one-way ANOVA followed by Dunnett's test. ### $P < 0.001$ compared with irradiated cells. *$P < 0.05$; **$P < 0.01$; ***$P < 0.001$ compared with non-treated cells exposed to UVA.

Summary (สรุปผลการทดลอง)

This study illustrated the antimelanogenic action of phytochemicals and AVS073 formula with regard to modulation of GSH-GCL system and GST in melanoma cells irradiated with UVA. CA, FA and GA (used as the reference compounds of herbal extracts), AVS073 and AVS022 extracts at non cytotoxic concentrations suppressed UVA-induced tyrosinase activity and melanin production. To assess photoprotective effect of AVS022 and GA on keratinocyte HaCaT cells, they were shown to inhibit UVA-induced cytotoxicity and MMP-1 upregulation. Photoprotection by polyherbal extracts and phytochemicals (CA, FA and GA), the possible active ingredients of the herbal formula extracts studied, against melanogenesis and MMP-1 activation was found to associate with upregulation of antioxidant defenses including CAT, GSH, GPx and GST at cellular and molecular levels. Phytochemicals including CA, FA and GA present in the herbal extracts may be accountable for the pharmacological activity of the herbal formulas studied. Further studies using physiologically relevant skin models such as primary skin cells, co-cultured skin cells and *in vivo* are needed in order to confirm photoprotective effects of promising herbal extracts and phytochemicals.

Output ที่ได้จากโครงการ

1. ผลงานวิจัยได้รับการตีพิมพ์ในวารสารวิชาการระดับนานาชาติ (เอกสารแนบในภาคผนวก)

   1.1 ผลงานวิจัยที่ได้รับการตีพิมพ์แล้ว (published)

- **Panich U**, Pluemsamran T, Tangsupa-a-nan V, Wattanarangsan J, Phadungrakwittaya R, Akarasereenont P, Laohapand T. Protective effect of AVS073, a polyherbal formula, against UVA-induced melanogenesis through a redox mechanism involving glutathione-related antioxidant defense. BMC Complement Altern Med 2013;13:159-168.
- Pluemsamran T, Tripatara P, Phadungrakwittaya R, Akarasereenont P, Laohapand T, **Panich U**. Redox mechanisms of AVS022, an oriental polyherbal formula, and its component herbs in protection against induction of matrix metalloproteinase-1 in UVA-irradiated keratinocyte HaCaT cells. Evid Based Complement Alternat Med. 2013;2013:739473-739482.
- Thangboonjit W**,** Limsaengurai S**,** Pluemsamran T, **Panich U**. Comparative evaluation of antityrosinase and antioxidant activities of dietary phenolics and their activities in melanoma cells exposed to UVA. Siriraj Med J 2014;66:5-10.

1.2 ผลงานวิจัยอยู่ในระหว่างการพิจารณาเพื่อรอรับการตีพิมพ์ (submitted)

- Anyamanee Chaiprasongsuk, Tasanee Onkoksoong, Thanyawan Pluemsamran, Saowalak Limsaengurai, Uraiwan Panich*. Photoprotection by dietary phenolics against melanogenesis induced by UVA through Nrf2-dependent antioxidant responses. Submitted to *Free Radical Biology & Medicine*.
- Lapatsanant Chaisiriwong, Rungsima Wanitphakdeedecha, Panitta Sittinamsuwan, Somponnat Sampattavanich, Somruedee Chatsiricharoenkul, Woraphong Manuskiatti, Uraiwan Panich. Involvement of oxidative DNA damage and alteration of antioxidant defense system in patients with basal cell carcinoma: a case-control study. Submitted to *Cancer Epidemiology, Biomarkers & Prevention*

2. การนำผลงานวิจัยไปใช้ประโยชน์

- เชิงวิชาการ: มีการพัฒนาการเรียนการสอนและมีส่วนในการผลิตนักศึกษาบัณฑิตศึกษาระดับปริญญาโท 2 คน

3. กิจกรรมอื่นๆ ที่เกี่ยวข้อง ได้แก่

การนำเสนอผลงานในการประชุมระดับนานาชาติ;

- **Panich U**, Onkoksoong T, Chaiprasongsuk A, Pluemsamran T, and Limsaengurai S. Protection against UVA-induced melanogenesis by dietary Phenolics through Nrf2-mediated antioxidant defenses. Free Rad Biol Med 2014; 76 (Suppl 1): S88. The 21st Annual Meeting of the Society for Free Radical Biology and Medicine (SFRBM), Seattle, USA; 19-23 Nov 2014.

ภาคผนวก

1. เอกสารต้นฉบับ (manuscript)

กรุณาดูเอกสารแนบ

ลงนาม.....

(รศ. ดร. พญ.อุไรวรรณ พานิช)

(หัวหน้าโครงการวิจัยผู้รับทุน)

ภาคผนวก

BMC Complementary & Alternative Medicine

RESEARCH ARTICLE Open Access

Protective effect of AVS073, a polyherbal formula, against UVA-induced melanogenesis through a redox mechanism involving glutathione-related antioxidant defense

Uraiwan Panich[1*], Thanyawan Pluemsamran[1], Vanida Tangsupa-a-nan[1], Jantanee Wattanarangsan[1], Rattana Phadungrakwittaya[1], Pravit Akarasereenont[1,2] and Tawee Laohapand[2]

Abstract

Background: Ayurved Siriraj Brand Wattana formula (AVS073), a Thai herbal formula, has traditionally been used for health promotion and prevention of age-related problems. Ultraviolet A (UVA) is recognized to play a vital role in stimulation of melanin synthesis responsible for abnormal skin pigmentation possibly mediated by photooxidative stress. We thus aimed to study the inhibitory effect of AVS073 extracts on UVA-induced melanogenesis via a redox mechanism involving glutathione (GSH) synthesis and glutathione S-transferase (GST) using human melanoma (G361) cell culture.

Methods: The standardization of AVS073 extracts was carried out by TLC and UHPLC to obtain fingerprinting profiles of the formula, which identified several phenolic compounds including gallic acid (GA) in the formula. Antimelanogenic actions of AVS073 (up to 60 μg/ml) and GA (up to 10 μg/ml) were investigated by measuring tyrosinase activity and mRNA as well as melanin level in G361 cells irradiated with UVA. Moreover, antioxidant actions of the herbal formula and GA were determined by evaluating oxidant formation and modulation of GSH-related antioxidant defenses including GSH content, GST activity and mRNA level of γ-glutamate cysteine ligase catalytic (γ-GCLC) and modifier (γ-GCLM) subunit and GST.

Results: AVS073 extracts and GA, used as a reference compound, suppressed UVA-augmented tyrosinase activity and mRNA and melanin formation. In addition, pretreatment with AVS073 and GA was able to inhibit cellular oxidative stress, GSH depletion, GST inactivation and downregulation of γ-GCLC, γ-GCLM and GST mRNA in G361 cells exposed to UVA radiation.

Conclusions: AVS073 formula exerted antimelanogenic effects possibly through improving the redox state by upregulation of GSH and GST. Moreover, pharmacological activity of the polyherbal formula would be attributed to combined action of different phenolic compounds present in the formula.

Keywords: Ayurved siriraj brand wattana formula, UVA, Melanogenesis, Glutathione, Antioxidant

Background

Herbal formula used for maintaining skin health and curing various ailments including skin problems has become increasing popular. Ayurved Siriraj Brand Wattana formula (AVS073), a Thai herbal formula, has traditionally been used for health promotion and prevention of age-related problems such as loss of appetite, gastrointestinal dysmotility and weakness. The formula is composed of 15 medicinal plants, *Piper nigrum* (L.), *Boesenbergia rotunda* (L.) Manf., *Cyperus rotundus* (L.), *Tinospora crispa*, *Terminalia chebula* Retz., *Cladogynos orientalis*, *Derris scandens* (Roxb.) Benth., *Anamirta cocculus* L., *Drypetes roxburghii* (Wall.), *Cinnamomum siamense* Craib., *Ferulaa assa-foetida* L., *Aegle maemelos* L., *Conioselinum univitatum* Trucz., *Saussurea lappa* Clark., *Cryptolepis buchanani* Roem. & Schult. Several *in vitro* and *in vivo* studies demonstrated that the extracts of

* Correspondence: uraiwan.pan@mahidol.ac.th
[1]Department of Pharmacology, Faculty of Medicine Siriraj Hospital, Mahidol University, Bangkok 10700, Thailand
Full list of author information is available at the end of the article

AVS073's components have a wide range of pharmacological properties, in particular, antioxidant, antiinflammatory, immunomodulating and anticancer actions [1-5]. Furthermore, the herbal components of AVS073 formula including *T. chebula* [6] and *S. Lappa* [7] were observed to yield whitening activities and inhibitory action against oxidative stress of the skin. Since having fair skin is desirable in the Eastern culture that leads to increased demand for whitening products, efforts have thus been made to develop medicinal plants as effective and safe antimelanogenic agents.

Ultraviolet (UV) radiation has been recognized as a main environmental factor contributed to hyperpigmentation or hypermelanosis through augmentation of melanin synthesis primarily controlled by tyrosinase [8]. Deleterious effects on the skin due to abnormal production of melanin have been also discussed because excess melanin could result in genotoxicity and may involve pathogenesis of malignant melanoma [9].

Previous studies have reported that UVA-induced oxidative stress through induction of oxidant formation and disruption of antioxidant defense system was correlated to elevation of melanogenesis [10,11]. Therefore, promotion of antioxidant defense capacity might be useful for the prevention of hypermelanosis. Glutathione (GSH)-related antioxidant enzymes including γ-glutamate cysteine ligase (γ-GCL), the rate-limiting enzyme in cellular GSH synthesis, and glutathione S-transferase (GST) are important detoxification enzymes vital to prevent the skin from photooxidative stress due to their abilities to maintain the redox state [12]. Since oxidative stress induced by UVA is implicated in hypermelanosis through induction of tyrosinase responsible for melanin synthesis, compounds that act as tyrosinase inhibitors and/or antioxidants could serve as a depigmenting agent [13]. Various melanin-producing cells including melanoma cell lines have been widely employed as models to investigate biology of melanogenesis and the effects of putative antimelanogenic agents [14,15]. Our study was carried out using human melanoma cell line (G361), one of lightly-pigmented cell types shown to be highly susceptible to accumulate oxidative damage mediated by UVA irradiation [16]. In order to develop AVS073 formula, a poly herbal formula, as a putative depigmenting agent, we thus aimed to investigate the antimelanogenic effect of AVS073 formula and its redox mechanisms in association with modulation of GSH-related antioxidant defense.

Methods

Materials

Human melanoma cell line G361 from American Type Culture Collection (ATCC, Rockville, Md, USA) was a generous gift from Assoc. Prof. Tengamnuay, Faculty of Pharmaceutical Sciences, Chulalongkorn University. Dulbecco's modified Eagle medium (DMEM) and cell culture reagents were purchased from Invitrogen (NY, USA). The highest quality chemicals and reagents available were used and purchased from Sigma-Aldrich (MO, USA or Germany), unless otherwise indicated.

Preparation and chromatographic fingerprint analysis of AVS073 formula extracts

AVS073 powder was obtained from Manufacturing Unit of Herbal Medicines and Products, manufactured under GMP by Ayurved Thamrong School, Center of Applied Thai Traditional Medicine (CATTM), Faculty of Medicine Siriraj Hospital, Mahidol University, Thailand. The whole dried AVS073 was accurately weighed (50 g) and extracted using 500 mL of 80% (v/v) ethanol as the extraction solvent. The sample solution was mixed for 10 min and centrifuged at 9,000 rpm for 10 min at 4°C. Then, the supernatant was evaporated under reduced pressure by rotary evaporator and kept frozen overnight prior to lyophilization. The lyophilized powder (5 mg) dissolved in 1 ml of methanol (50%, v/v) was used in thin layer chromatography (TLC) or ultra-high performance liquid chromatography (UHPLC) with photodiode array (PDA) detection for AVS073 analysis. The layout of the fingerprint analysis of AVS073 and its 15 components was shown in Figures 1 and 2. As shown in Figure 1, TLC-densitometric analysis was performed using a mobile phase (hexane/ethyl acetate/acetic acid = 31:14:5 v/v/v) for the separation of phenolics. TLC chromatograms showed the presence of phenolics in AVS073 extract and identification of phenolics was carried out by comparing retardation factor (Rf) values of phenolic reference markers. Gallic acid (GA) was detected in AVS073 extracts with Rf = 0.18 (Figure 1B). Moreover, two- and three- dimensional UHPLC chromatogram fingerprints were shown in Figure 2. The separations were performed on a reverse phase column (BEH C18, 1.7 μm, 2.1×100 mm, Water, Milford, MA). The mobile phases were composed of acetonitrile (B) and 0.1% o-phosphoric acid (A) using a gradient elution of 95-90% A at 0–5 min; 90-80% A at 5–8 min; 80-0% A at 8–10 min; 0-95% A at 10–11 min. The flow rate was 0.3 mL/minute. Phenolic peaks in the UHPLC fingerprint of AVS073 were analyzed and a prominent peak at a retention time (Rt) of 1.678 min was identified as GA by comparing the Rt and absorption spectrum of GA marker. Additionally, quantitative analysis of GA present in AVS073 extracts was carried out using the UHPLC method and GA content in the whole dried AVS073 extract was found to be 0.0342% w/w.

Treatment of cells with AVS073 extracts and UVA irradiation

G361 melanoma cells were cultured in DMEM supplemented with 10% fetal bovine serum (FBS), 100

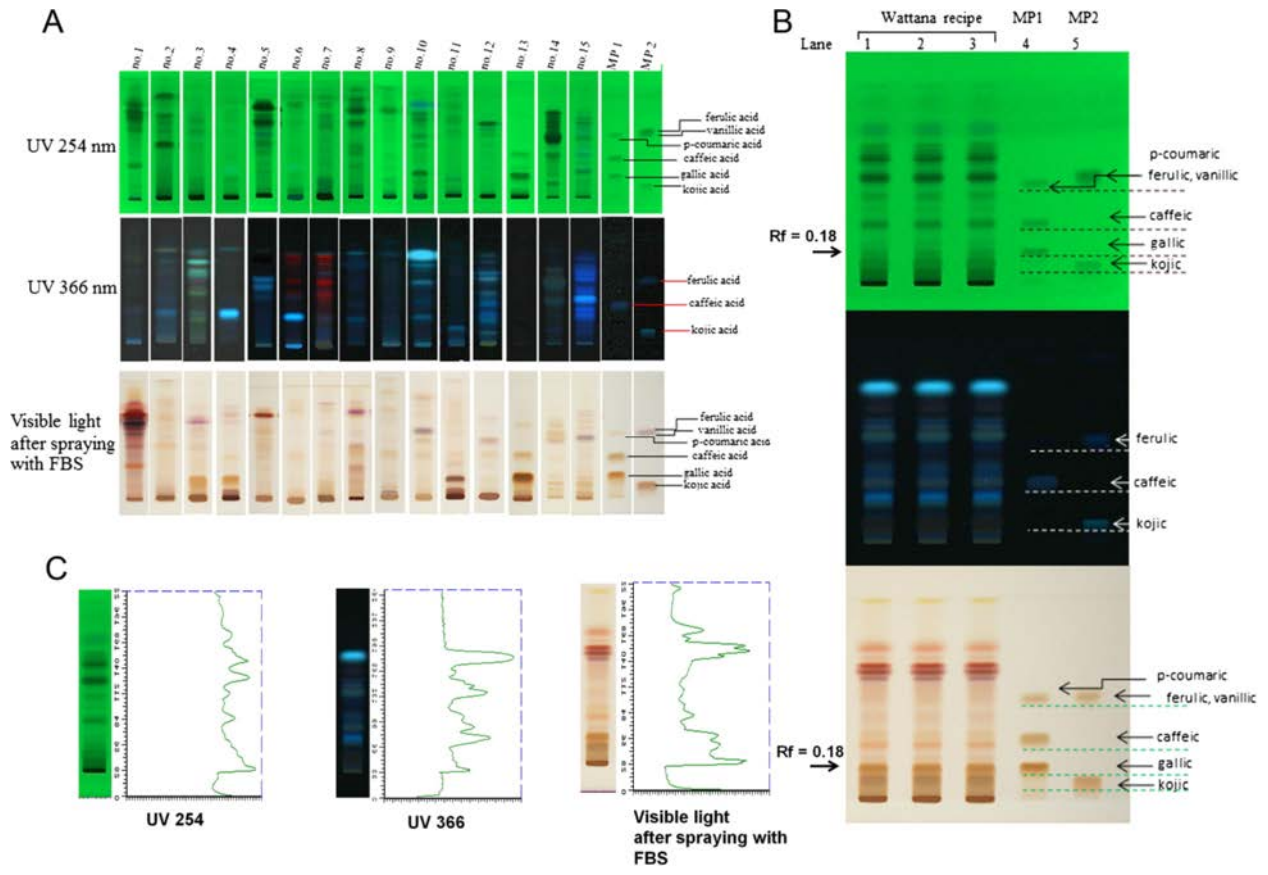

Figure 1 TLC fingerprints of AVS073 and its 15 components visualized at 254 and 366 nm under UV and visible light (after spraying with fast blue salt: FBS), respectively. (A) 15 components of AVS073 were *P. nigrum*, *B. rotunda*, *C. rotundus*, *T. crispa*, *T. chebula*, *C. orientalis*, *D. scandens*, *A. cocculus*, *D. roxburghii*, *C. siamense*, *F. assa-foetida*, *A. maemelos*, *C. univitatum*, *S. lappa*, and *C. buchanani*; lane1-15: component no. 1–15; lane16: mixed phenolic markers (MP1): gallic acid, caffeic acid and *p*-coumaric acid; lane17: mixed phenolic markers (MP2): kojic acid, vanillic acid and ferulic acid (from bottom to top). **(B)** Wattana (AVS073) formula; lane1-3; 3 replicates of AVS073; lane 4: MP1; lane 5: MP2. **(C)** Densitometric fingerprint of AVS073.

units/ml penicillin and 100 μg/ml streptomycin at 37°C in a humidified atmosphere containing 5% CO_2 (P_{CO2} = 40 Torr) (a Forma Scientific CO_2 Water Jacketed Incubator). AVS073 extracts and GA used as a positive control were dissolved in 80% ethanol, the final concentration of which was less than 0.5% (v/v) in culture medium. G361 cells were treated with AVS073 extracts (7.5, 15, 30 and 60 μg/ml) and GA (2.5, 5 and 10 μg/ml) for 30 min before UV exposure for all assays and for 24 h without UV irradiation for cytotoxicity study. Cells were washed with phosphate buffered saline (PBS) and PBS was added to the cells prior to UVA (320–400 nm) exposure to avoid generation of medium-derived toxic photoproducts. For melanin content assay, the UVA dose of 16 J/cm^2 was selected since the dose of 8 J/cm^2 did not significantly alter melanin synthesis and both UVA doses of 8 and 16 J/cm^2 did not affect G361 cell viability [17]. The source of UVA (330–400 nm) was xenon arc lamp (Dermalight ultrA1; Hoenle, Martinsried, Germany). After the treatment, cell lysates were prepared as previously described [17].

Cell viability assay

In order to confirm that antimelanogenic effects of AVS073 formula was not due to cytotoxicity of the formula extracts causing a decrease in cell numbers. Cell viability was assessed using 3-(4,5-dimethylthiazol-2-yl) 2,2 diphenyltetrazolium bromide (MTT) reduction assay. Metabolically viable cells were identified by measuring the purple formazan, a product of MTT reduction. Absorbance of the purple formazan was measured at 595 nm by a spectrophotometer (SpectraMax M2 of Molecular Device, CA, USA).

Tyrosinase activity assay

Cellular tyrosinase activity was determined by assessing the rate of L-DOPA oxidation as previously described [11]. L-DOPA was added as the substrates to each

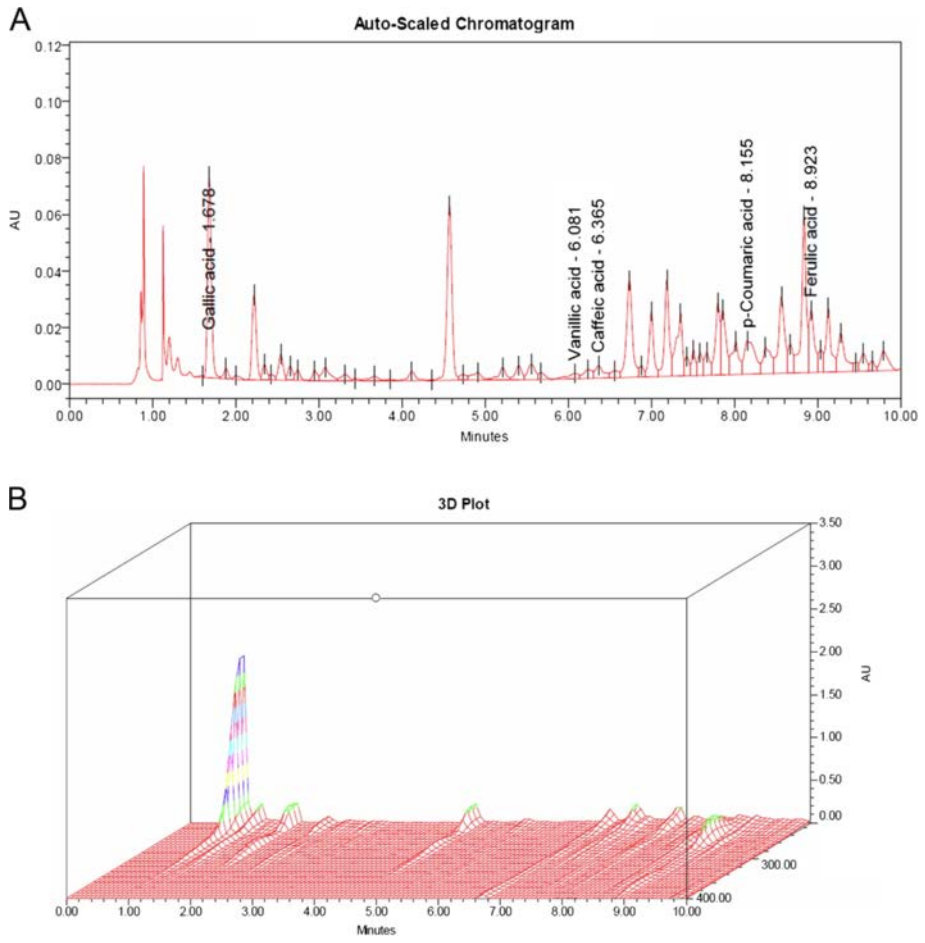

Figure 2 UHPLC chromatogram of the AVS073 formula. (A) Two-dimensional UHPLC chromatogram (UV absorbance at 280 nm). **(B)** Three-dimensional UHPLC-PDA chromatogram (range 210–400 nm).

sample to initiate the enzymatic reaction at 37°C. Absorbance of dopachrome formation was measured spectrophotometrically at 475 nm every 10 min for 1 h at 37°C by a spectrophotometer. The tyrosinase activity was calculated by comparing to standard curves using tyrosinase (2,034 U/mg) and was expressed as unit/mg protein. The data are expressed as a percentage of the tyrosinase activity (unit/mg protein) of the untreated control cells without UV irradiation (100%).

Melanin content assay

Melanin production induced by a UVA dose of 16 J/cm^2 was assessed as previously described [11]. 1 N NaOH was used to lyse the cells and dissolve melanin, which was then determined spectrophotometrically at 475 nm. The melanin contents were calculated by comparing to a standard curve derived using synthetic melanin (0–250 μg/ml) and expressed as a percentage of the melanin contents (μg/mg protein) of the untreated control cells without UV irradiation (100%).

Determination of intracellular oxidant formation

The inhibitory effects of AVS073 and GA on UVA (8 J/cm^2)-dependent reactive oxygen species (ROS) formation in G361 cells were measured using 2′,7′-Dichlorofluorescein diacetate (DCFH-DA), a stable and non-fluorescent dye. Within the cells, DCFH-DA was hydrolyzed by esterases to non-fluorescent DCFH, which was readily oxidized by intracellular oxidants to fluorescent 2,7-dichlorofluorescein (DCF). After UVA irradiation, cells were subjected to phenol red-free DMEM containing DCFHDA (5 μM) for 1 h. Then, the DCF fluorescence was monitored for 20 min at 485-nm excitation and 530-nm emission using a spectrofluorometer. The data are expressed as a percentage of intracellular oxidant formation (relative fluorescence units, RFU) of the untreated control cells without UV irradiation (100%).

Measurement of intracellular glutathione level

A fluorometric assay based on the specific reaction of GSH with the fluorescent probe *o*-phthalaldehyde (OPA)

was carried out to assess intracellular GSH as previously described [18]. After UVA treatment, cells were lysed with 6.5% (w/v) trichloroacetic acid (TCA). The assay mixture contained cell lysate, buffer (100 mM KH_2PO_4, 10 mM EDTA and 1 mM NaOH, pH 8.0) and 1 mg/ml OPA in methanol. The fluorescence of the GSH-OPA adduct was measured with excitation and emission wavelengths of 350 and 420 nm, respectively. The GSH levels were calculated in comparison to the standard and the results are expressed as a percentage of the GSH content (nmol/mg protein) of the untreated control cells without UV irradiation (100%).

Measurement of glutathione-S-transferase activity

GST activity was investigated by following the kit protocol from Cayman chemical (Ann Arbor, MI). The GST catalyzed the conjugation of GSH with 1-chloro-2,4-dinitrobenzene (CDNB) to produce GSH-DNB conjugate spectrophotometrically determined at 340 nm immediately and every 30 second for 10 min. 100 mM CDNB were used to produce the reaction of either sample or positive control GST with 200 mM GSH in assay buffer. The data are expressed as a percentage of the GST activity (μmol/min/mg protein) of the untreated control cells without UV irradiation (100%).

Protein content assay

The protein content was determined using the Bio-Rad Protein Assay Kit (Bio-Rad, Germany) with bovine serum albumin (BSA) as the standard. Values for each sample are means of triplicate measurements.

Quantitative real-time reverse transcriptase-polymerase chain reaction: determination of tyrosinase, γ-GCLC, γ-GCLM and GST mRNA expression

G361 cells pretreated with or without AVS073 (7.5, 15 and 30 μg/ml) and GA (1.25, 2.5 and 5 μg/ml) were exposed to UVA (8 J/cm^2). At 2 h following UV irradiation, preparation of total RNA was carried out using the illustra RNAspin Mini RNA Isolation Kit (GE Healthcare, UK) and total RNA was reverse transcribed using the ImProm-II Reverse Transcriptase (Promega, Medison, USA) following the kit manual. 25 μl of reaction mixtures contained 5 μl cDNA template, 12.5 μl Master Mix, 10 μM forward primer (1 μl), 10 μM reversed primer (1 μl) and 5.5 μl water. Real-time PCR was carried out in triplicate for each sample on the ABI Prism 7500 Real Time PCR System (Applied Biosystems, USA). The amplification reactions were run under the following conditions: 95°C for 10 min, 40 cycles at 95°C for 15 s, 60°C for 40 s, and 72°C for 40 s. mRNA levels were determined using FastStart Universal SYBR Green Master (ROX). Primers for PCR were designed using the Primer Express software version 3.0 (Applied Biosystems, USA). Sequences of PCR primer sets for tyrosinase, γ-GCLC, γ-GCLM, GST and GAPDH (in 5′-3′ direction) were as follows:

Tyrosinase (product sizes = 114 bp)
Sense primer: TCTTCTCCTCTTGGCAGATTGTC
Antisense primer: TGTCATGGTTTCCAGGATTACG
γ-GCLC (product sizes = 160 bp)
Sense primer: GCTGTCTTGCAGGGAATGTT
Antisense primer: ACACACCTTCCTTCCCATTG
γ-GCLM (product sizes = 200 bp)
Sense primer: TTGGAGTTGCACAGCTGGATTC
Antisense primer: TGGTTTTACCTGTGCCCACTG
GST (product sizes = 72 bp)
Sense primer: CCTGTACCAGTCCAATACCATCCT
Antisense primer: TCCTGCTGGTCCTTCCCATA
GAPDH (product size = 124 bp)
Sense primer: GAAATCCCATCACCATCTTCC
Antisense primer: AAATGAGCCCCAGCCTTCTC

Amplification of a single product was verified using the melt curve analysis. The mRNA level was normalized with reference to the amount of housekeeping gene transcripts (GAPDH mRNA). The mean Ct from mRNA expression in cDNA from each sample was compared with the mean Ct

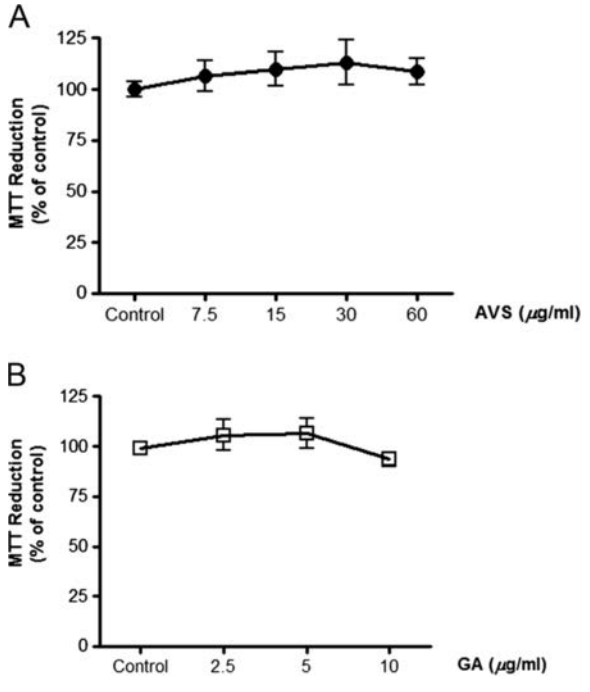

Figure 3 Effects of AVS073 extracts (A) and GA (B) on cell viability without UVA irradiation. Cell viability was expressed as a percentage of control (100%, the untreated control cells without UV irradiation).

from GAPDH determinations from the same cDNA samples in order to determine tyrosinase, γ-GCLC, γ-GCLM and GST mRNA. The results are expressed as fold change in gene expression calculated using the $2^{-\Delta\Delta Ct}$ method. For the control (untreated cells without UV irradiation), $\Delta\Delta C_t$ equals zero and 2^0 equals one, so that the fold change in gene expression relative to the control equals one, by definition. For the cells treated with AVS073, assessment of $2^{-\Delta\Delta Ct}$ determined the fold change in gene expression relative to the control.

Statistical analysis

Values are expressed as means ± standard error of the mean (SEM) analysed from data taken from at least 3 separate experiments performed on different days. The significance of individual treatment groups in comparison to the UV-irradiated groups was determined with one-way analysis of variance (ANOVA) followed by Tukey's *post hoc* test or independent *t*-test (Student's; 2 populations) using Prism (GraphPad Software Inc., San Diego, CA). Values of $p < 0.05$ were considered statistically significant.

Results

Inhibition of UVA-induced tyrosinase activity and melanin synthesis by AVS073

At first, cytotoxicity of the herbal formula and GA on G361 cells was assessed in order to indicate that the inhibitory effects of AVS073 and GA on melanin synthesis were not due to reduced number of cells. MTT assay demonstrated that the formula up to 60 μg/ml and GA up to 10 μg/ml did not affect cell viability (Figure 3A and 3B). The depigmenting effects of the herbal extracts and GA were assessed by measuring tyrosinase activity and melanin production in G361 cells irradiated with a UVA dose of 8 and 16 J/cm^2, respectively. UVA irradiation caused 65.6 ± 11.9% ($p < 0.001$) and 42.6 ± 5% ($p < 0.001$) induction in tyrosinase activity and melanin production, respectively. However, UVA-mediated enhanced tyrosinase activity (Figure 4A and 4B) and melanin content

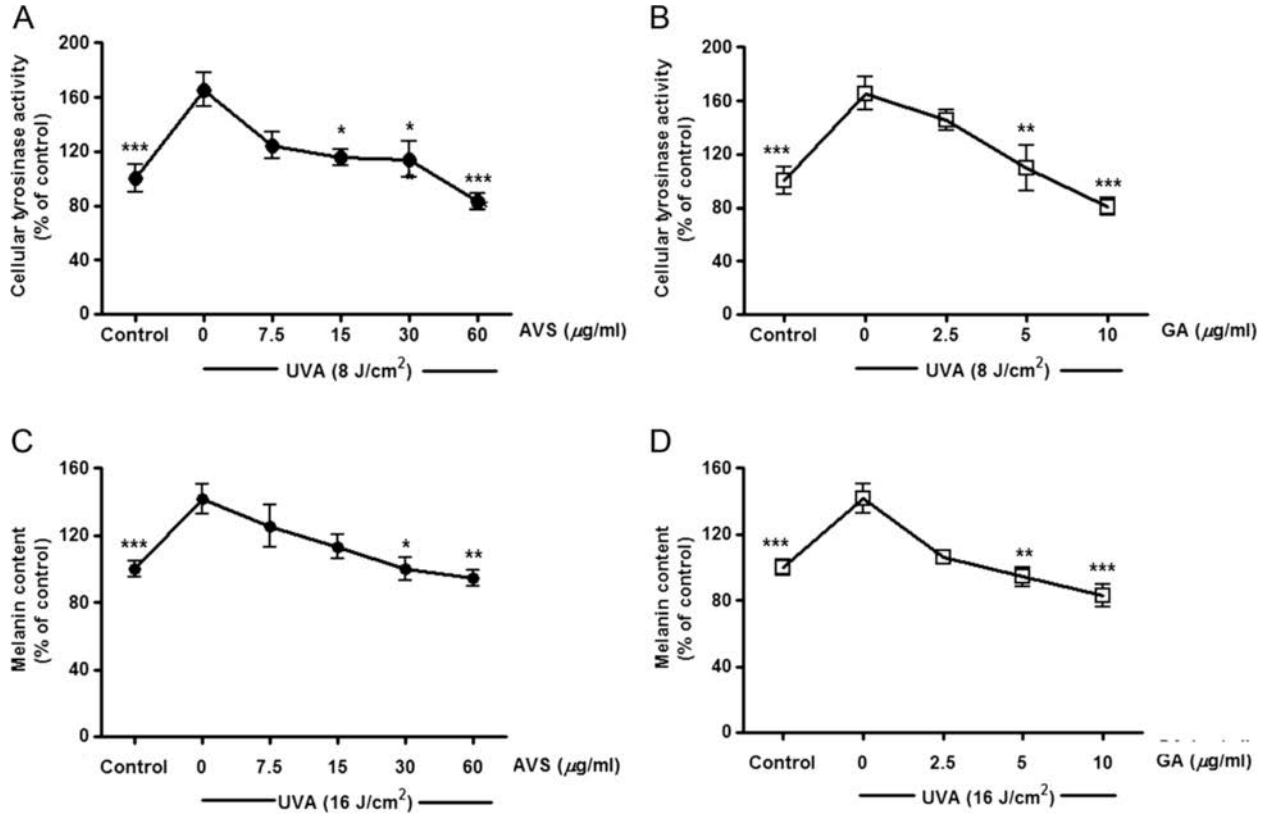

Figure 4 Inhibition of UVA-induced tyrosinase activity (A and B) and melanin synthesis (C and D) by AVS073 and GA. The tyrosinase activity and melanin production induced by a single UVA dose of 8 or 16 J/cm^2, respectively, related to the protein concentration were expressed as a percentage of control (100%, the untreated control cells without UV irradiation). Values are expressed as mean±SEM. The statistical significance of differences between the control and UVA-irradiated cells was determined by Student's t test and between UVA-irradiated and AVS073 extracts- or GA-treated cells by one-way ANOVA followed by Tukey's *post hoc* test. *$p < 0.05$; **$p < 0.01$; ***$p < 0.001$ compared with AVS073- or GA-treated cells without UV irradiation.

(Figure 5C and 5D) was markedly inhibited by AVS073 extracts and GA in a concentration-dependent manner.

Inhibition of UVA-induced ROS formation, GSH depletion and GST inactivation by AVS073

The redox mechanisms associated with antimelanogenic effects of AVS073 were assessed by investigating GSH-related antioxidant defenses including GSH level and GST activity. Irradiation of G361 cells with UVA (8 J/cm^2) caused a substantial elevation in intracellular oxidant production by 93.6 ± 11.7% ($p < 0.01$) in irradiated cells compared to nonirradiated cells. In contrast, pretreatment of cells with AVS073 (15–60 μg/ml) (Figure 5A) and GA (2.5-10 μg/ml) (Figure 5B) resulted in a dose-dependent inhibition of UVA-induced oxidant generation. Moreover, a significant decline in GSH content by 52.5 ± 7.2% ($p < 0.001$) and GST activity by 53.5 ± 9.4% ($p < 0.001$) (Figure 6) was observed in irradiated G361 cells compared to nonirradiated cells. Nevertheless, AVS073 extracts and GA were observed to protect against the loss of GSH (Figure 6A and 6B) and inactivation of GST (Figure 6C and 6D) in a concentration-dependent manner.

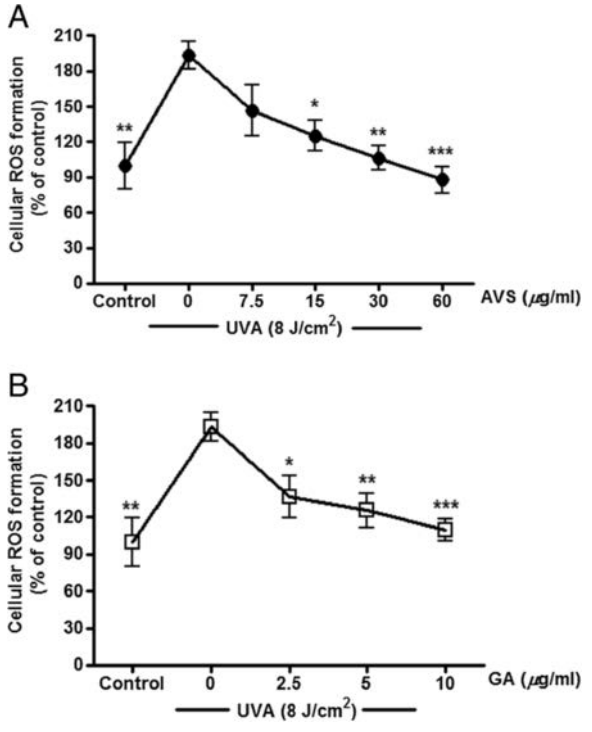

Figure 5 Inhibition of UVA-induced ROS formation by AVS073 (A) and GA (B). Oxidant formation was assessed by measurement of fluorescence of the DCF. Values are expressed as mean±SEM. The statistical significance of differences between the control and UVA-irradiated cells was determined by Student's t test and between UVA-irradiated and AVS073 extracts- or GA-treated cells by one-way ANOVA followed by Tukey's *post hoc* test. *$p < 0.05$; **$p < 0.01$; ***$p < 0.001$ compared with AVS073- or GA-treated cells without UV irradiation.

Inhibition of UVA-induced upregulation of tyrosinase mRNA and downregulation of γ-GCLC, γ-GCLM and GST by AVS073

The quantitative analysis of gene expression changes was carried out in order to investigate the effects of AVS073 (7.5-30 μg/ml) and GA (1.25-5 μg/ml) on increased melanogenesis at mRNA level at 2 h after irradiation. In agreement with the data observed in the study of tyrosinase activity, a rise in tyrosinase mRNA expression (2.2 ± 0.2-fold change; $p < 0.01$) was observed in response to UVA irradiation (8 J/cm^2), although AVS073 (Figure 7A) and GA (Figure 7B) significantly diminished tyrsoinase mRNA levels. Furthermore, while UVA exposure led to reduction of mRNA levels of γ-GCLC (0.51 ± 0.01-fold decrease; $p < 0.001$), γ-GCLM (0.59 ± 0.04-fold decrease; $p < 0.001$) and GST (0.74 ± 0.04-fold decrease; $p < 0.001$), upregulation of their mRNA was detected in the cells pretreated with AVS073 extracts (Figure 7C and 7E) and GA (Figure 7D and 7F).

Discussion and conclusion

Potential medicinal plants containing antioxidant properties have gain remarkable attention in development of novel whitening products since UVA-dependent oxidative stress is recognized to aggravate hyperpigmentation, a common skin problem that physically and emotionally affects mostly Asian women. Assays for tyrosinase activity and melanin production are common screening methods used to determine antimelanogenic effects of putative compounds. Additionally, medicinal plants possessing antioxidant properties play a crucial role in the protection of photooxidative stress through different redox mechanisms including quenching free radicals and improving antioxidant defense capacity. Our observation suggested that AVS073 formula at non-cytotoxic concentrations was able to substantially inhibit UVA-dependent increased melanin production and tyrosinase activity and mRNA expression in G361 cells. The antioxidant roles of AVS073 in regulation of melanogenesis were also investigated in our study. We previously demonstrated that ROS production in response to UV irradiation correlated with upregulation of tyrosinase and melanin synthesis in human melanoma cells [11]. In this study, the extracts of AVS073 formula were found to suppress UVA-induced ROS formation in relation to modulation of GSH-related antioxidant defense. GSH-related antioxidant defense including GSH-GCL system and GST is important for the cells to cope with oxidative stress as their actions involve restoration of intracellular redox homeostasis and detoxification of UV-dependent generation of oxidants implicated in skin damage [19]. In addition, it is well

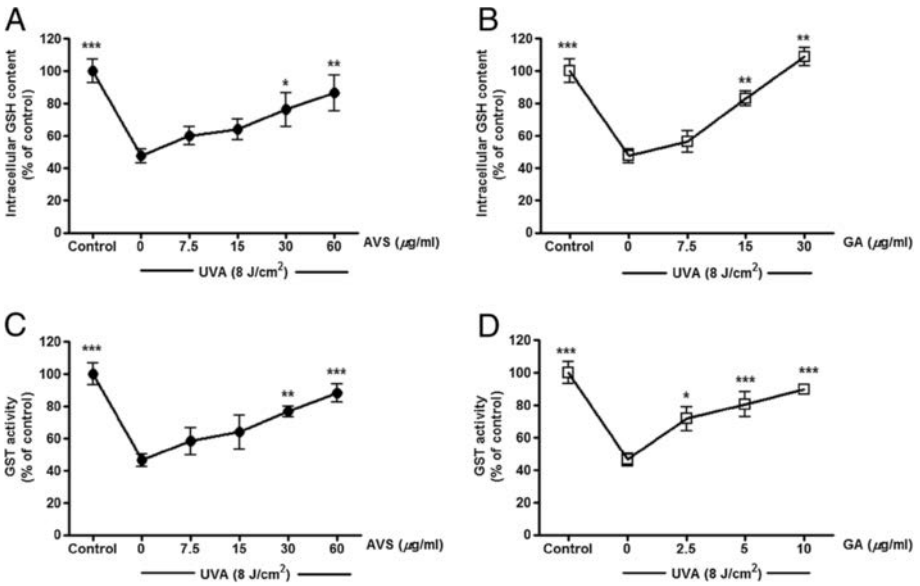

Figure 6 Inhibition of UVA-induced GSH depletion (A and B) and GST inactivation (C and D) by AVS073 and GA. GSH level and GST activity were determined by measurement of fluorescence of the GSH-OPA adduct and absorbance of the GSH-CDNB, respectively. The GSH content and GST activity related to the protein concentrations were expressed as a percentage of control (100%, untreated cells without UV irradiation). Values are expressed as mean±SEM. The statistical significance of differences between the control and UVA-irradiated cells was determined by Student's t test and between UVA-irradiated and AVS073 extracts- or GA-treated cells by one-way ANOVA followed by Tukey's *post hoc* test. *$p < 0.05$; **$p < 0.01$; ***$p < 0.001$ compared with AVS073- or GA-treated cells without UV irradiation.

recognized that GSH is capable of modulating melanogenesis and the opposite regulation of tyrosinase by GSH has been observed in previous studies suggesting that promotion of GSH content was associated with a decrease in melanogenesis in human melanoma cells [11]. Since insufficient elimination of oxidants appears to induce tyrosinase activity and melanin production, GSH-related detoxifying antioxidants may thus play a role in the regulation of melanogenesis and/or neutralization of toxic intermediates generated during melanogenic process [20]. Pretreatment of irradiated G361 cells with the AVS073 extracts was found to upregulate GSH levels and GST activity in our study. We then determined whether AVS073 also affected the transcriptional regulation of GSH biosynthesis and GST and found that the extracts were able to protect against UVA-induced downregulation of γ-GCLC, γ-GCLM and GST mRNA. Nevertheless, further investigations using physiologically relevant skin models, e.g., primary human melanocytes, are required since various pigment cell types have different redox states that might affect melanin biosynthesis in response to UVA exposure.

In addition, the fingerprint profile of the AVS073 extracts was carried out using TLC and UHPLC analysis to ensure consistent quality of preparations of the herbal extracts studied. While the chromatogram showed the presence of several phenolic compounds including GA in the AVS073 formula, which was then used as the positive control to screen antimelanogenic effects of the herbal formula, GA content in the AVS073 extracts was observed to be 0.0342% w/w, which was very low, and its concentration at 5 μg/ml was required to achieve a significant inhibition of UVA-induced tyrosinase activity (Figure 4B) and melanin content (Figure 4B) in G361 cells. Therefore, GA could not be solely a phenolic compound contributed to biological activity of the AVS073 extracts and antimelanogenic effect of the formula may be attributed to combined effect of multiple phytochemicals present in the formula. It is thus important to further identify active components and/or ingredients of the whole formula and its constituent herbs responsible for the pharmacological activities of the AVS073 formula. There is considerable interest in screening of botanical products including herbal formulas possessing antioxidant properties accountable for depigmenting activity in order to develop effective and safe whitening agents. Previous *in vitro* and *in vivo* studies have shown that *P. nigrum* [21], *C. rotundus* [1], *T. chebula* [22], *D. scandens* [23], *F. asafoetida* [24], *S. lappa* [3,7], *C. buchanani* [23] provided powerful free radical scavenging activities and/or restored antioxidant defense system including GSH or GST at the cellular and molecular level. *T. chebula* fruit also exhibited inhibitory effects on UVB-induced oxidative stress and damage of human

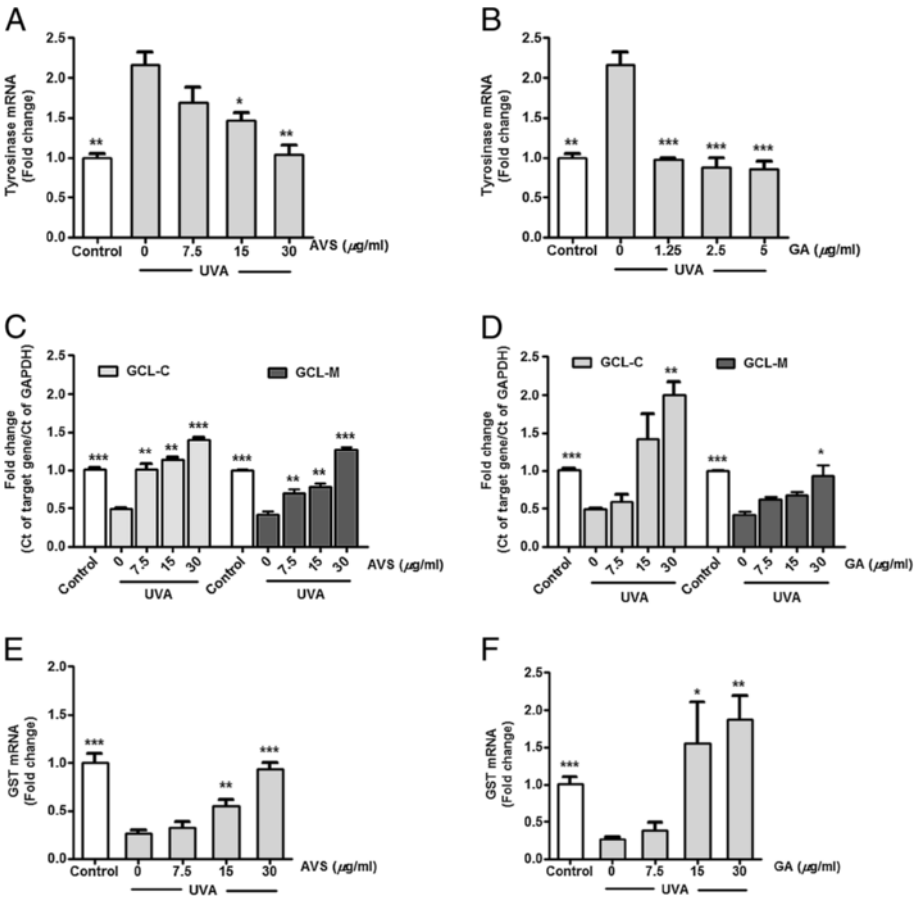

Figure 7 Inhibition of UVA-induced upregulation of tyrosinase mRNA (A and B) and downregulation of γ-GCLC and γ-GCLM (C and D) as well as GST (E and F) by AVS073 and GA. The data shown as the fold change in gene expression normalized to GAPDH and relative to the control sample. Values given are mean±SEM. The statistical significance of differences between the control and UVA-irradiated cells was determined by Student's t test and between UVA-irradiated and AVS073 extracts- or GA-treated cells by one-way ANOVA followed by Tukey's *post hoc* test. *$p < 0.05$; **$p < 0.01$; ***$p < 0.001$ compared with AVS073- or GA-treated cells without UV irradiation.

epidermal keratinocytes [22]. Furthermore, in agreement with our observation on the antimelanogenic effects of GA on G361 and B16F10 melanoma cells [16], GA, an important phenolic acid present in AVS073 formula (Figure 2A), was also shown to protect against UVA-induced melanogenesis in this study. It may be possible that the antimelanogenic effects of AVS073 formula may be attributed to antioxidant actions of several phenolic compounds including GA in neutralizing ROS generated by UV but not direct effects since treatment of G361 cells with the herbal extracts alone at the highest concentration tested (60 μg/ml) for 30 min without UVA irradiation did not significantly affect tyrosinase activity, melanin content, ROS formation, GSH level and GST activity (Table 1).

Table 1 The effects of AVS073 extracts alone at the highest concentration tested (60 μg/ml) on tyrosinase activity, melanin content, ROS formation, GSH level and GST activity in G361 cells compared to control group

Assay	% of control		*p*-value
	Unirradiated and untreated control	AVS073 alone without irradiation	
Tyrosinase activity	100 ± 10.3	99.5 ± 5.5	> 0.05
Melanin content	100 ± 4.7	110.06 ± 15.2	> 0.05
ROS formation	100 ± 7.8	87.1 ± 9.3	> 0.05
GSH level	100 ± 7.1	94.36 ± 5.5	> 0.05
GST activity	100 ± 6.7	106.24 ± 6.6	> 0.05

Results are expressed as mean ± SEM.

In summary, the AVS073 formula, a Thai herbal formula, provided inhibitory effects on melanogenesis in association with the redox mechanism involving upregulation of GSH biosynthesis as well as GST activity and mRNA. Our observation could give pharmacological evidence for the traditional use of the herbal formula and further studies are warranted to develop this formula and/or to identify active ingredients as effective depigmenting agents.

Abbreviations

AVS073: Ayurved siriraj brand wattana formula™; BSA: Bovine serum albumin; CDNB: 1-Chloro-2,4-dinitrobenzene; DCFH-DA: 2′, 7′-Dichlorofluorescein diacetate; DMEM: Dulbecco's modified eagle medium; FBS: Fetal bovine serum; GA: Gallic acid; γ-GCLC: γ-Glutamate cysteine ligase catalytic subunit; γ-GCLM: γ-Glutamate cysteine ligase modifier subunit; GMP: Good manufacturing practice; GSH: Glutathione; GST: Glutathione S-transferase; MP: Mixed phenolic markers; MTT: 3-(4,5-Dimethylthiazol-2-yl)-2,5-diphenyltetrazolium bromide; OPA: *o*-Phthalaldehyde; PBS: Phosphate buffered saline; Rf: Retardation factor; ROS: Reactive oxygen species; Rt: Retention time; TCA: Trichloroacetic acid; TLC: Thin layer chromatography; UHPLC: Ultra-high performance liquid chromatography; UV: Ultraviolet.

Competing interests

The authors declare that they have no completing interests.

Authors' contributions

UP designed the study, analyzed the data and wrote the manuscript. TP and VT performed the experimental studies of cellular melanogenesis and antioxidant defense. JW and RP carried out the chromatographic fingerprint analysis. PA wrote the manuscript. TL conceived the study and provided the herbal samples. All authors read and approved the final manuscript.

Acknowledgements

Appreciation is expressed to Thailand Research Fund (Grant no. RSA5580012) and Department of Pharmacology and the "Chalermphrakiat" Grant, the Faculty of Medicine Siriraj Hospital, Mahidol University, for research funding.

Author details

[1]Department of Pharmacology, Faculty of Medicine Siriraj Hospital, Mahidol University, Bangkok 10700, Thailand. [2]Center of Applied Thai Traditional Medicine, Faculty of Medicine Siriraj Hospital, Mahidol University, Bangkok 10700, Thailand.

Received: 7 December 2012 Accepted: 28 June 2013
Published: 5 July 2013

References

1. Seo WG, Pae HO, Oh GS, Chai KY, Kwon TO, Yun YG, Kim NY, Chung HT: **Inhibitory effects of methanol extract of cyperus rotundus rhizomes on nitric oxide and superoxide productions by murine macrophage cell line, RAW 264.7 Cells.** *J Ethnopharmacol* 2001, **76:**59–64.
2. Lee HS, Won NH, Kim KH, Lee H, Jun W, Lee KW: **Antioxidant effects of aqueous extract of *Terminalia Chebula* in vivo and in vitro.** *Biol Pharm Bull* 2005, **28:**1639–1644.
3. Pathak N, Khandelwal S: **Cytoprotective and immunomodulating properties of piperine on murine splenocytes: an in vitro study.** *Eur J Pharmacol* 2007, **576:**160–170.
4. Subramaniam D, Giridharan P, Murmu N, Shankaranarayanan NP, May R, Houchen CW, Ramanujam RP, Balakrishnan A, Vishwakarma RA, Anant S: **Activation of apoptosis by 1-hydroxy-5,7-dimethoxy-2-naphthalene-carboxaldehyde, a novel compound from *Aegle marmelos*.** *Cancer Res* 2008, **68:**8573–8581.
5. Iranshahy M, Iranshahi M: **Traditional uses, phytochemistry and pharmacology of asafoetida (Ferula assa-foetida oleo-gum-resin)-a review.** *J Ethnopharmacol* 2011, **134:**1–10.
6. Suguna L, Singh S, Sivakumar P, Sampath P, Chandrakasan G: **Influence of *Terminalia chebula* on dermal wound healing in rats.** *Phytother Res* 2002, **16:**227–231.
7. Choi JY, Choi EH, Jung HW, Oh JS, Lee WH, Lee JG, Son JK, Kim Y, Lee SH: **Melanogenesis inhibitory compounds from Saussureae Radix.** *Arch Pharm Res* 2008, **31:**294–299.
8. Schallreuter KU, Kothari S, Chavan B, Spencer JD: **Regulation of melanogenesis-controversies and new concepts.** *Exp Dermatol* 2008, **17:**395–404.
9. Miyamura Y, Coelho SG, Schlenz K, Batzer J, Smuda C, Choi W, Brenner M, Passeron T, Zhang G, Kolbe L, Wolber R, Hearing VJ: **The deceptive nature of UVA tanning versus the modest protective effects of UVB tanning on human skin.** *Pigment Cell Melanoma Res* 2011, **24:**136–147.
10. Hu ZM, Zhou Q, Lei TC, Ding SF, Xu SZ: **Effects of hydroquinone and its glucoside derivatives on melanogenesis and antioxidation: Biosafety as skin whitening agents.** *J Dermatol Sci* 2009, **55:**179–184.
11. Panich U, Tangsupaanan V, Onkoksoong T, Kongtaphan K, Kasetsinsombat K, Akarasereenont P, Wongkajornsilp A: **Inhibition of UVA-mediated melanogenesis by ascorbic acid through modulation of antioxidant defense and nitric oxide system.** *Arch Pharm Res* 2011, **34:**811–820.
12. Dinkova-Kostova AT, Fahey JW, Wade KL, Jenkins SN, Shapiro TA, Fuchs EJ, Kerns ML, Talalay P: **Induction of the phase 2 response in mouse and human skin by sulforaphane-containing broccoli sprout extracts.** *Cancer Epidemiol Biomarkers Prev* 2007, **16:**847–851.
13. Briganti S, Camera E, Picardo M: **Chemical and instrumental approaches to treat hyperpigmentation.** *Pigment Cell Res* 2003, **16:**101–110.
14. Sapkota K, Park SE, Kim JE, Kim S, Choi HS, Chun HS, Kim SJ: **Antioxidant and antimelanogenic properties of chestnut flower extract.** *Biosci Biotechnol Biochem* 2010, **74:**1527–1533.
15. Shirasugi I, Sakakibara Y, Yamasaki M, Nishiyama K, Matsui T, Liu MC, Suiko M: **Novel screening method for potential skin-whitening compounds by a luciferase reporter assay.** *Biosci Biotechnol Biochem* 2010, **74:**2253–2258.
16. Panich U, Onkoksoong T, Limsaengurai S, Akarasereenont P, Wongkajornsilp A: **UVA-induced melanogenesis and modulation of glutathione redox system in different melanoma cell lines: the protective effect of gallic acid.** *J Photochem Photobiol B* 2012, **108:**16–22.
17. Panich U, Kongtaphan K, Onkoksoong T, Jaemsak K, Phadungrakwittaya R, Thaworn A, Akarasereenont P, Wongkajornsilp A: **Modulation of antioxidant defense by *Alpinia galanga* and *Curcuma aromatica* extracts correlates with their inhibition of UVA-induced melanogenesis.** *Cell Biol Toxicol* 2010, **26:**103–116.
18. Ketsawatsakul U: **Modulation by bicarbonate of the protective effects of phenolic antioxidants on peroxynitrite-mediated cell cytotoxicity.** *Science Asia* 2007, **33:**273–282.
19. Larsson P, Ollinger K, Rosdahl I: **Ultraviolet (UV)A- and UVB-induced redox alterations and activation of nuclear factor-kappaB in human melanocytes-protective effects of alpha-tocopherol.** *Br J Dermatol* 2006, **155:**292–300.
20. Meyskens FL Jr, Farmer P, Fruehauf JP: **Redox regulation in human melanocytes and melanoma.** *Pigment Cell Res* 2001, **14:**148–154.
21. Kapoor IP, Singh B, Singh G, De Heluani CS, De Lampasona MP, Catalan CA: **Chemistry and in vitro antioxidant activity of volatile oil and oleoresins of black pepper (*Piper nigrum*).** *J Agric Food Chem* 2009, **57:**5358–5364.
22. Na M, Bae K, Kang SS, Min BS, Yoo JK, Kamiryo Y, Senoo Y, Yokoo S, Miwa N: **Cytoprotective effect on oxidative stress and inhibitory effect on cellular aging of *Terminalia chebula* fruit.** *Phytother Res* 2004, **18:**737–741.
23. Laupattarakasem P, Houghton PJ, Hoult JR, Itharat A: **An evaluation of the activity related to inflammation of four plants used in Thailand to treat arthritis.** *J Ethnopharmacol* 2003, **85:**207–215.
24. Saleem M, Alam A, Sultana S: **Asafoetida inhibits early events of carcinogenesis: a chemopreventive study.** *Life Sci* 2001, **68:**1913–1921.

doi:10.1186/1472-6882-13-159
Cite this article as: Panich *et al.*: Protective effect of AVS073, a polyherbal formula, against UVA-induced melanogenesis through a redox mechanism involving glutathione-related antioxidant defense. *BMC Complementary and Alternative Medicine* 2013 **13**:159.

Hindawi Publishing Corporation
Evidence-Based Complementary and Alternative Medicine
Volume 2013, Article ID 739473, 10 pages
http://dx.doi.org/10.1155/2013/739473

Research Article

Redox Mechanisms of AVS022, an Oriental Polyherbal Formula, and Its Component Herbs in Protection against Induction of Matrix Metalloproteinase-1 in UVA-Irradiated Keratinocyte HaCaT Cells

Thanyawan Pluemsamran,[1] Pinpat Tripatara,[1] Rattana Phadungrakwittaya,[1] Pravit Akarasereenont,[1,2] Tawee Laohapand,[2] and Uraiwan Panich[1]

[1] *Department of Pharmacology, Faculty of Medicine Siriraj Hospital, Mahidol University, Bangkok 10700, Thailand*
[2] *Center of Applied Thai Traditional Medicine, Faculty of Medicine Siriraj Hospital, Mahidol University, Bangkok 10700, Th iland*

Correspondence should be addressed to Uraiwan Panich; uraiwan.pan@mahidol.ac.th

Received 7 June 2013; Accepted 26 July 2013

Academic Editor: Benny Tan Kwong Huat

Ayurved Siriraj HaRak (AVS022) formula has been used for topical remedy of dermatologic disorders. Oxidative stress induced by ultraviolet (UV) A irradiation could be implicated in photoaged skin through triggering matrix metalloproteinase-1 (MMP-1). We, therefore, explored the antioxidant mechanisms by which AVS022 formulation and its individual components protected against UVA-dependent MMP-1 upregulation in keratinocyte HaCaT cells. TLC analysis revealed the presence of multiple phenolics including gallic acid (GA) in the AVS022 extracts. We demonstrated that pretreatment with the whole formula and individual herbal components except *T. triandra* protected against increased MMP-1 activity in irradiated HaCaT cells. Moreover, all herbal extracts and GA, used as the reference compound, were able to reverse cytotoxicity, oxidant production, glutathione (GSH) loss, and inactivation of catalase and glutathione peroxidase (GPx). *F. racemosa* was observed to yield the strongest abilities to abolish UVA-mediated induction of MMP-1 and impairment of antioxidant defenses including GSH and catalase. Our observations suggest that upregulation of endogenous antioxidants could be the mechanisms by which AVS022 and its herbal components suppressed UVA-stimulated MMP-1 in HaCaT cells. In addition, pharmacological actions of AVS022 formula may be attributed to the antioxidant potential of its components, in particular *F. racemosa*, and several phenolics including GA.

1. Introduction

Demands for alternative medicines including herbal remedies continue to increase. Herbal treatment for dermatologic diseases and cosmetic problems has existed for thousands of years [1]. Ayurved Siriraj HaRak (AVS022) formula, a Th i polyherbal formula consisting of 5 medicinal plants, has been used in Thai traditional medicine for the remedy of skin disorders. Thus, exploring pharmacological activities of the AVS022 polyherbal formula and its constituent herbs is of signific nce in order to gain scientifi evidence on the effic y and safety of traditional herbal medicine. Th AVS022 formula is composed of the root extracts of 5 herbs, *Capparis micracantha* DC., *Clerodendrum indicum* L., *Harrisonia perforata* Merr., *Ficus racemosa* L., and *Tiliacora triandra* (Colebr.) Diels. Previous *in vitro* and *in vivo* studies of *F. racemosa*, a medicinal plant used in Indian ayurvedic medicine, reported that it exerted several pharmacological actions including anti-inflammatory, anticancer, and antioxidant activities [2–4]. Additionally, various phytochemical constituents including racemic acid and alkaloids isolated from *F. racemosa* and *T. triandra*, respectively, which are also the herbal components of AVS022 formula, were demonstrated to possess biological activities [5, 6].

Ultraviolet A (UVA) (315–400 nm) has been recognized as a primary environmental cause of photodamage and

premalignant changes of the skin cells through cytotoxicity of keratinocytes and activation of metalloproteinase-1 (MMP-1), a major collagenolytic enzyme generated by keratinocytes and fibroblasts. Since MMP-1 is contributed to skin cell damage and collagen fragmentation affecting the skin's structural integrity [7], development of dermatological products that effectively suppress MMP-1 at cellular and molecular levels could be a targeting strategy for photoaging prevention. Medicinal plants and phytochemicals including phenolic acids providing antioxidant properties have been observed to abrogate damaging effects of UVA on the skin through inhibition of activity and expression of MMP-1 in keratinocytes or fibroblasts [8–10]. We previously reported that impaired capacity of antioxidant defenses including catalase, glutathione peroxidase (GPx), and glutathione (GSH) involved UVA-stimulated MMP-1 activity, and therefore, upregulation of endogenous antioxidants may represent mechanisms underlying photoprotective effects of phytochemicals [10]. We, thus, assessed antioxidant mechanisms of AVS022 extracts, its 5 plant components, and gallic acid (GA), an antioxidant phenolic present in the formula, in protecting against UVA-dependent cell toxicity and MMP-1 augmentation by assessing cellular oxidant generation, GSH level, and catalase and GPx activities in immortalized human keratinocyte (HaCaT) cells.

2. Materials and Methods

2.1. Materials. Human keratinocyte cell line (HaCaT) from Cell Lines Service (CLS, Heidelberg, Germany) was a kind gift from Professor Pa-thai Yenchitsomanus, Department of Research and Development, Faculty of Medicine Siriraj Hospital, Mahidol University. Dulbecco's modifi d Eagle's media (DMEM) were purchased from Invitrogen (NY, USA), and chemicals and reagents of the highest quality available were obtained from Sigma-Aldrich (MO, USA or Germany).

2.2. Preparation of AVS022 Formula Extracts. AVS022 composed of 20% (w/w) of each herb; *H. perforate*, *C. micracantha*, *C. indicum*, *F. racemosa*, and *T. triandra*, was prepared by Unit of Thai Herbal Pharmaceuticals of Center of Applied Thai Traditional Medicine, Faculty of Medicine Siriraj Hospital, Mahidol University, Tha land. All plant materials were purchased from Tai-hua-jan drugstore and authenticated by two experienced Th i traditional practitioners using macroscopic identific tion and organoleptic techniques which based on anatomical characteristics of the individual plant parts and color, fracture, smell, or taste. Then the specimens were sorted, washed, oven-dried, and crushed. Th powdered drug was extracted by dynamic maceration method. One hundred grams of the powdered herb was weighed and placed in a container with 1L of 80% (v/v) ethanol. Th mixture was constantly stirred with magnetic stirrer for 10 minutes, and then the liquid was filtered and the marcs were pressed. Th clarifie liquid was evaporated under reduced pressure by rotary evaporator and kept frozen overnight prior to lyophilization. The extraction procedure for individual plant was the same with previously referred to procedure. One hundred milligrams of the lyophilized powder was accurately weighed and dissolved in 1 mL of 80% ethanol, mixed, and centrifuged at 15,000 rpm for 10 minutes at 4°C. The sample solution was filtered through a 0.2 μm membrane filter and was used for thin layer chromatography (TLC) analysis.

2.3. TLC Fingerprinting of AVS022 Formula Extracts. Th filtrate of sample solution was loaded to TLC silica gel 60 F 254 (Merck, Germany) using sample applicator (Camag Linomat 5, Switzerland). Solvent system of hexane: ethyl acetate: acetic acid (31: 14 : 5 v/v/v) was used as mobile phase for phenolic separation. The detection was examined under 254 nm UV light and visible light after spraying with fast blue salt (FBS). Th identific tion of phenolics in AVS022 was carried out by comparing its TLC chromatogram with those of phenolic reference markers. Five phenolic reference markers including caffeic acid, ferulic acid, gallic acid, kaempferol, and quercetin were used. The TLC chromatograms showed the presence of caffeic acid, ferulic acid, and GA in the AVS022 extracts, and caffeic acid and GA were detected under both 254 nm UV light and visible light (after spraying with FBS) as shown in Figure 1.

2.4. Cell Cultures and Treatment. HaCaT cells were cultured in DMEM/F12 medium supplemented with 10% fetal bovine serum (FBS) and 1% penicillin (100 units/mL)/streptomycin (100 μg/mL) at 37°C in a humidified air of 5% CO_2 (P_{CO_2} = 40 Torr) (a Forma Scientifi CO_2 Water-Jacketed Incubator). Cells were treated with the AVS022 extract; each component extract or GA used as the reference compound dissolved in 80% ethanol, and the final concentration of ethanol in culture medium did not exceed 0.05% (v/v). To assess photoprotective and antioxidant effects, cells were treated with herbal extracts at concentrations up to 60 μg/mL and GA up to 5 μg/mL for 30 min before UVA (330–400 nm) exposure. UVA intensity verific tion and selection of a UVA dose (4 J/cm^2) and time point afte irradiation were previously described [10]. GA was used as the reference phenolic in this study because it was shown to possess stronger inhibitory activity than that of caff ic acid and ferulic acid against oxidant formation in HaCaT cells exposed to UVA (4 J/cm^2) (data not shown). Assays for cell viability, oxidant formation, GSH content, and antioxidant enzyme activities were carried out at 1 h time point and for MMP-1 activity at 24 h time point after UVA exposure.

2.5. Cell Lysate Preparation. Cells were harvested by centrifugation and lysed with buffer containing 50 mM Tris-HCl, 10 mM ethylene diaminetetraacetic acid (EDTA), 1% (v/v) Triton X-100, phenylmethylsulfonyl fluoride (PMSF) (100 mg/mL), and pepstatin A (1 mg/mL) in DMSO and leupeptin (1 mg/mL) in H_2O, pH 6.8. Th cells were centrifuged at 10,000 rpm for 10 min and the supernatant was then collected. Protein concentration was determined using the Bio-Rad Protein Assay Kit (Bio-Rad, Germany).

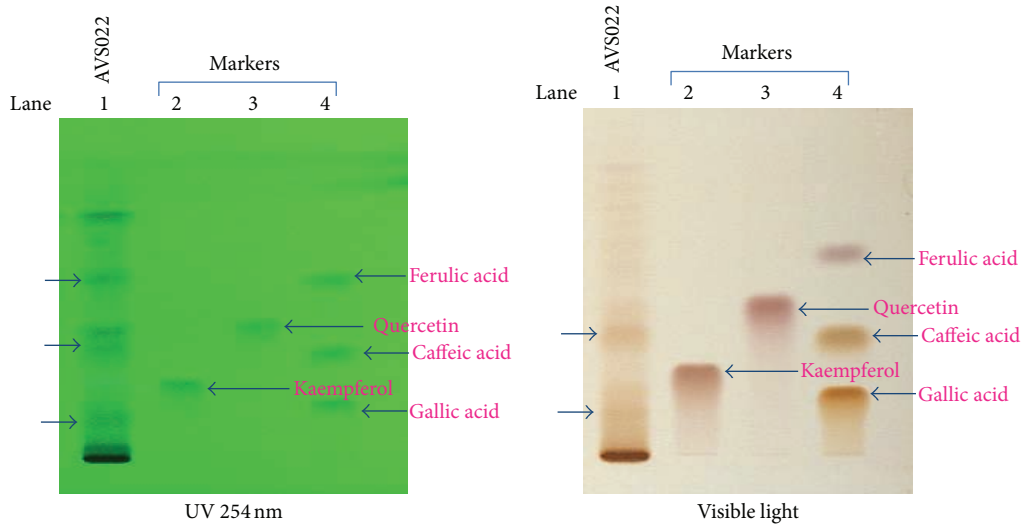

Figur e 1: TLC fingerprinting of AVS022 extracts visualized under UV light (254 nm) (a) and visible light (after spraying with FBS) (b).

2.6. Cell Viability Assay. 3-(4,5-Dimethylthiazol-2-yl)2,2 diphenyltetrazolium bromide (MTT) assay, based on the reduction of the yellow tetrazolium salt to purple formazan, was carried out to identify metabolically viable cells using a spectrophotometer (SpectraMax M2 of Molecular Device, CA, USA). Cell viability was expressed as a percentage of the control (100%, untreated cells without UV exposure).

2.7. MMP-1 Activity Assay by Zymography. Conditioned supernatants were collected for detecting MMP-1 activity using a zymography following the protocol previously reported [10]. Briefly, gelatinase substrate or samples were electrophoresized on nonreducing 10% sodium dodecyl sulphate-polyacrylamide gel electrophoresis (SDS-PAGE) containing gelatin. Then gels were washed twice with 2.5% Triton X-100 to eliminate SDS and allow MMP-1 renaturation. Th gels were then incubated in the reaction buffer containing 50 mM Tris-HCl, pH 8.8, supplemented with 1% Triton X-100, 10 mM $CaCl_2$, 1 μM $ZnCl_2$, and 0.02% Na_3N for 24 h at 37° to generate MMP-1-induced degradation of gelatin. Th gels were stained with 0.006% Coomassie Blue G-250, and gelatinolytic activity of MMP-1 in the gel was visualized as nonstained bands on the blue background. The gels were scanned using a CAMAG TLC scanner (Muttenz, Switzerland), and integrated density of each band was analyzed to determine MMP-1 activity using the ImageMaster software (Hoefer Pharmacia Biotech). Data was represented as arbitrary densitometric units of MMP-1 activity per 1,000,000 cells.

2.8. Assay for Cellular ROS Formation. Dichlorofluorescein (DCFH) assay, based on the oxidation of nonfluorescent DCFH by intracellular ROS to fluorescent 2,7-DCF, was performed to evaluate formation of ROS. After cells were subjected to UVA (4 J/cm^2), cells were incubated in DMEM without phenol red and loaded with 5 μM DCFHDA for 1 h at 37°C. DCF fluorescence intensity was monitored for 30 min at excitation and emission wavelengths of 485 and 530 nm using a spectrofluorometer. Th data are represented as a percentage of ROS production (relative fl orescence units, RFU) of the nontreated control cells without UVA exposure (100%).

2.9. Cellular Glutathione Content Assay. GSH level was measured using the fluorescent probe *o*-phthalaldehyde- (OPA-) based fluorometric method, principally by the reaction of GSH with OPA at pH 8. Th cell extracts were prepared using 6.5% (w/v) trichloroacetic acid (TCA), and the GSH content assay was carried out as described previously [11]. Th GSH content was detected by fluorescence intensity of the GSH-OPA adduct at excitation/emission wavelengths of 350/420 nm. GSH level was calculated using a GSH standard curve and was represented as μM/mg protein.

2.10. Catalase Activity Assay. Catalase activity was measured colorimetrically by following the kit protocol from Cayman chemical (Ann Arbor, MI, USA). In principle, the enzyme reacted with methanol in the presence of H_2O_2 to produce the formaldehyde, which was determined spectrophotometrically at 540 nm using 4-amino-3-hydrazino-5-mercapto-1,2,4-triazole (Purpald). The standard curve was obtained using a formaldehyde standard. One unit of CAT activity was calculated as the amount of enzyme producing 1.0 nmol of formaldehyde per min at 25°C and represented as nmol/min/mg protein.

2.11. Glutathione Peroxidase Activity Assay. GPx activity was assessed by following manufacturer's protocol (Trevigen, Gaithersburg, MD, USA). Th activity was indirectly measured by a coupled reaction with glutathione reductase (GR) causing reduction of oxidized glutathione. Th oxidation of

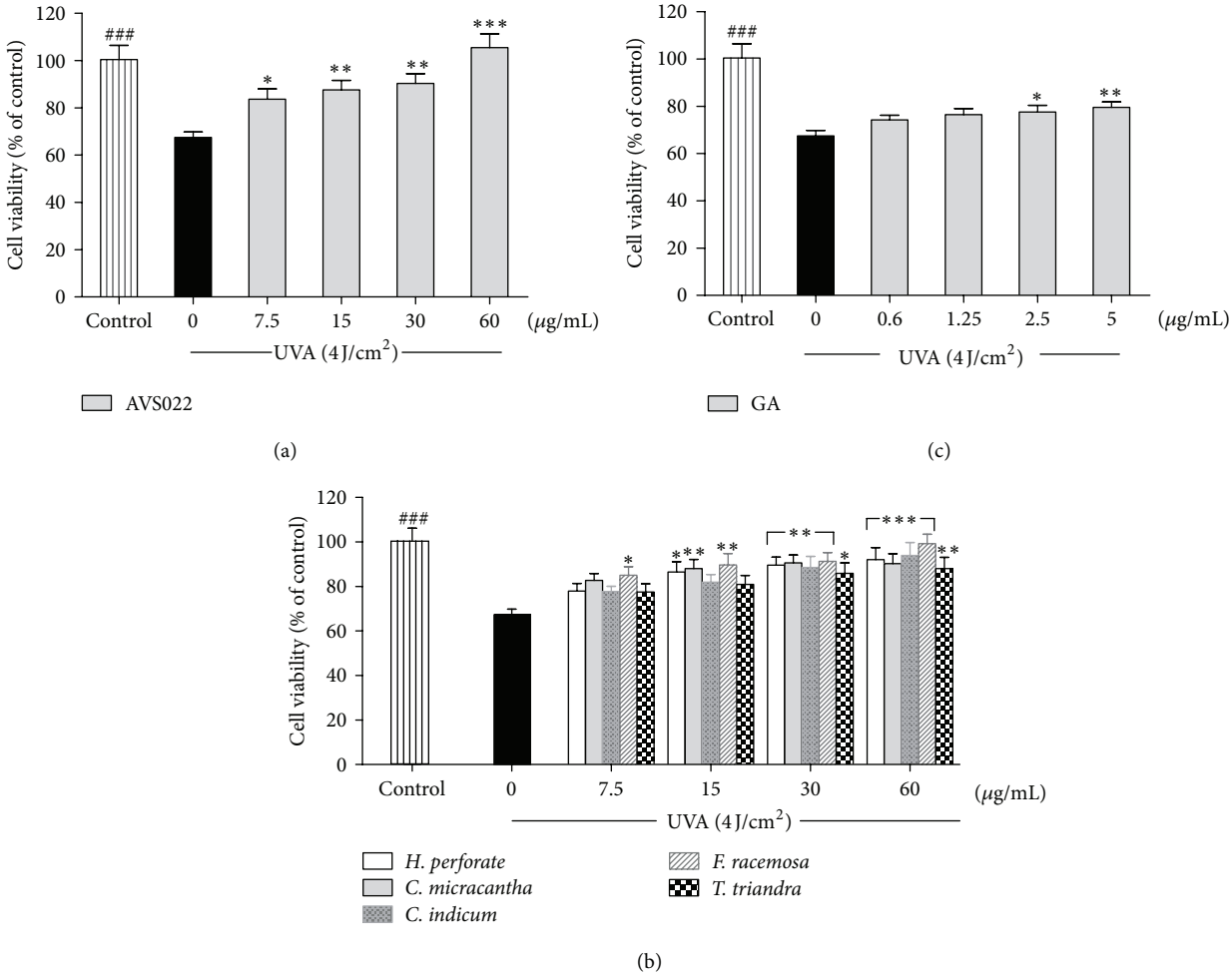

Figure 2: Inhibition of UVA- (4 J/cm^2) induced HaCaT cell toxicity by the whole formula (a) and individual component herbs (b) of AVS022 and GA (c). Data was represented as mean ± SEM. Th statistical signific nce of differences between the control and irradiated cells was assessed by Student's t-test and between UVA-irradiated and herb extracts- or GA-treated cells by one-way ANOVA followed by Dunnett's test. $^{###}P < 0.001$ compared with irradiated cells. $^{*}P < 0.05$; $^{**}P < 0.01$; $^{***}P < 0.001$ compared with nontreated cells exposed to UVA.

NADPH to NADP$^+$ is accompanied by decreased absorbance at 340 nm as previously described [10]. One unit of GPx activity was determined as the amount of enzyme converting 1 nmol of NADPH to NADP$^+$ per min at 25°C and represented as units/mg of protein.

2.12. Statistical Analysis. Data are represented as means ± standard error of the mean (SEM) of separate experiments ($n \geq 3$) conducted on different days. Th significic nce of individual treatment groups compared with irradiated groups was calculated using one-way analysis of variance (ANOVA) followed by Dunnett's test or by independent t-test (Student's; 2 populations) using Prism (GraphPad Software Inc., San Diego, CA, USA).

3. Results

3.1. Inhibition of Cytotoxicity and MMP-1 Activation in Irradiated HaCaT Cells. Treatment of HaCaT with the AVS022 formula and each component herb at concentrations ranging from 7.5 to 60 μg/mL and GA from 0.6 to 5 μg/mL for 24 h without UVA exposure did not result in cytotoxicity (data not shown). Whereas a UVA dose of 4 J/cm^2 caused a substantial decrease in cell viability by 32.95 ± 2.3% ($P < 0.001$) compared to nonirradiated cells, pretreatment with AVS022 (Figure 2(a)), its individual constituents (Figure 2(b)), and GA (Figure 2(c)) was able to signific ntly and dose-dependently hamper cytotoxicity induced by UVA irradiation. In addition, among 5 herbs, *F. racemosa* was observed to yield the greatest cytoprotective effect because it blocked UVA-mediated HaCaT toxicity at lower concentrations (7.5 μg/mL) than those required for the 4 herbs.

We further examined inhibition of UVA-stimulated MMP-1 activity by herb extracts and GA since MMP-1 is a major metalloproteinase for collagen destruction, a hallmark of photoaging. As shown in Figure 3, UVA (4 J/cm^2) markedly stimulated activity of MMP-1 by 206 ± 2.3% ($P < 0.001$) compared to nonirradiated cells, although a

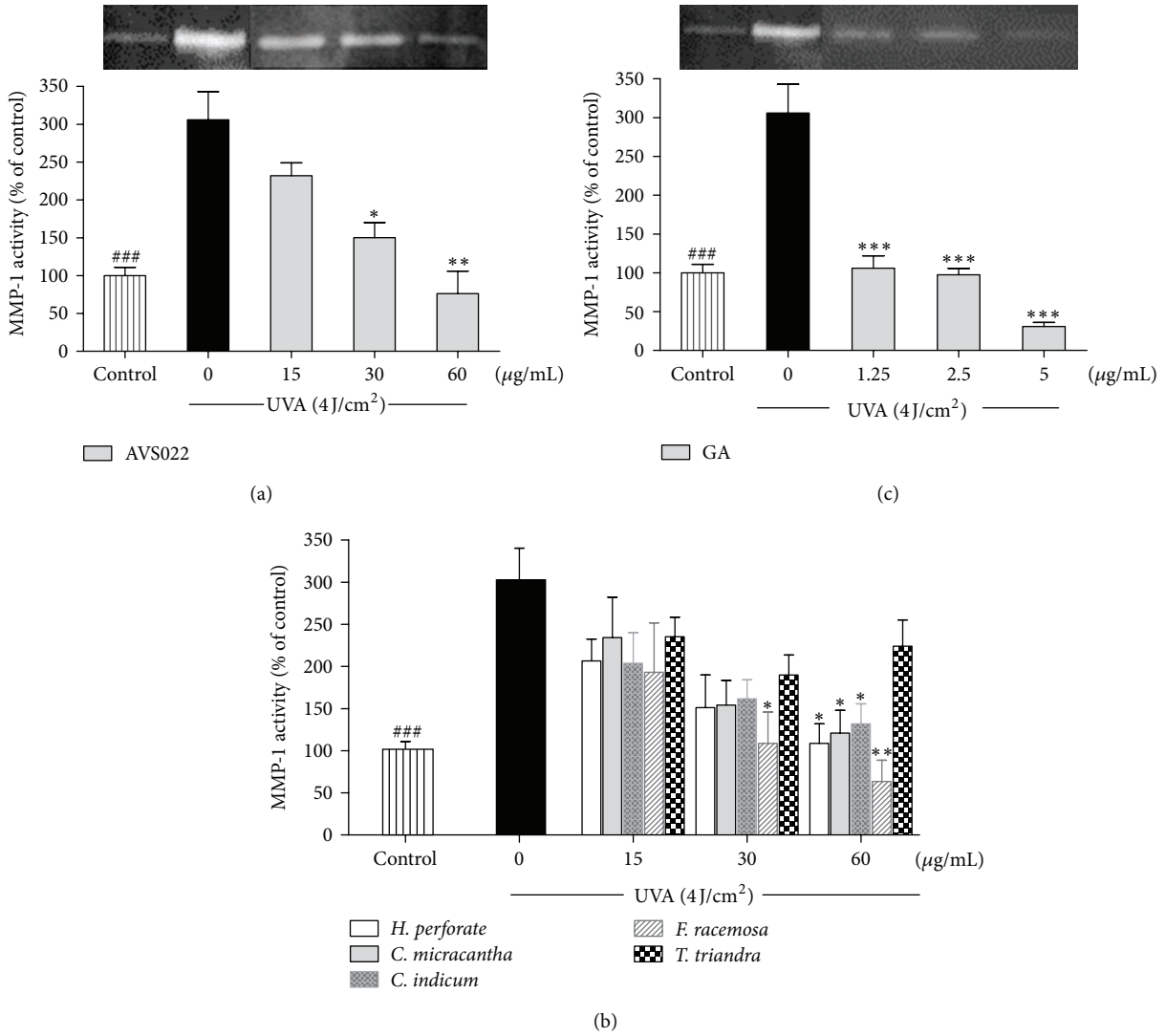

Figure 3: Inhibition of UVA-stimulated MMP-1 activity in HaCaT cells by the whole formula (a) and individual component herbs (b) of AVS022 and GA (c). Zymography analysis of secreted MMP-1 was performed as described in Section 2. Data was represented as mean ± SEM. Th statistical signific nce of differences between the control and irradiated cells was evaluated by Student's t-test and between UVA-irradiated and herb extracts- or GA-treated cells by one-way ANOVA followed by Dunnett's test. $^{###}P < 0.001$ compared with irradiated cells. $^{*}P < 0.05$; $^{**}P < 0.01$; $^{***}P < 0.001$ compared with nontreated cells exposed to UVA.

significant and dose-dependent reduction of MMP-1 activity was observed in HaCaT cells pretreated with the whole formulation of AVS022 (Figure 3(a)), its component herbs but not *T. triandra* (Figure 3(b)), and GA (Figure 3(c)) compared with unpretreated cells following UV irradiation. In agreement with the photoprotective effect on HaCaT cell cytotoxicity, among 5 herb components of AVS022 formula, *F. racemosa* presented the strongest protective activity against UVA-induced enhanced MMP-1 activity since lower concentrations (30 μg/mL) of *F. racemosa* than those of other 4 components were capable of suppressing MMP-1 stimulation.

3.2. Inhibition of ROS Formation and GSH Loss in Irradiated HaCaT Cells. Level of cellular ROS and GSH is an important marker to indicate cellular redox status. We assessed whether redox mechanisms were involved in the inhibitory effects of herb extracts studied and GA on UVA-dependent cytotoxicity and MMP-1 upregulation. Figures 4 and 5 demonstrated that, at 1h postirradiation, UVA exposure (4 J/cm^2) led to a substantial increase in ROS by 38.54 ± 2.1% ($P < 0.001$) and a dramatic decline in GSH level by 49.3 ± 1.3% ($P < 0.001$). In contrast, pretreatment of HaCaT cells with the whole formula (Figures 4(a) and 5(a)) and the individual components of AVS022 (Figures 4(b) and 5(b)) and GA (Figures 4(c) and 5(c)) caused a significant and dose-dependent inhibition of ROS formation and GSH loss as compared to unpretreated cells following UV irradiation. Furthermore, among all 5 components of AVS022, *F. racemosa* was shown to have the highest inhibitory effect on UVA-mediated reduced GSH content because the inhibitory concentrations (7.5 μg/mL) of *F. racemosa* were lower than those required for the 4 herbs.

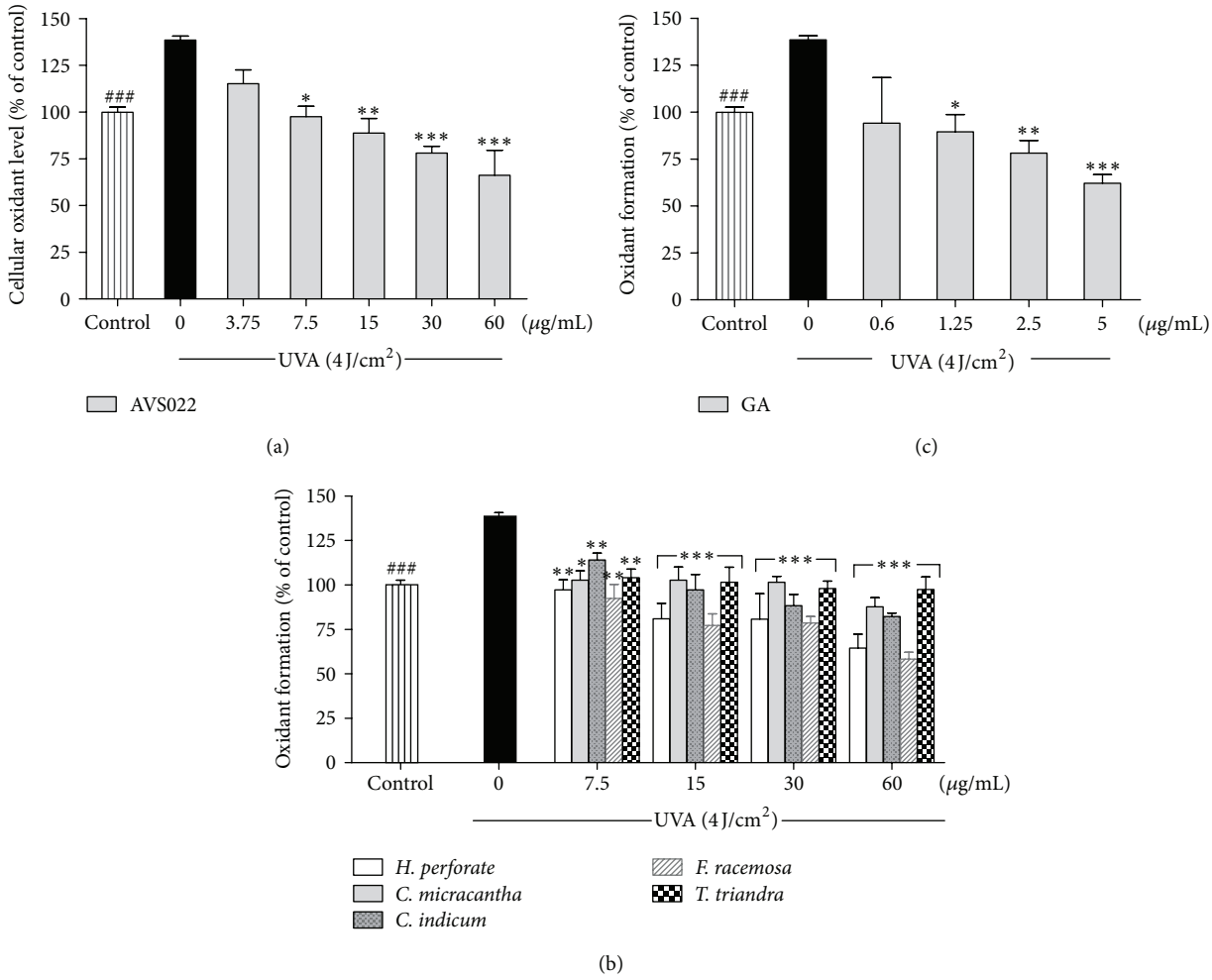

Figure 4: Inhibition of UVA-induced cellular ROS formation in HaCaT cells by the whole formula (a) and individual component herbs (b) of AVS022 and GA (c). The fluorescent DCF as an indicator of ROS formation was measured at 485 nm excitation and 530 nm emission as described in Section 2. Data were represented as a percentage of control (100%, nonirradiated and nontreated cells) using a microplate reader. Th statistical signific nce of differences between the control and irradiated cells was determined by Student's t-test and between UVA-irradiated and herb extracts- or GA-treated cells by one-way ANOVA followed by Dunnett's test. $^{\#\#\#}P < 0.001$ compared with irradiated cells. $^{*}P < 0.05$; $^{**}P < 0.01$; $^{***}P < 0.001$ compared with nontreated cells exposed to UVA.

3.3. Inhibition of Catalase and Glutathione Peroxidase Inactivation in Irradiated HaCaT Cells. To further investigate redox mechanisms of herbal extracts studied and GA with respect to modulation of endogenous antioxidants, as shown in Figures 6 and 7, enzymatic assays revealed that, compared to nonirradiated control cells, UVA (4 J/cm^2) irradiation drastically reduced catalase activity by 43.53 ± 7.7% ($P < 0.001$) and GPx activity by 66 ± 8.4% ($P < 0.001$). Nevertheless, addition of AVS022, each component herb, and GA prior to UVA exposure was able to dose-dependently reverse inactivation of both catalase and GPx compared to irradiated cells in the absence of herb extracts or GA. In agreement with our findings for cytotoxicity, MMP-1 activity, and GSH level, among all 5 components of AVS022, *F. racemosa* was shown to exert the most potent protection against UVA-dependent catalase inactivation.

4. Discussion

Development of herbs employed in a traditional medicine as promising photoprotective agents has gained considerable attention in dermatology research because pharmacologically active phytochemicals identified and isolated from several medicinal plants have been reported to yield antioxidant actions benefici l for the skin [12]. Since UVA irradiation-mediated oxidative stress of the skin is involved in keratinocyte toxicity and activation of MMP-1 accountable for photoaged skin, we, therefore, explored redox mechanisms of the whole formula and individual component herbs of AVS022 and GA, a reference phenolic compound, in protection against UVA-mediated cytotoxicity and MMP-1 induction in keratinocyte HaCaT cells. Our study demonstrated that AVS022, its constituent herbs, and GA significantly abrogated HaCaT cell toxicity mediated by UVA

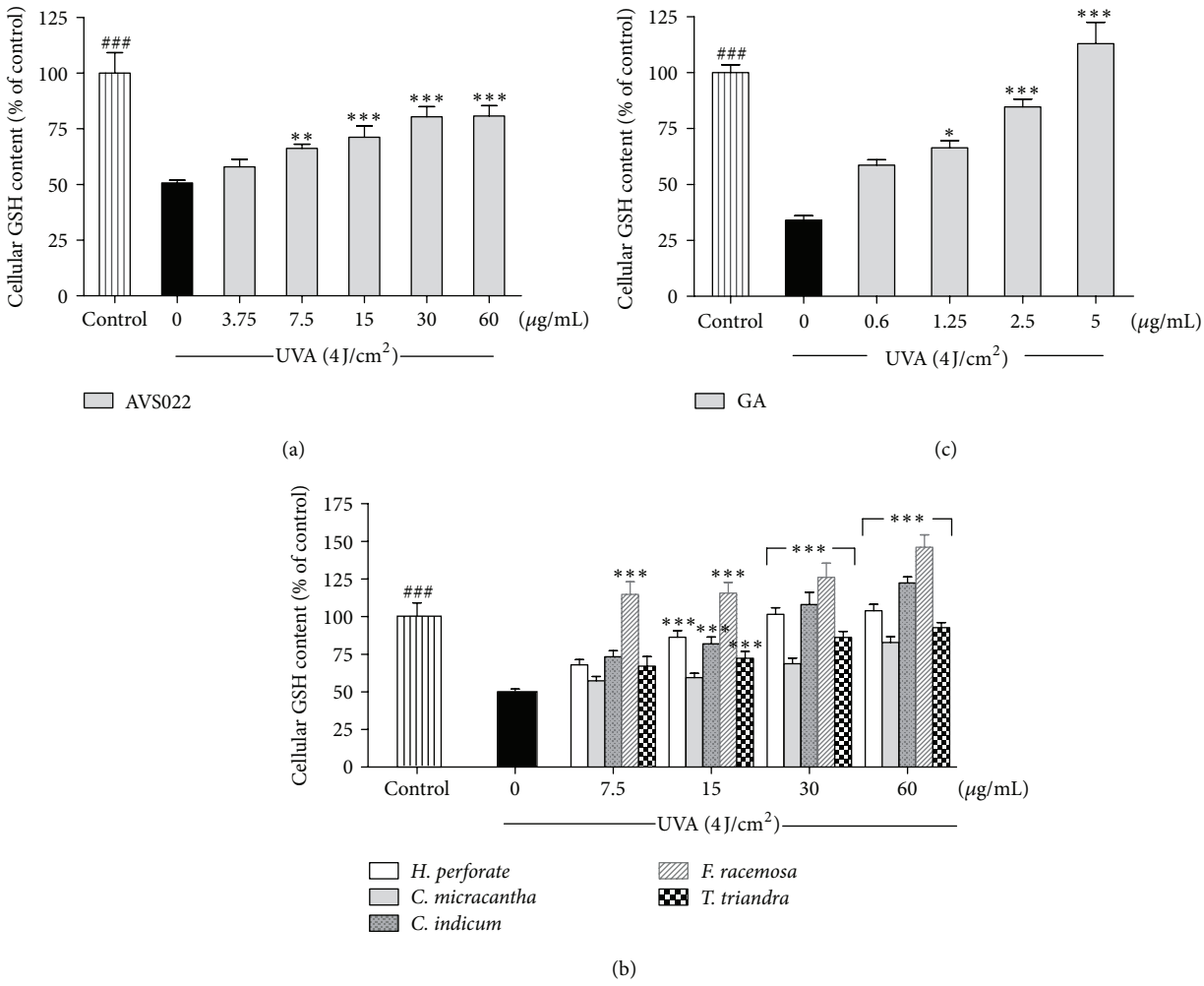

Figur e 5: Inhibition of UVA-dependent GSH loss in HaCaT cells by the whole formula (a) and individual component herbs (b) of AVS022 and GA (c). GSH level was detected by fluorescence intensity of the GSH-OPA adduct at 350 nm excitation and 420 nm emission as described in Section 2. The statistical signific nce of differences between the control and irradiated cells was evaluated by Student's t-test and between UVA-irradiated and herb extracts- or GA-treated cells by one-way ANOVA followed by Dunnett's test. $^{###}P < 0.001$ compared with irradiated cells. $^{*}P < 0.05$; $^{**}P < 0.01$; $^{***}P < 0.001$ compared with nontreated cells exposed to UVA.

(4 J/cm^2). Stimulation of MMP-1 activity by UVA was also suppressed by the whole formula and its individual herbal components except *T. triandra* component of AVS022 and GA. Previous studies reported that photooxidative stress is possibly involved in MMP-1 regulation in skin cells including keratinocytes [13, 14], and improving antioxidant defense system may thus be mechanisms underlying the photoprotective effects of phytochemicals ubiquitously present in medicinal plants. ROS accumulation in photoaged skins has been suggested to associate with increased MMP-1 expression, which could be reversed by promoting capacity of antioxidant defenses including catalase [15], GSH, and GPx [10, 16]. Th y are essential endogenous antioxidant defenses controlling redox balance accountable for protection against photooxidative stress in the keratinocytes and skin carcinogenesis [17, 18], and redox regulation of MMP-1 might, therefore, represent a strategy for photoaging prevention. We further investigated whether protective effects of the whole formula and each component of AVS022 and GA on UVA-mediated increased ROS formation and GSH depletion as well as inactivation of catalase and GPx were involved in the inhibition of MMP-1 activity. Our data indicated that pretreatment of irradiated HaCaT cells with the herbal extracts or GA abolished UVA-dependent GSH depletion and catalase and GPx inactivation.

Since AVS022 is a polyherbal formulation composed of 5 medicinal plants, combinations of multiple active ingredients in different plants can make pharmacological action of AVS022 complex. We, thus, examined the modulation of MMP-1 and antioxidant defense capacity by AVS022 and individual component in our study. Zymographic analysis of MMP-1 activity showed that combination of 5 herbs did not yield synergistic protection against UVA-dependent enhanced MMP-1 activity and the *F. racemosa* component was primarily contributed to biological activities of the AVS022 formula because *F. racemosa* appeared to yield the

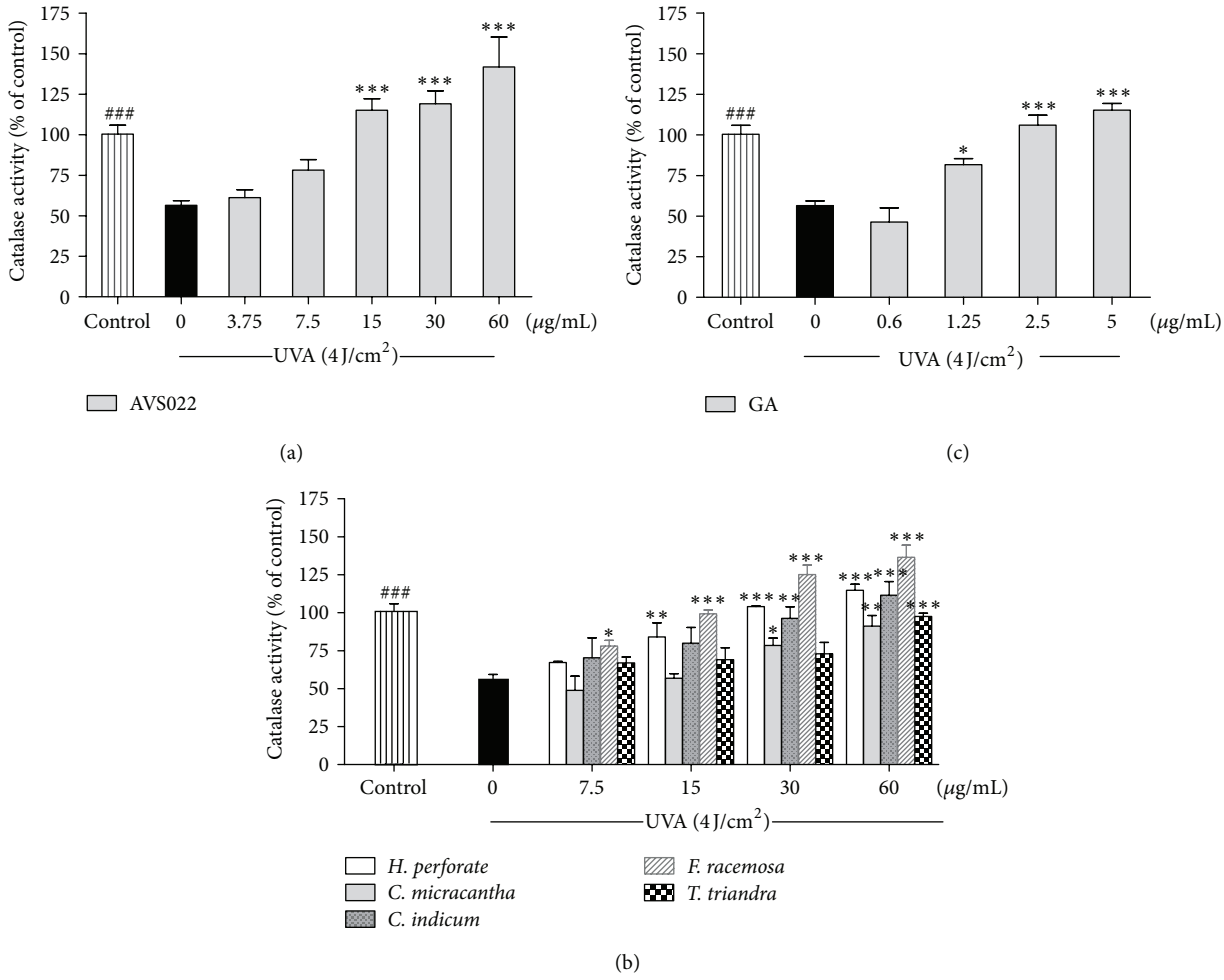

Figur e 6: Inhibition of UVA-mediated catalase inactivation in HaCaT cells by the whole formula (a) and individual component herbs (b) of AVS022 and GA (c). The formaldehyde generated was determined spectrophotometrically with Purpald as a chromogen at 540 nm as described in Section 2. The statistical signific nce of differences between the control and irradiated cells was assessed by Student's t-test and between UVA-irradiated and herb extracts- or GA-treated cells by one-way ANOVA followed by Dunnett's test. $^{###}P < 0.001$ compared with irradiated cells. $^{*}P < 0.05$; $^{**}P < 0.01$; $^{***}P < 0.001$ compared with nontreated cells exposed to UVA.

most potent protective effect on UVA-induced MMP-1 activity. Furthermore, *F. racemosa* exerted the greatest abilities than the other 4 herbs to inhibit cytotoxicity, GSH depletion, and catalase inactivation mediated by UVA irradiation. In accordance with our study on free radical scavenging activity of all 5 herbal components using DPPH (1,1-diphenyl-2-picrylhydrazyl) assay, *F. racemosa* extracts possessed the strongest DPPH radical scavenging activity (data not shown). Our findings also suggested that protection against induction of MMP-1 by UVA appeared to correlate to the abilities of herbal extracts to improve the redox balance as *T. triandra*, which failed to suppress UVA-induced MMP-1 activation, had lower antioxidant activities than *F. racemosa* in restoring antioxidant defense system studied. Moreover, as reported in our previous study showing the protective effects of caff ic and ferulic acids on UVA-dependent MMP-1 stimulation in HaCaT cells, phenolic acids including caffeic, ferulic, and gallic acids identifi d in the AVS022 extracts could be possible active ingredients responsible for the biological activity of AVS022. Our data in this study is also consistent with previous studies for GA in modulation of redox system in different melanoma cell lines [19]. Nevertheless, further investigations concerning qualitative and quantitative analyses of phytochemicals present in the AVS022 formula and its component herbs using analytical techniques with high sensitivity and resolution (e.g., HPLC) are needed in order to identify possible active constituents responsible for photoprotective effects of the plant extracts.

Th mechanisms by which AVS022 extracts suppressed activation of MMP-1 in HaCaT cells exposed to UVA were probably attributed to the attenuation of UVA-mediated ROS accumulation as a result of the augmentation of endogenous antioxidant capacity and did not involve the direct effects of the herbal extracts on the cells because treatment with the formula or each component herbs alone for 30 min in the absence of UVA irradiation did not substantially aff ct MMP-1 activity (data not shown). Additionally, inhibition of UV-induced MMP-1 activity and expression by natural

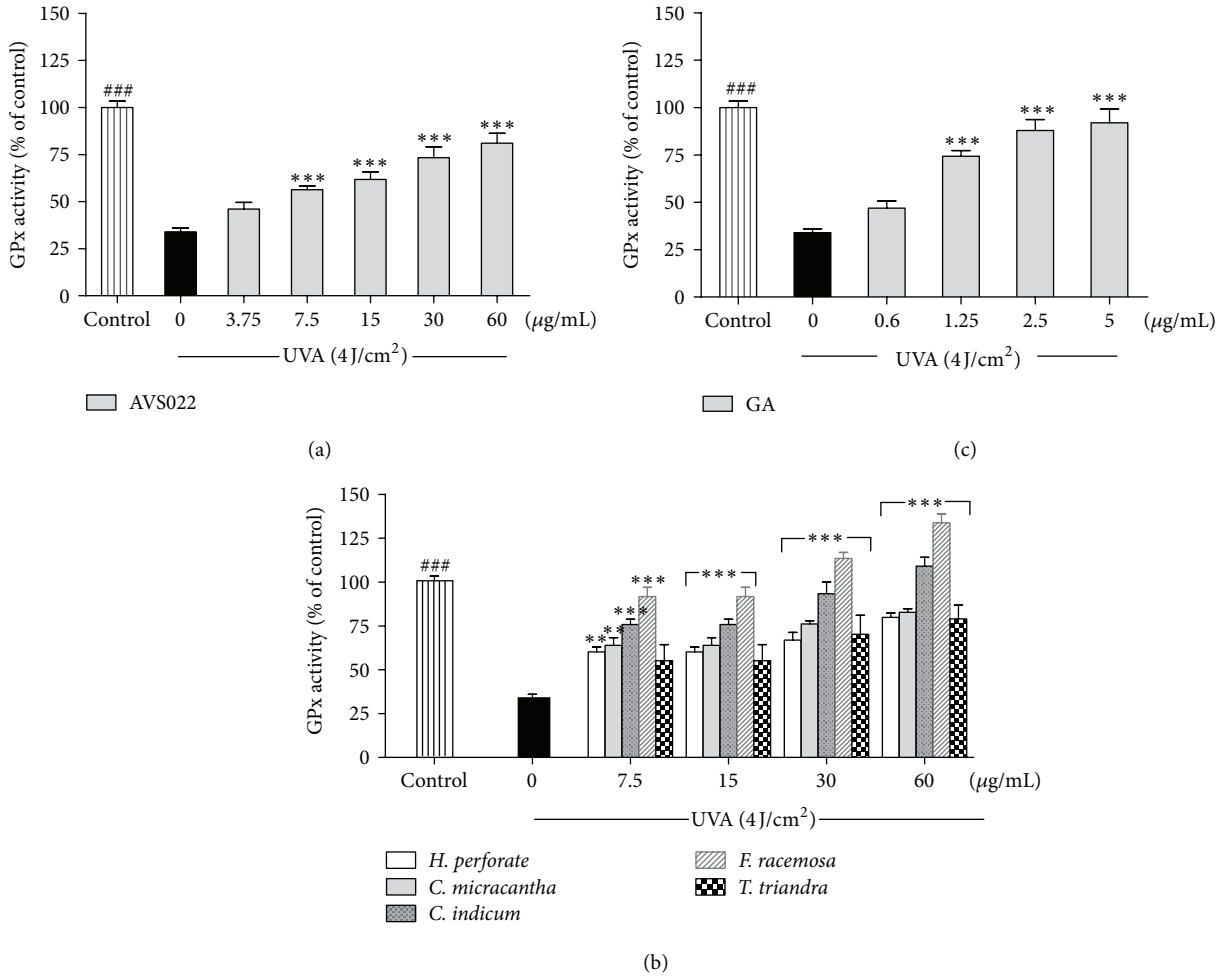

Figur e 7: Inhibition of UVA-dependent GPx inactivation in HaCaT cells by the whole formula (a) and individual component herbs (b) of AVS022 and GA (c). GPx activity was evaluated as described in Section 2. The statistical signific nce of differences between the control and irradiated cells was determined by Student's t-test and between UVA-irradiated and herb extracts- or GA-treated cells by one-way ANOVA followed by Dunnett's test. $^{###}P < 0.001$ compared with irradiated cells. $^{*}P < 0.05$; $^{**}P < 0.01$; $^{***}P < 0.001$ compared with nontreated cells exposed to UVA.

products derived from medicinal plants could be regulated by multiple signal pathways including AP-1 and NF-kappa B transcription factors and MAP kinase [8, 14, 20]. Quercetin, a polyphenol commonly found in diet and medicinal plants, was demonstrated to block photocarcinogenesis in epidermal JB6 cells through downregulation of AP-1, NF-kappa B, and MAPK activities as well as activation of antioxidant transcription factor [21]. Further study is, thus, needed to explore an association between MMP-1 mediated by MAP kinase and redox modulation at molecular levels in keratinocytes exposed to UV irradiation.

In conclusion, protective mechanisms by which AVS022, an oriental herbal formula, and its herbal components exerted inhibitory effects on UVA-induced MMP-1 activity involved regulation of endogenous antioxidants including GSH, catalase, and GPx. Additionally, antioxidant potential of the component herbs, particularly *F. racemosa*, and several phenolic compounds (e.g., GA) may be contributed to the pharmacological actions of AVS022 formula. Thi study could provide pharmacological evidence for polyherbal formula and its constituent herbs. Further identific tion of active compounds to validate biological activities of the formula is needed in order to develop the herbal formula containing antioxidant phytochemicals as effective photoprotective agents.

Conflict of Interests

The authors declare that there is no conflict of interests.

Acknowledgments

This work was supported by Thailand Research Fund (Grants nos. RSA5580012 and DBG5380040) and the "Chalermphrakiat" Grant, Faculty of Medicine Siriraj Hospital, Mahidol University. Appreciation is expressed to Assistant Professor Chanitra Thuwajit, Department of Immunology, Faculty

of Medicine Siriraj Hospital, Mahidol University, for valuable suggestion and support concerning gelatin zymography.

References

[1] J. Koo and S. Arain, "Traditional chinese medicine for the treatment of dermatologic disorders," *Archives of Dermatology*, vol. 134, no. 11, pp. 1388–1393, 1998.

[2] N. Khan and S. Sultana, "Chemomodulatory effect of *Ficus racemosa* extract against chemically induced renal carcinogenesis and oxidative damage response in Wistar rats," *Life Sciences*, vol. 77, no. 11, pp. 1194–1210, 2005.

[3] S. C. Mandal, T. K. Maity, J. Das, B. P. Saba, and M. Pal, "Anti-inflammatory evaluation of *Ficus racemosa* Linn. leaf extract," *Journal of Ethnopharmacology*, vol. 72, no. 1-2, pp. 87–92, 2000.

[4] V. P. Veerapur, K. R. Prabhakar, V. K. Parihar et al., "*Ficus racemosa* stem bark extract: a potent antioxidant and a probable natural radioprotector," *Evidence-Based Complementary and Alternative Medicine*, vol. 6, no. 3, pp. 317–324, 2009.

[5] R. W. Li, D. N. Leach, S. P. Myers, G. D. Lin, G. J. Leach, and P. C. Waterman, "A new anti-inflammatory glucoside from *Ficus racemosa* L," *Planta Medica*, vol. 70, no. 5, pp. 421–426, 2004.

[6] S. Sureram, S. P. D. Senadeera, P. Hongmanee, C. Mahidol, S. Ruchirawat, and P. Kittakoop, "Antimycobacterial activity of bisbenzylisoquinoline alkaloids from *Tiliacora triandra* against multidrug-resistant isolates of *Mycobacterium tuberculosis*," *Bioorganic and Medicinal Chemistry Letters*, vol. 22, no. 8, pp. 2902–2905, 2012.

[7] G. J. Fisher, T. Quan, T. Purohit et al., "Collagen fragmentation promotes oxidative stress and elevates matrix metalloproteinase-1 in fibroblasts in aged human skin," *American Journal of Pathology*, vol. 174, no. 1, pp. 101–114, 2009.

[8] Y. P. Hwang, K. N. Oh, H. J. Yun, and H. G. Jeong, "The flavonoids apigenin and luteolin suppress ultraviolet A-induced matrix metalloproteinase-1 expression via MAPKs and AP-1-dependent signaling in HaCaT cells," *Journal of Dermatological Science*, vol. 61, no. 1, pp. 23–31, 2011.

[9] E. A. Offord, J. C. Gautier, O. Avanti et al., "Photoprotective potential of lycopene, β-carotene, vitamin E, vitamin C and carnosic acid in UVA-irradiated human skin fibroblasts," *Free Radical Biology and Medicine*, vol. 32, no. 12, pp. 1293–1303, 2002.

[10] T. Pluemsamran, T. Onkoksoong, and U. Panich, "Caffeic acid and ferulic acid inhibit UVA-induced matrix metalloproteinase-1 through regulation of antioxidant defense system in keratinocyte HaCaT cells," *Photochemistry and Photobiology*, vol. 88, no. 4, pp. 961–968, 2012.

[11] U. Ketsawatsakul, "Modulation by bicarbonate the protective effects of phenolic antioxidants on peroxynitrite-mediated cell cytotoxicity," *ScienceAsia*, vol. 33, no. 3, pp. 273–282, 2007.

[12] V. M. Adhami, D. N. Syed, N. Khan, and F. Afaq, "Phytochemicals for prevention of solar ultraviolet radiation-induced damages," *Photochemistry and Photobiology*, vol. 84, no. 2, pp. 489–500, 2008.

[13] J. H. Lee, J. H. Chung, and K. H. Cho, "The effects of epigallocatechin-3-gallate on extracellular matrix metabolism," *Journal of Dermatological Science*, vol. 40, no. 3, pp. 195–204, 2005.

[14] M. J. Piao, R. Zhang, N. H. Lee, and J. W. Hyun, "Phloroglucinol attenuates ultraviolet B radiation-induced matrix metalloproteinase-1 production in human keratinocytes via inhibitory actions against mitogen-activated protein kinases and activator protein-1," *Photochemistry and Photobiology*, vol. 88, no. 2, pp. 381–388, 2012.

[15] M. H. Shin, G. E. Rhie, Y. K. Kim et al., "H_2O_2 accumulation by catalase reduction changes MAP kinase signaling in aged human skin in vivo," *Journal of Investigative Dermatology*, vol. 125, no. 2, pp. 221–229, 2005.

[16] G. Park, D. S. Jang, and M. S. Oh, "Juglans mandshurica leaf extract protects skin fibroblasts from damage by regulating the oxidative defense system," *Biochemical and Biophysical Research Communications*, vol. 421, no. 2, pp. 343–348, 2012.

[17] M. Isoir, V. Buard, P. Gasser, P. Voisin, E. Lati, and M. Benderitter, "Human keratinocyte radiosensitivity is linked to redox modulation," *Journal of Dermatological Science*, vol. 41, no. 1, pp. 55–65, 2006.

[18] Y. Zhao, L. Chaiswing, T. D. Oberley et al., "A mechanism-based antioxidant approach for the reduction of skin carcinogenesis," *Cancer Research*, vol. 65, no. 4, pp. 1401–1405, 2005.

[19] U. Panich, T. Onkoksoong, S. Limsaengurai, P. Akarasereenont, and A. Wongkajornsilp, "UVA-induced melanogenesis and modulation of glutathione redox system in different melanoma cell lines: the protective effect of gallic acid," *Journal of Photochemistry and Photobiology B*, vol. 108, pp. 16–22, 2012.

[20] J. Y. Bae, J. S. Choi, Y. J. Choi et al., "(-)Epigallocatechin gallate hampers collagen destruction and collagenase activation in ultraviolet-B-irradiated human dermal fibroblasts: Involvement of mitogen-activated protein kinase," *Food and Chemical Toxicology*, vol. 46, no. 4, pp. 1298–1307, 2008.

[21] M. Ding, J. Zhao, L. Bowman, Y. Lu, and X. Shi, "Inhibition of AP-1 and MAPK signaling and activation of Nrf2/ARE pathway by quercitrin," *International Journal of Oncology*, vol. 36, no. 1, pp. 59–67, 2010.

Comparative Evaluation of Antityrosinase and Antioxidant Activities of Dietary Phenolics and their Activities in Melanoma Cells Exposed to UVA

Weerawon Thangboonjit, M.D., Saowalak Limsaeng-u-rai, B.Sc. Thanyawan Pluemsamran, B.Sc., Uraiwan Panich, M.D., Ph.D.
Department of Pharmacology, Faculty of Medicine Siriraj Hospital, Mahidol University, Bangkok 10700, Thailand.

ABSTRACT

Background: Dietary phenolics have been shown to possess antityrosinase and antioxidant properties which account for their pharmacological effect against ultraviolet (UV)-mediated skin pigmentation. Hence, this study assessed the correlation between antityrosinase and antioxidant activities of various phenolic acids including caffeic acid (CA), ferulic acid (FA), gallic acid (GA), *p*-coumaric acid (PA) and quercetin using cell-free systems including mushroom tyrosinase and DPPH (1,1-diphenyl-2-picrylhydrazyl) assays and human melanoma (G361) cell culture model.

Methods: Antityrosinase and free radical (FR) scavenging activities of all test phenolics were determined using mushroom tyrosinase and DPPH assays, respectively. Inhibition of cellular melanogenesis with regard to regulation of intracellular oxidant formation and glutathione (GSH) content was assessed in UVA-irradiated G361 melanoma cells.

Results: The IC_{30} values for the mushroom tyrosinase inhibition activity showed a rank order of quercetin ≈ PA > kojic acid (KA) ≈ CA ≈ FA > GA. For the FR scavenging activity, IC_{30} values demonstrated a rank order of GA ≈ CA ≈ FA > quercetin > PA ≈ KA. In addition, both CA and FA were observed to suppress UVA-induced tyrosinase activity and melanin content in G361 cells, although CA exerted greater antimelanogenic effect than FA. Pretreatment with CA was also able to reduce oxidant generation and restore GSH content in irradiated cells.

Conclusion: Cell-free systems showed that antityrosinase activity of test phenolics was not associated with their FR scavenging activity. Moreover, we have herein reported the correlation between depigmenting effect and antioxidant action of CA in G361 cells.

Keywords: Phenolic acids, antioxidant, tyrosinase, melanogenesis, glutathione

Siriraj Med J 2014;66:5-10
E-journal: http://www.sirirajmedj.com

INTRODUCTION

Dietary phenolics have been attractive for dermatology research since they possess powerful antioxidant properties, which might be responsible for their inhibitory effect on skin hyperpigmentation. Melanin plays an essential role in protection against UV irradiation-induced skin damage, although abnormal accumulation of melanin can result in dermatologic problems including malignant melanoma and cosmetic concern. Recently, an underlying mechanism of melanogenesis involved in oxidative stress has been proposed[1] and attempts have thus been made to investigate the antimelanogenic effect of natural products-derived antioxidant properties. Tyrosinase is a copper-containing monooxygenase which accounts for melanin formation in melanocytes and/or melanoma cells and so has become a key target for screening of novel whitening agents. Cell-free system assays of antityrosinase and FR scavenging activities are spectrophotometric methods which have been widely employed to screen promising whitening and antioxidant agents, respectively, because such techniques are sensitive, rapid, convenient and inexpensive.[2,3]

UVA has been postulated to contribute to skin pigmentation through oxidative stress, which takes place when there is an increase in cellular oxidant production.[4]

Correspondence to: Uraiwan Panich
E-mail: uraiwan.pan@mahidol.ac.th
Received 13 March 2013
Revised 28 November 2013
Accepted 1 July 2013

Moreover, previous reports have suggested that compounds having abilities to inhibit oxidative stress would be useful in regulation of melanogenesis through mitigating tyrosinase activity and melanin synthesis.[5,6] Since antioxidant action of putative whitening agents may be involved in their antityrosinase effects, the objective of our study was therefore to investigate the correlation between antityrosinase and antioxidant activities of various phenolic acids including caffeic acid (CA), ferulic acid (FA), gallic acid (GA), *p*-coumaric acid (PA) and quercetin as well as kojic acid (KA), a well-known tyrosinase inhibitor (Fig 1). Different classes of phenolics were tested in this study. CA, FA and PA are cinnamic acid derivatives, GA is a benzoic acid derivative and quercetin is a flavonoid. Cell-free systems including mushroom tyrosinase and DPPH (1,1-diphenyl-2-picrylhydrazyl) assays and human melanoma (G361) cells irradiated with UVA were used to evaluate antityrosinase and antioxidant actions of test phenolics.

MATERIALS AND METHODS

Materials

Chemicals and reagents of the highest quality available were used and obtained from Sigma-Aldrich (MO, USA or Germany). Human melanoma cell lines (G361) from American Type Culture Collection (ATCC, Rockville, MD, USA) was a kind gift from Assoc. Prof. Tengamnuay, Faculty of Pharmaceutical Sciences, Chulalongkorn University. Cell culture medium and reagents were purchased from Invitrogen (NY, USA).

Mushroom tyrosinase assay

The activity of mushroom tyrosinase was assayed as previously described[1] using L-3,4-dihydroxyphenylalanine (L-DOPA) as a substrate and KA was used as a reference compound. The sample solution (20 μl) and mushroom tyrosinase (40 μl) in 20 mM phosphate buffer (480 units/ml) were added to PBS (120 μl, 20 mM) in a 96-well plate. The reactions were initiated by adding L-DOPA (20 μl) and the reaction mixture was further incubated for 5 min at 25°C. Then, the optical density (OD) of the reaction mixture, which was proportional to the amount of dopachrome produced, was determined at 470 nm. The percentage inhibition of tyrosinase activity was calculated using the following equation; [1-(C-D)/(A-B)] x 100, in which A represents the OD of the reaction mixture containing the enzyme without the test sample, B represents the OD of PBS only, C represents the OD of the reaction mixture containing the enzyme and the test sample and D represents the OD of the reaction mixture containing the test sample without the enzyme.

Measurement of free radical scavenging activity

DPPH is a stable free radical commonly used to determine FR scavenging activity.[13] Briefly, test samples (100 μL) in 80% ethanol were added to a solution of 0.2% (w/v) DPPH radical (100 μL) in ethanol in a 96-well plate. The absorbance was monitored spectrophotometrically at 520 nm at 0 and 15 mins by a microplate reader. The FR scavenging activity was evaluated as a decrease in the absorbance of DPPH radical and the scavenging activity percentage was calculated using the equation; $[(A_0\text{-}A_{15})/Ac] \times 100$, in which A_0 is the absorbance of the test sample at 0 min, A_{15} is the absorbance of the test sample at 15 mins and Ac is the absorbance of the control sample at 0 min.

Treatment of cells with phenolic acids and UVA irradiation

Human melanoma G361 cells were maintained in DMEM supplemented with 10% fetal bovine serum and antibiotic solution [1% penicillin (100 units/ml)-streptomycin (100 μg/ml)] at 37°C in humidified air containing 5% CO_2 (P_{CO2} = 40 Torr) (a Forma Scientific CO_2 Water Jacketed Incubator). G361 cells were seeded at 0.5×10^6 cells/well in a 24-well plate for all cell-based assays used to study cellular tyrosinase activity, melanin content, cellular GSH level and oxidant formation. In all cell-based assays, the cells were treated with CA or FA for 30 mins in the PBS before cells were subjected to UVA (320-400 nm) irradiation. The cells were irradiated with UVA light for 5 mins 43 s or 11 mins 26 s to achieve a single UVA dose of 8 J/cm^2 or 16 J/cm^2, respectively.[6] The source of UVA was an xenon arc lamp (Dermalight ultrA1; Hoenle, Germany). The UVA dose of 8 J/cm^2 was applied in our study except for melanin content since such dose did not markedly enhance melanin formation and thus the dose of 16 J/cm^2 was chosen. Moreover, the UVA doses applied in this study were physiologically relevant and did not affect G361 cell viability[6]. The cells were harvested for the assays at 1 h after UV irradiation and cell lysates were prepared using lysis buffer containing 50 mM TrisHCl, 10 mM ethylene diaminetetraacetic acid (EDTA), 1% (v/v) Triton X100, phenylmethylsulfonyl fluoride (PMSF) (100 mg/ml) and pepstatin A (1 mg/ml) in DMSO, and leupeptin (1 mg/ml) in H2O, pH 6.8[1].

Cellular tyrosinase activity assay

Tyrosinase activity was determined by assessing the rate of L-DOPA oxidation to dopachrome as described previously.[1,13] Briefly, cell lysate (90 μl) was loaded onto a 96-well plate and 20 mM L-DOPA (10 μl) was added as the substrate to induce the reaction. Conversion of L-DOPA to dopachrome was measured spectrophotometrically at 475 nm every 10 mins for 1 h at 37°C by a microplate reader. The data have been shown as a percentage of the tyrosinase activity (unit/mg protein) of untreated and non-irradiated control cells (100%).

Melanin content assay

For evaluation of melanin synthesis as described previously,[14] the cell pellets were solubilized in 1 M NaOH and the optical density was measured at 475 nm using a microplate reader. The results were expressed as a percentage of the melanin content (μg/mg protein) of untreated and non-irradiated control cells (100%).

Measurement of intracellular glutathione content

GSH content was evaluated using the fluorescent

probe *o*-phthalaldehyde (OPA) reacting with GSH at pH 8 as previously described[6]. After cells were subjected to UVA irradiation, cells were lysed with 6.5% (w/v) trichloroacetic acid (TCA). The TCA extracts were loaded onto 96-well plates together with buffer (100 mM KH_2PO_4, 10 mM EDTA and 1 mM NaOH) and then OPA (1 mg/ml in methanol). The fluorescence was determined at 350 nm excitation and 420 nm emission. The GSH levels were calculated by comparing with standard curves using known concentrations of GSH. The results have been shown as a percentage of the GSH content (nmol/mg of protein) of the untreated and non-irradiated control cells (100%).

Determination of protein content

The total protein concentration of cell lysates was determined using the Bio-Rad Protein Assay Kit (Bio-Rad, Germany).

Determination of intracellular oxidant formation

2′, 7′-Dichlorodihydrofluorescin diacetate (DCFH-DA), a stable and non-fluorescent dye, was used to determine oxidant formation in G361 cells as previously demonstrated.[6] After cells were irradiated with UVA, cells were treated with phenol red-free DMEM containing 5 μM DCFHDA for 1 h. DCF fluorescence was determined for 20 mins at 485 nm excitation and 530 nm emission using a spectrofluorometer. The data have been shown as a percentage of intracellular oxidant formation (relative fluorescence units/RFU) of the untreated and non-irradiated control cells (100%).

Statistical analysis

Data are represented as means ± standard error of the means (SEM) from at least 3 independent experiments. The statistical significance of differences between the control and UVA-irradiated cells was evaluated by Student's *t*-test and between UVA-irradiated and phenolic-treated cells by one-way analysis of variance (ANOVA) followed by Tukey's *post hoc* test.

RESULTS

Mushroom tyrosinase inhibitory activity and FR scavenging activity of phenolics

All test phenolics including CA, FA, GA, PA and quercetin (7.5-120 μM) as well as positive control, KA, were shown to exert a dose-dependent protection against mushroom tyrosinase-mediated oxidation of L-DOPA. The IC_{30} value in Table 1 showed a rank order of quercetin ≈ PA > KA ≈ CA ≈ FA > GA for the inhibition of mushroom tyrosinase activity. Additionally, DPPH assay was performed to determine FR scavenging activity of the studied compounds. Based on the IC_{30} values, the rank order of the DPPH radical scavenging activity of the compounds was GA ≈ CA ≈ FA > quercetin > PA ≈ KA.

The effects of CA and FA on UVA-induced tyrosinase activity and melanin synthesis

Since CA and FA exerted powerful FR scavenging activity, they were then chosen for study of their inhibitory effects on UVA-mediated increased melanogenesis in G361 melanoma cells. The cytotoxicity of CA and FA on G361 cells was also assessed by MTT assay. We observed that treatment of the cells with CA and FA up to 120 μM for 24 h did not affect cell viability, indicating that protection by test phenolics against UVA-mediated melanogenesis was not due to reduction in cell numbers.

UVA irradiation led to 49.1 ± 6% ($p < 0.001$) and 36.6 ± 4.2% ($p < 0.001$) induction in tyrosinase activity and melanin content, respectively (Fig 2). However, pretreatment of UVA-irradiated cells with CA and FA

TABLE 1. IC_{30} values of the phenolics for mushroom tyrosinase inhibitory activity and FR scavenging activity.

Test compounds	IC_{30} (μM)	
	Antityrosinase activity	FR scavenging activity
Caffeic acid	$43.09 \pm 2.3^{\#\#\#}$	$14.85 \pm 3.9^{***}$
Ferulic acid	$51.85 \pm 1.7^{\#\#}$	$11.97 \pm 0.6^{***}$
Gallic acid	79.89 ± 6.5	$7.0 \pm 0.5^{***}$
Quercetin	$22.43 \pm 1.5^{*,***}$	$74.23 \pm 9.7^{\#\#\#}$
p-coumaric acid	$22.86 \pm 2.1^{*,***}$	> 120
Kojic acid	$42.78 \pm 6.5^{\#\#\#}$	> 120

For antityrosinase activity: *p<0.05 compared with CA and KA. ***p<0.001 compared with FA and GA. ##p<0.01; ###p<0.001 compared with GA. For FR scavenging activity: ***p<0.001 compared with quercetin, PA and KA. ###p<0.001 compared with PA and KA.

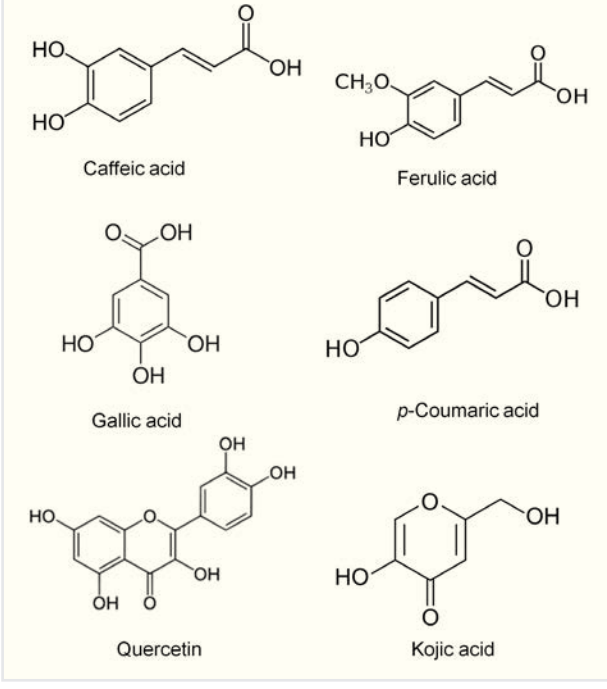

Fig 1. Chemical structure of test phenolics.[7-12]

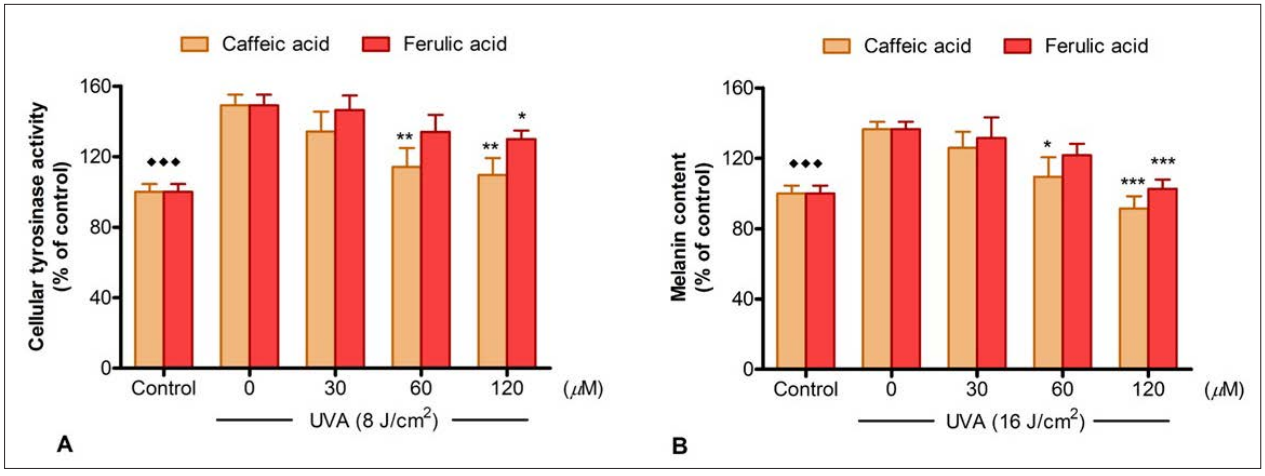

Fig 2. Protection by CA and FA against UVA-mediated melanogenesis in G361 cells. Cellular tyrosinase activity (A) and melanin formation (B) induced by a single dose of UVA at 8 or 16 J/cm^2, respectively. ♦♦♦ $p < 0.001$ compared with UVA-irradiated cells. *$p < 0.05$; **$p < 0.01$; ***$p < 0.001$ compared with untreated cells exposed to UVA.

resulted in a substantial decline in tyrosinase activity (Fig 2A) and melanin content (Fig 2B) in a concentration-dependent manner. Our data also showed that CA had a greater antimelanogenic effect than that of FA since a lower dose of CA was required to prevent induction of tyrosinase activity and melanin content in irradiated cells.

The effects of CA on UVA-induced oxidant formation and GSH content

Protection by CA against oxidant formation and GSH loss in UVA-irradiated G361 cells was then assessed because it was more potent than FA in inhibiting UVA-mediated melanogenesis. Irradiation of cells by a UVA dose of 8 J/cm^2 produced a 67.6 ± 7.2% (p<0.001) augmentation of oxidant formation compared to non-UVA-irradiated cells, although pretreatment with CA led to a dose-dependent decrease in cellular oxidant level in response to UVA irradiation (Fig 3A). In addition, while exposure of the cells to UVA irradiation (8 J/cm^2) substantially reduced GSH content by 45.98 ± 6.2% ($p < 0.001$) compared to non-irradiated cells, pretreatment with CA significantly blocked GSH depletion in a concentration-dependent manner (Fig 3B).

DISCUSSION

Screening for antityrosinase properties of various phenolic compounds possessing antioxidant actions has gained a lot of attention in order to develop putative whitening agents. Several reports have suggested that compounds yielding antioxidant properties could also serve as potential antityrosinase agents capable of blocking melanin synthesis.[6,15] GA, CA and FA are phenolic acids naturally present in a variety of medicinal plants used for skin problems including hyperpigmentation, probably, through their antioxidant actions.[16-19] Therefore, we carried out comparative *in vitro* evaluation of antityrosinase and antioxidant activities of several natural phenolics. By using cell-free system models, our data showed that protection by the test phenolics against mushroom tyrosinase activity were not correlated with their FR scavenging activities because GA possessed lower inhibitory effects

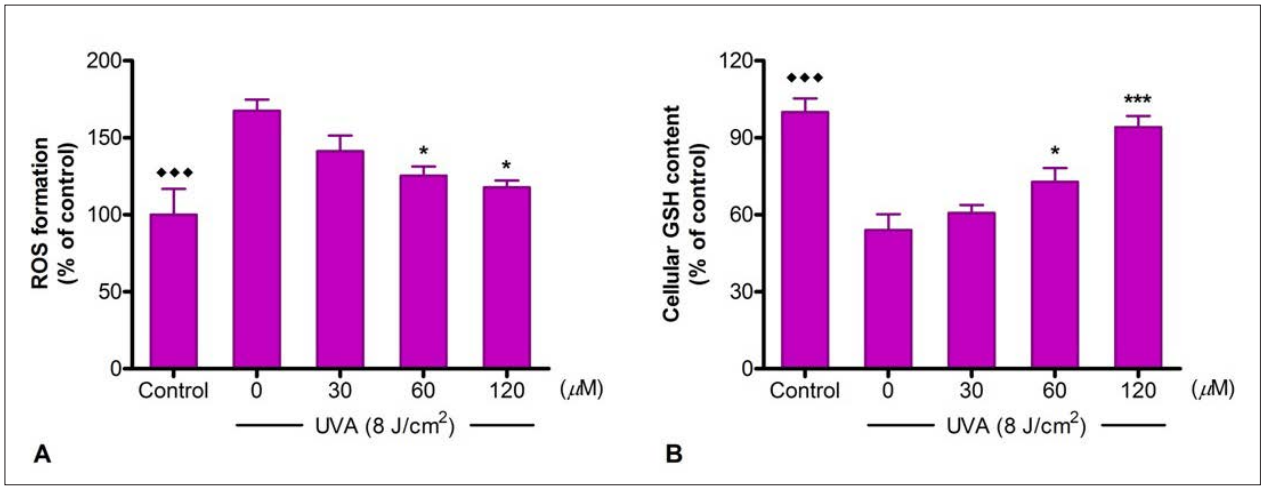

Fig 3. Protection by CA against UVA-mediated oxidant formation and GSH loss in G361 cells. Cellular oxidant formation (A) and GSH content (B). ♦♦♦ $P < 0.001$ compared with UVA-irradiated cells. *p<0.05; **p<0.01; ***p<0.001 compared with untreated cells exposed to UVA.

on mushroom tyrosinase than quercetin, PA, CA and FA, while it yielded greater FR scavenging activity than quercetin and PA. Furthermore, CA and FA were demonstrated to possess antityrosinase and antioxidant activity, while our findings in the mushroom tyrosinase assay did not relate to that observed in cellular tyrosinase study. CA and FA were shown to have comparable inhibitory activities against mushroom tyrosinase and DPPH free radicals in a cell-free system, whereas CA provided greater protective effect than FA on UVA-mediated melanogenesis in G361 cells. Furthermore, our previous study showed that GA, which yielded lower abilities to inhibit mushroom tyrosinase than CA and FA in this study, was more effective than CA and FA in inhibiting UVA-mediated cellular melanogenesis as a lower concentration of GA (15 μM) than that of CA (60 and 120 μM) and FA (120 μM) was required to reduce tyrosinase activity and melanin content in UVA-irradiated G361 cells.[19]

Tyrosinase catalyzes two distinct rate-limiting steps in melanin biosynthesis; the hydroxylation of tyrosine to L-DOPA and the oxidation of L-DOPA to DOPAquinone, a highly reactive o-quinone, readily converted to dopachrome eventually leading to melanin production involving a series of complex chemical reactions including oxidation-reduction reactions.[20] Antityrosinase properties of depigmenting compounds may be attributed to different actions including competitive inhibition at the copper catalytic site of tyrosinase and non-competitive inhibition against L-DOPA oxidation, reduction of *o*-quinone to prevent dopachrome formation and detoxification of ROS involved in melanin formation.[21,22] Therefore, compounds that are effective in inhibition of mushroom tyrosinase activity may not serve as powerful FR scavengers. Well-known tyrosinase inhibitors including arbutin, hydroquinone and KA are competitive tyrosinase inhibitors, but are not represented as strong FR scavengers. Our study confirmed that while KA had a greater ability than GA to inhibit mushroom tyrosinase activity, its FR scavenging activity was weaker than that of GA. Therefore, developing dietary phenolics as candidate and effective depigmenting agents is promising since they could have a potential to interfere with various steps of melanin formation.

UVA irradiation-mediated GSH depletion has been proposed to be responsible for abnormal melanogenesis.[6,19] Our study demonstrated that the antimelanogenic effect of CA was associated with its ability to restore redox balance through upregulation of GSH content in the irradiated cells. Indeed, inhibitory activity of phenolics against mushroom tyrosinase appeared to be uncorrelated with that against cellular melanogenesis. It is probably because of different depigmenting mechanisms involving various targets such as direct inhibition of tyrosinase activity, transcriptional and/or translational regulations of tyrosinase, chemical reactions involved in melanin formation, melanosome transfer and/or distribution, melanocyte viability and abilities of a compound to permeate into the cells, these account for their intracellular availability and activity.[23-25] Our observations were consistent with previous studies reporting that while citrus fruit extract exhibited a weak inhibitory activity against mushroom tyrosinase, it was capable of protection against melanogenesis in both cultured B16 melanoma cells and brown guinea pig skin exposed to UVB.[26]

Therefore, suppression of melanogenesis cannot be attributed to inhibitory activity against tyrosinase or antioxidant activity alone. Furthermore, model systems and cell types employed should be taken into consideration when assessing antityrosinase properties of depigmenting agents.

ACKNOWLEDGMENTS

Appreciation is expressed to the Thailand Research Fund (Grant no. RSA5580012) and the "Chalermphrakiat" Grant, Faculty of Medicine Siriraj Hospital, Mahidol University for research funding and support.

REFERENCES

1. Panich U, Tangsupaanan V, Onkoksoong T, Kongtaphan K, Kasetsinsombat K, Akarasereenont P, Wongkajornsilp A. Inhibition of UVA-mediated melanogenesis by ascorbic acid through modulation of antioxidant defense and nitric oxide system. Arch Pharm Res. 2011 May;34(5):811-20.
2. Magalhaes LM, Segundo MA, Reis S, Lima JL. Methodological aspects about *in vitro* evaluation of antioxidant properties. Anal Chim Acta. 2008 Apr 14;613(1):1-19.
3. Seo SY, Sharma VK, Sharma N. Mushroom tyrosinase: recent prospects. J Agric Food Chem. 2003 May 7;51(10):2837-53.
4. Jiang S, Liu XM, Dai X, Zhou Q, Lei TC, Beermann F, et al. Regulation of DHICA-mediated antioxidation by dopachrome tautomerase: implication for skin photoprotection against UVA radiation. Free Radic Biol Med. 2010 May 1;48(9):1144-51.
5. Chou TH, Ding HY, Hung WJ, Liang CH. Antioxidative characteristics and inhibition of alpha-melanocyte-stimulating hormone-stimulated melanogenesis of vanillin and vanillic acid from *Origanum vulgare*. Exp Dermatol. 2010 Aug;19(8):742-50.
6. Panich U, Kongtaphan K, Onkoksoong T, Jaemsak K, Phadungrakwittaya R, Thaworn A, et al. Modulation of antioxidant defense by *Alpinia galanga* and Curcuma aromatica extracts correlates with their inhibition of UVA-induced melanogenesis. Cell Biol Toxicol. 2010 Apr;26(2):103-16.
7. Caffeic acid [image on the internet]. 2008 Sep 5; cited 2012 Dec 12. Available from: http://en.wikipedia.org/wiki/File:Kaffees%C3%A4ure.svg#file
8. *p*-Coumaric acid [image on the internet]. 2007 Apr 1; cited 2012 Dec 12. Available from: http://en.wikipedia.org/wiki/File:Coumaric_acid_acsv.svg
9. Ferulic acid [image on the internet]. 2007 Apr 1; cited 2012 Dec 12. Available from: http://en.wikipedia.org/wiki/File:Ferulic_acid_acsv.svg
10. Gallic acid [image on the internet]. 2007 Feb 1 [updated 2009 Jan 3]; cited 2012 Dec 12. Available from: http://en.wikipedia.org/wiki/File:Gallic_acid.svg
11. Kojic acid [image on the internet]. 2010 Apr 23; cited 2012 Dec 12. Available from: http://en.wikipedia.org/wiki/File:KojicAcid.svg
12. Quercetin [image on the internet]. 2008 Apr 5; cited 2012 Dec 12. Available from: http://en.wikipedia.org/wiki/File:Quercetin.svg
13. Huang D, Ou B, Prior RL. The chemistry behind antioxidant capacity assays. J Agric Food Chem. 2005 Mar 23;53(6):1841-56.
14. Carsberg CJ, Warenius HM, Friedmann PS. Ultraviolet radiation-induced melanogenesis in human melanocytes. Effects of modulating protein kinase C. J Cell Sci. 1994 Sep;107 (Pt 9):2591-7.
15. Niki Y, Yoshida M, Ando H, Wakamatsu K, Ito S, Harada N, et al. 1-(2,4-Dihydroxyphenyl)-3-(2,4-dimethoxy-3-methylpheny) propane inhibits melanin synthesis by dual mechanisms. J Dermatol Sci. 2011Aug;63(2):115-21.
16. Mukherjee PK, Maity N, Nema NK, Sarkar BK. Bioactive compounds from natural resources against skin aging. Phytomedicine. 2011 Dec 15;19(1):64-73.
17. Choi SW, Lee SK, Kim EO, Oh JH, Yoon KS, Parris N, et al. Antioxidant and Antimelanogenic Activities of Polyamine Conjugates from Corn Bran and Related Hydroxycinnamic Acids. J Agric Food Chem. 2007 May 16;55(10):3920-5.
18. Yoshioka S, Terashita T, Yoshizumi H, Shirasaka N. Inhibitory effects of whisky polyphenols on melanogenesis in mouse B16 melanoma cells. Biosci Biotechnol Biochem. 2011;75(12):2278-82.

19. Panich U, Onkoksoong T, Limsaengurai S, Akarasereenont P, Wongkajornsilp A. UVA-induced melanogenesis and modulation of glutathione redox system in different melanoma cell lines: the protective effect of gallic acid. J Photochem Photobiol B. 2012 Mar 1;108: 16-22.
20. Ito S, Wakamatsu K. Chemistry of mixed melanogenesis--pivotal roles of dopaquinone. Photochem Photobiol. 2008 May-Jun;84(3):582-92.
21. Hori I, Nihei K, Kubo I. Structural criteria for depigmenting mechanism of arbutin. Phytother Res. 2004 Jun;18(6):475-9.
22. Briganti S, Camera E, Picardo M. Chemical and instrumental approaches to treat hyperpigmentation. Pigment Cell Res. 2003 Apr;16(2):101-10.
23. Virador VM, Kobayashi N, Matsunaga J, Hearing VJ. A standardized protocol for assessing regulators of pigmentation. Anal Biochem. 1999 Jun;270(2):207-19.
24. Espin JC, Garcia-Ruiz PA, Tudela J, Garcia-Canovas F. Study of stereospecificity in mushroom tyrosinase. Biochem J. 1998 Apr;331(pt2):547-51.
25. Chang TS. An updated review of tyrosinase inhibitors. Int J Mol Sci. 2009 Jun;10(6):2440-75.
26. Itoh K, Hirata N, Masuda M, Naruto S, Murata K, Wakabayashi K, Matsuda H. Inhibitory effects of Citrus hassaku extract and its flavanone glycosides on melanogenesis. Biol Pharm Bull. 2009 Mar;32(3):410-5.

Elsevier Editorial System(tm) for Free Radical Biology and Medicine
Manuscript Draft

Manuscript Number:

Title: Photoprotection by dietary phenolics against melanogenesis induced by UVA through Nrf2-dependent antioxidant responses

Article Type: Original Research/ Original Contribution

Keywords: phenolics; antioxidant; ultraviolet A; melanogenesis; nuclear factor E2-related factor 2 (Nrf2)

Corresponding Author: Dr. Uraiwan Panich, M.D., Ph.D.

Corresponding Author's Institution: Faculty of Medicine Siriraj Hospital, Mahidol University

First Author: Anyamanee Chaiprasongsuk

Order of Authors: Anyamanee Chaiprasongsuk; Tasanee Onkoksoong, MSc.; Thanyawan Pluemsamran; Saowalak Limsaengurai; Uraiwan Panich, M.D., Ph.D.

Abstract: The roles of dietary phenolics possessing antioxidant and ultraviolet (UV)-absorbing and properties in inhibition of UV-mediated skin pigmentation have been widely investigated in order to develop effective and safe whitening products. UVA has been shown to induce melanogenesis through interference with redox state by increased reactive oxygen species (ROS) production and reduced antioxidant defense capacity in melanocytes and/or B16F10 melanoma cells. Nuclear factor E2-related factor 2-antioxidant response element (Nrf2-ARE) plays a crucial role in cellular response to oxidative stress through regulating the transcription of antioxidant genes including glutamate cysteine ligase (GCL), glutathione S-transferase (GST) and NAD(P)H quinone oxidoreductase1 (NQO1). In this study, we first investigated whether genetic silencing of Nrf2 using small-interfering RNA (siRNA) affected melanogenesis in primary human epidermal melanocytes (HEMn) and B16F10 melanoma cells subjected to UVA (8 J/cm2) exposure. Then, we explored the antimelanogenic actions of various phytochemicals including caffeic acid (CA) and ferulic acid (FA), phenolics without UVA-blocking properties as well as quercetin (QU) and rutin (RU), phenolics with UVA-blocking properties, and avobenzone (AV), an efficient and widely-used UVA filter, in association with modulation of Nrf2-mediated antioxidant defenses in response to UVA (8 J/cm2) irradiation in B16F10 cells. Nrf2 silencing was observed to promote melanin content as well as tyrosinase activity and protein level in both HEMn and B16F10 cells in response to UVA exposure. In addition, a single dose of UVA irradiation resulted in time-dependent alterations of Nrf2 nuclear accumulation and its target antioxidant proteins including GCLC, GST and NQO1 B16F10 cells. Stimulation of melanogenesis by UVA correlated with increased formation of ROS and oxidative DNA damage (8-OHdG level), depletion of GSH and an early transient downregulation of Nrf2 nuclear translocation, Nrf2-ARE transcriptional activity and its downstream antioxidants in B16F10 cells exposed to UVA irradiation. All test compounds (up to 30 μM) exerted anti-melanogenic effects with respect to their abilities to suppress UVA-mediated ROS and 8-OHdG formation as well as GSH loss in B16F10 cells. Moreover, while CA, QU and AV alone without UVA challenge did not significantly affect Nrf2 nuclear accumulation and transcriptional activity, they could potentially reverse downregulation of Nrf2 nuclear translocation, its transactivation, mRNA and protein levels of Nrf2 target antioxidants including GCLC, GST and NQO1 and enzyme activities of GST and NQO1 in UVA-irradiated cells. Among all test compounds, QU produced the greatest inhibitory effect on UVA-mediated melanogenesis, oxidative damage and downregulation of Nrf2-dependent

antioxidant defenses. In conclusion, defective Nrf2 may promote melanogenesis under UVA-induced oxidative stress. Antioxidant and UVA blocking compounds could effectively provide an early protection against UVA-induced melanogenesis in correlation with their antioxidant potentials through indirect regulatory effect on Nrf2-ARE pathway.

Suggested Reviewers: Helmut Sies M.D., Ph.D.
Professor Emeritus, Biochemistry and Molecular Biology , Faculty of Medicine, Heinrich Heine University Düsseldorf
hhh@ncsu.edu
He is an expert in molecular basis
of actions of oxidants and antioxidants.

Wondrak Georg Ph.D.
Associate Professor, Pharmacology & Toxicology, College of Pharmacy, University of Arizona Cancer Center
wondrak@pharmacy.arizona.edu
He is an expert in redox drug discovery targeting skin cancer and solar photodamage.

Young-Joon Surh Ph.D.
Professor, Tumor Microenvironment Global Core Research Center, College of Pharmacy, Seoul National University
surh@plaza.snu.ac.kr
He is an expert in redox-sensitive transcription factors including Nrf2 in cancer chemoprevention and redox mechanisms of natural products.

Ruza Pandel Ph.D.
Professor, Faculty of Health Studies, University of Ljubljana
ruza.pandel@zf.uni-lj.si
She is an expert in cell biology of photoaged skin.

ภาควิชาเภสัชวิทยา
คณะแพทยศาสตร์ศิริราชพยาบาล
มหาวิทยาลัยมหิดล บางกอกน้อย กรุงเทพฯ
๑๐๗๐๐
โทร. ๔๑๙๗๕๖๕, ๔๑๙๗๕๖๙
โทรสาร. ๔๑๑๕๐๒๖

DEPARTMENT OF PHARMACOLOGY
FACULTY OF MEDICINE SIRIRAJ HOSPITAL
MAHIDOL UNIVERSITY,
BANGKOK 10700
THAILAND
TEL. (662) 4197565, 4197569
FAX. (662) 4115026

Jun 22, 2015

Dear Editor,

I wish to submit the following manuscript to be considered for publication as a Research Communication in *Free Biology & Medicine*.

'Photoprotection by dietary phenolics against melanogenesis induced by UVA through Nrf2-dependent antioxidant responses'

The corresponding author is: Dr. Uraiwan Panich

In this study, we investigated whether genetic silencing of Nrf2 using small-interfering RNA (siRNA) affected melanogenesis in primary human epidermal melanocytes (HEMn) and B16F10 melanoma cells subjected to UVA (8 J/cm^2) exposure. Then, we explored the antimelanogenic actions of various phytochemicals including caffeic acid (CA) and ferulic acid (FA), phenolics without UVA-blocking properties as well as quercetin (QU) and rutin (RU), phenolics with UVA-blocking properties, and avobenzone (AV), an efficient and widely-used UVA filter, in association with modulation of Nrf2-mediated antioxidant defenses in response to UVA (8 J/cm^2) irradiation in B16F10 cells. We observed that Nrf2 silencing was observed to promote melanin content as well as tyrosinase activity and protein level in both HEMn and B16F10 cells in response to UVA exposure. In addition, a single dose of UVA irradiation resulted in time-dependent alterations of Nrf2 nuclear accumulation and its target antioxidant proteins including GCLC, GST and NQO1. We reported for the first time that defective Nrf2 may promote melanogenesis under UVA-induced oxidative stress. Antioxidant and UVA blocking compounds could effectively provide an early protection against UVA-induced melanogenesis in correlation with their antioxidant potentials through indirect regulatory effect on Nrf2-ARE pathway.

I confirm that the above manuscript has not been published in this or a substantially similar form (in print or electronically including on a website) nor accepted for publication elsewhere.

Suggested reviewers

1. Professor Helmut Sies
   Institution: Faculty of Medicine, Heinrich Heine University Düsseldorf
   Email address: hhh@ncsu.edu

2. Associate Professor Wondrak Georg
   Institution: College of Pharmacy, University of Arizona
   Email address: wondrak@pharmacy.arizona.edu
3. Professor Young-Joon Surh
   Institution: College of Pharmacy, Seoul National University
   Email address: surh@plaza.snu.ac.kr
4. Professor Ruza Pandel
   Institution: Faculty of Health Studies, University of Ljubljana
   Email address: ruza.pandel@zf.uni-lj.si

Yours sincerely,

Uraiwan Panich, M.D., Ph.D.

HIGHLIGHTS

- Depletion of Nrf2 could stimulate melanogenesis under UVA-mediated oxidative stress.
- A single dose of UVA irradiation resulted in time-dependent alterations of Nrf2 nuclear accumulation and its target antioxidant proteins including GCLC, GST and NQO1 B16F10 cells.
- Antioxidant and UVA blocking compounds could effectively provide an early protection against UVA-induced melanogenesis in correlation with their antioxidant potentials through indirect regulatory effect on Nrf2-ARE pathway.
- To avoid excessive activation of Nrf2, which could harm the cells, indirect modulation of Nrf2-ARE pathway to promote redox balance by photoprotective compounds with antioxidant or sunscreen properties may provide a pharmacological insight for protection against photooxidative damage and hyperpigmentation.

Photoprotection by dietary phenolics against melanogenesis induced by UVA through Nrf2-dependent antioxidant responses

Anyamanee Chaiprasongsuk, Tasanee Onkoksoong, Thanyawan Pluemsamran, Saowalak Limsaengurai, Uraiwan Panich*

Department of Pharmacology, Faculty of Medicine Siriraj Hospital, Mahidol University, Bangkok 10700, Thailand

*Corresponding author. Address: Department of Pharmacology, Faculty of Medicine Siriraj Hospital, Mahidol University, Bangkok 10700, Thailand. Tel.: +66-(0)2-419-7569; Fax: +66-(0)2-411-5026.

E-mail address: uraiwan.pan@mahidol.ac.th

ABSTRACT

The roles of dietary phenolics possessing antioxidant and ultraviolet (UV)-absorbing and properties in inhibition of UV-mediated skin pigmentation have been widely investigated in order to develop effective and safe whitening products. UVA has been shown to induce melanogenesis through interference with redox state by increased reactive oxygen species (ROS) production and reduced antioxidant defense capacity in melanocytes and/or B16F10 melanoma cells. Nuclear factor E2-related factor 2-antioxidant response element (Nrf2-ARE) plays a crucial role in cellular response to oxidative stress through regulating the transcription of antioxidant genes including glutamate cysteine ligase (GCL), glutathione S-transferase (GST) and NAD(P)H quinone oxidoreductase-1 (NQO1). In this study, we first investigated whether genetic silencing of Nrf2 using small-interfering RNA (siRNA) affected melanogenesis in primary human epidermal melanocytes (HEMn) and B16F10 melanoma cells subjected to UVA (8 J/cm^2) exposure. Then, we explored the antimelanogenic actions of various phytochemicals including caffeic acid (CA) and ferulic acid (FA), phenolics without UVA-blocking properties as well as quercetin (QU) and rutin (RU), phenolics with UVA-blocking properties, and avobenzone (AV), an efficient and widely-used UVA filter, in association with modulation of Nrf2-mediated antioxidant defenses in response to UVA (8 J/cm^2) irradiation in B16F10 cells. Nrf2 silencing was observed to promote melanin content as well as tyrosinase activity and protein level in both HEMn and B16F10 cells in response to UVA exposure. In addition, a single dose of UVA irradiation resulted in time-dependent alterations of Nrf2 nuclear accumulation and its target antioxidant proteins including GCLC, GST and NQO1 B16F10 cells. Stimulation of melanogenesis by UVA correlated with increased formation of ROS and oxidative DNA damage (8-OHdG level), depletion of GSH and an early transient downregulation of Nrf2 nuclear translocation, Nrf2-ARE

transcriptional activity and its downstream antioxidants in B16F10 cells exposed to UVA irradiation. All test compounds (up to 30 μM) exerted anti-melanogenic effects with respect to their abilities to suppress UVA-mediated ROS and 8-OHdG formation as well as GSH loss in B16F10 cells. Moreover, while CA, QU and AV alone without UVA challenge did not significantly affect Nrf2 nuclear accumulation and transcriptional activity, they could potentially reverse downregulation of Nrf2 nuclear translocation, its transactivation, mRNA and protein levels of Nrf2 target antioxidants including GCLC, GST and NQO1 and enzyme activities of GST and NQO1 in UVA-irradiated cells. Among all test compounds, QU produced the greatest inhibitory effect on UVA-mediated melanogenesis, oxidative damage and downregulation of Nrf2-dependent antioxidant defenses. In conclusion, defective Nrf2 may promote melanogenesis under UVA-induced oxidative stress. Antioxidant and UVA blocking compounds could effectively provide an early protection against UVA-induced melanogenesis in correlation with their antioxidant potentials through indirect regulatory effect on Nrf2-ARE pathway.

KEY WORDS: phenolics; antioxidant; ultraviolet A; melanogenesis; nuclear factor E2-related factor 2 (Nrf2)

Abbreviations: ARE, antioxidant response element; AV, avobenzone; CA, caffeic acid; CDNB, 1-chloro-2,4-dinitrobenzene; DCPIP, 2,6-dichloroindophenol; DMEM, dulbecco's modified Eagle medium; DPBS, dulbecco`s phosphate buffered saline; DTNB, (5,5′-dithio-bis-2-(nitrobenzoic acid); FA, ferulic acid; γ-GCL, γ-glutamate cysteine ligase; γ-GCLC, γ-glutamate cysteine ligase catalytic subunit; γ-GCLM, γ-glutamate cysteine ligase modifier subunit; GSH, glutathione; GSSG, glutathione reductase; GST, glutathione S-transferase; H_2DCFDA, non-fluorescent dichlorofluorescein; HEMn, primary human epidermal melanocytes; NQO1, NAD(P)H quinone oxidoreductase1; Nrf2, nuclear factor E2-related factor 2; 8-OHdG, 8-hydroxy-2'–deoxyguanosine; QU, quercetin; RNAi, RNA interference; ROS, reactive oxygen species; RU, rutin; siCtrl, non-silencing siRNA controls; siNrf2, siRNA against Nrf2; siRNA, small-interfering RNA; UVA, ultraviolet A

INTRODUCTION

Oxidative stress induced by ultraviolet A (UVA) radiation has been recognized to play a crucial role in physiological and biological stress responses of skin cells including dysregulation of melanogenesis in melanocytes and/or melanoma cells [1, 2]. Whereas melanin plays a beneficial role in protecting the skin against damaging effects of UV radiation, excessive formation of melanin could be harmful, in particular following UV exposure [3, 4]. Diet- and plant-derived phytochemicals have been proposed as good candidates for effective and safe photoprotective agents, possibly, due to their antioxidant and UV-absorbing properties [5, 6].

Since UVA exposure has been demonstrated to play a crucial role in increased melanogenesis partly through induction of oxidative stress and impairment of antioxidant defense in melanocytes and/or melanoma cells [7, 8], improvement of antioxidant defense system to cope with the overwhelmed oxidative stress could thus be one of effective and safe approaches to inhibit melanogenesis and photodamaged skin. Nuclear factor E2-related factor 2 (Nrf2) is an important transcription factor controlling cellular response to oxidative stress in various tissues including the skin by binding to the antioxidant response element (ARE), present in the promoter region of genes encoding for phase II detoxification and antioxidant enzymes, and initiating the transcription of its target genes including γ-glutamate cysteine ligase (γ-GCL), the rate-limiting enzyme for GSH synthesis, glutathione S-transferase (GST) and NAD(P)H quinone oxidoreductase-1 (NQO1) [9]. Activation of the Nrf2-dependent antioxidant response has been reported to play a beneficial role in cellular function and integrity by protecting skin cells including melanocytes against damaging effects from oxidative insults including UV radiation [10-13]. Additionally, Nrf2 overexpression has recently been shown to suppress melanogenesis through abrogation of melanin production

and tyrosinase protein expression [14]. Dietary phytochemicals including caffeic acid (CA), ferulic acid (FA), quercetin (QU) and rutin (RU) found abundantly in plant-based diets and beverages as well as UVA blocking agents were shown to produce antioxidant, photoprotective and depigmenting actions [15-18]. We previously reported that inhibition of melanogenesis and photoprotection by dietary phenolics involved promotions of antioxidant defenses in HaCaT keratinocyte and melanoma cell lines exposed to UVA irradiation [19-21]. Nevertheless, there has been no report investigating antimelanogenic effects of compounds with antioxidant and UVA blocking properties in correlation to modulation of Nrf2-ARE signaling pathway and its downstream antioxidants in response to oxidative stress induced by UVA irradiation. In this study, we therefore examined whether depletion of Nrf2 using small-interfering RNA-mediated silencing of Nrf2 affected melanogenesis in primary human epidermal melanocytes (HEMn) and B16F10 melanoma cells in the presence and absence of UVA challenge. Additionally, we explored the underlying mechanisms of dietary phenolics without UVA absorbing properties; CA and FA, and with UVA absorbing properties; QU and RU, as well as AV, an efficient and widely-used UVA filter which does not possess antioxidant activity, in protecting B16F10 cells against UVA-induced melanogenesis in association with inhibition of oxidative stress and oxidative DNA damage (8-hydroxy-2'–deoxyguanosine; 8-OHdG) through modulation of Nrf2-ARE signaling and its downstream antioxidants.

MATERIALS AND METHODS

Cell cultures and treatment

Primary human epidermal melanocytes (HEMn) (Lonza, Basel, Switzerland) were grown in Medium 254 (#M-254-500) supplemented with human melanocyte growth supplement (HMGS) according to the manufacturer's instructions. B16F10 mouse melanoma cells (ATCC, Rockville, Md, USA), a gift from Assoc. Prof. Wajjwalku, Faculty of Veterinary Medicine, Kasetsart University, were grown in Dulbecco's modified Eagle medium (DMEM) supplemented with 10% fetal bovine serum (FBS) and 1% penicillin (100 units/ml)/streptomycin (100 μg/ml). All cells were maintained at 37 ^{o}C in a humidified air of 5% CO_2 (P_{CO2} = 40 Torr) (a Forma Scientific CO_2 Water Jacketed Incubator).

Cells were treated with test compounds (up to 30 μM) in Dulbecco`s phosphate buffered saline (DPBS) for 30 min before exposure to a single dose of UVA radiation (8 J/cm^2) as previously described [4]. The dose of UVA and concentrations of phenolics employed in this study were non-cytotoxic to both HEMn and B16F10 cells. Cells were washed, further incubated in serum-free medium and harvested at various time points after UVA irradiation. The UVA source was a xenon arc lamp (Dermalight ultrA1; Hoenle, Martinsried, Germany).

For preparation of cell lysate, cells were harvested and resuspended in lysis buffer consisted of 50 mM Tris-HCl, 10 mM ethylene diaminetetraacetic acid (EDTA), 1% (v/v) Triton X-100, phenylmethylsulfonyl fluoride (PMSF) (100 mg/ml) and pepstatin A (1 mg/ml) in DMSO and leupeptin (1 mg/ml) in H_2O, pH 6.8. The lysed cells were centrifuged at 10,000 rpm for 10 min at 4 ºC and the total lysates were collected and either assayed immediately or stored frozen at -80 °C.

Silencing of Nrf2 via RNA interference (RNAi)

A combination of four gene-specific small-interfering RNA (siRNA) against human Nrf2 (NM_006164) was used (FlexiTube GeneSolution GS4780 for NFE2L2, Qiagen; Cat.#:1027416). HEMn and B16F10 cells were transfected with 5 nM siRNA against Nrf2 (siNrf2) or equal molar non-silencing siRNA controls (siCtrl, Qiagen; Cat.#:1022076) for 48 h. These siRNAs were earlier complexed with liposome carrier (HiPerFect Transfection Reagent, Qiagen; Cat.#: 301705) at 0.08 μL/ng siRNA concentration by incubating mixture for 5-10 min at room temperature in serum-free culture medium. At 48 h post-transfection, cells were then washed with DPBS and subjected to UVA irradiation, following which melanin content, tyrosinase activity and protein were determined. Cells appeared normal morphologically and did not differ from untransfected cells in cell viability. At 48 h post-transfection, all siRNAs were verified to ensure achieving functional and specific silencing by evaluating mRNA and protein levels of Nrf2 and known Nrf2 target genes including GCLC, GCLM, GST and NQO1 before employment in all experiments. To evaluate melanogenic response of Nrf2-depleted cells to UVA irradiation, HEMn and B16F10 cells transfected with Nrf2-siRNA or nonsilencing negative control siRNA (siCtrl) were irradiated with 8 J/cm^2 of UVA and harvested at 1 h post-irradiation for determination of melanin content and tyrosinase activity and at 24 h post-irradiation for tyrosinase protein expression.

Melanin content assay

An evaluation of melanin production was performed as described previously [20]. Cells were harvested at 1 h after UV radiation (8 J/cm^2) and the cell pellets were solubilized in 1 N NaOH for 1 h to dissolve melanin, which was then measusred spectrophotometrically at 475

nm. The melanin content (μg/mg protein) was calculated by comparison to a standard curve derived using synthetic melanin.

Tyrosinase activity assay

The rate of L-DOPA oxidation was measured to assess cellular tyrosinase activity at 1 h following exposure to a UVA dose of 8 J/cm^2. The assay was performed as previously described [14]. Briefly, 20 mM L-DOPA used as the substrates was added to each lysate in a 96-well plate and absorbance of dopachrome formation was measured spectrophotometrically at 475 nm every 10 min for 1 h at 37 °C by a spectrophotometer. The tyrosinase activity (unit/mg protein) was calculated by comparison to a standard curve using tyrosinase (2034 U/mg).

Measurement of intracellular glutathione content

GSH level was spectrophotometrically measured using glutathione reductase (GSSG) : (5,5′-dithio-bis-2-(nitrobenzoic acid) (DTNB) enzymatic recycling method following the kit protocol from Sigma-Aldrich (MO, US). The assay is based on conversion of glutathione disulfide (GSSG) to GSH by GR in the presence of NADPH and GSH oxidation by the sulfhydryl reagent DTNB to produce the yellow TNB (5′-thio-2-nitrobenzoic acid) measured at 412 nm. The rate of TNB production is directly proportional to this recycling reaction in turn directly proportional to the concentration of GSH. The GSH level was calculated by comparing the valued obtained with a standard curve of GSH and was expressed in nmol/mg protein.

Measurement of glutathione-S-transferase activity

GST activity was measured following the kit protocol from Cayman chemical (Ann Arbor, MI). The assay is based on GST-catalyzed conjugation of GSH to 1-chloro-2,4-dinitrobenzene (CDNB) as a substrate. The GS-DNB conjugate was determined spectrophotometrically at 340 nm immediately and every 30 second for 10 min. 10 μl of 100 mM CDNB was added to start the reaction of 20 μl of sample or positive control GST with 20 μl of 200 mM GSH in 150 μl of assay buffer (100 mM potassium phosphate, pH 6.5, containing 0.1% Triton X-100). One unit of GST activity is defined as the amount of enzyme that catalyzes 1 nmol of GS-DNB conjugate/min and the results were expressed as nmol/min/mg protein).

Measurement of NQO1 activity

B16F10 cells were harvested at 4 h post-irradiation, and NQO1 activity in cell lysates was measured using 2,6-dichloroindophenol (DCPIP) as a substrate as previously described [22]. The assay was based on the activities for NAD(P)H-dependent reduction of DCPIP at 600 nm and the reaction was specifically inhibited by dicumarol. Briefly, reactions contained 25 mM Tris-HCl, pH 7.4, 0.17 mg/ml bovine serum albumin, 0.2 mM NADH and sample. 80 μM DCPIP was added to initiate the reactions and the NQO1 activity was measured as the dicumarol inhibitable reduction in absorbance at 600 nm. The NQO1 activity was expressed as nmole DCPIP reduced/min/mg protein.

Determination of protein content

Protein concentration was measured using the Bio-Rad Protein Assay Kit (Bio-Rad, Germany) and bovine serum albumin (BSA) was used as protein standard.

Determination of intracellular oxidant formation by flow cytometry

The assay is based on oxidation of non-fluorescent dichlorofluorescein (H_2DCFDA) by intracellular ROS to fluorescent 2,7-DCF. After UVA irradiation, cells were washed and incubated with serum-free DMEM for 30 min. Then, cells were incubated in DPBS with 5 μM H_2DCFDA at 37°C for 30 min and analysed by flow cytometery using a fluorescence activated cell sorter (FACS-calibur).

Protein preparation and western blot analysis

Protein extraction

Western blotting were carried out using whole cell extracts for detection of tyrosinase, GCLC, GST and NQO1 protein expressions and cytosolic, and nuclear extracts for Nrf2 levels. Whole cells were extracted by incubation for 10 min at 4 °C with RIPA (radioimmunoprecipitation assay) buffer containing 10% NP40, 5 M NaCl, 1 M HEPES (pH 7.4), 0.5 M EDTA (pH 8.0) and proteinase inhibitor cocktail. Cytosolic and nuclear extraction were prepared using a commercial kit according to the manufacturer's instructions (Sigma). Cells were washed with DPBS and collected in micro-centrifuge tubes. Cell pellets were suspended in 100 μl of hypotonic lysis buffer containing 0.01 M DTT and proteinase inhibitor cocktail. Cells were incubated on ice for 15 min and lysed in ice-cold cytosolic extraction buffer containing 10% IGEPAL CA-630. Lysate mixtures were centrifuged at 11,000 rpm for 1 min at 4°C, and the supernatant was collected as the cytosolic extract. Nuclear pellets were suspended in 60 µl of nuclear extraction buffer (20 mM HEPES, pH 7.9, 1.5 mM MgCl, 0.42 M NaCl, 0.2 mM EDTA, and 25% (v/v) Glycerol) containing 0.01 M DTT and proteinase inhibitor cocktail. The mixtures were incubated on ice with intermittent vortexing for 15-30 min. Then, extracts were centrifuged at 14,000 rpm for 10 min and the supernatant was collected as the nuclear extract.

Western blotting

Protein concentrations were quantified using the Bradford method (Bio-Rad, Germany). The proteins were resolved by a 10% (w/v) SDS-PAGE gel and transferred to a nitrocellulose membrane. The membranes were blocked with 5% skim milk (Tris-buffer saline containing 0.1% (v/v) Tween 20 and 5% (w/v) skim milk) for 1.5 h and then incubated overnight at 4ºC with the primary antibody against tyrosinase (ab178676; Abcam, Cambridge, MA, USA) (1:10000), Nrf2 (sc-722; Santa Cruz Biotechnology, Santa Cruz, CA) (1:2000), GCLC (ab53179; Abcam, Cambridge, MA, USA) (1:2000), GST (sc-459; Santa Cruz Biotechnology, Santa Cruz, CA) (1:1000) and NQO1 (ab34173; Abcam, Cambridge, MA, USA) (1:2000) in 5% skim milk. The membranes were washed 3 times with a PBS solution of 0.1% (v/v) Tween-20 for 30 min and incubated for 1.5 h at room temperature with the the HRP-conjucated secondary antibodies (ab6789 for anti-mouse and ab6721 for anti-rabbit HRP labeled secondary antibody; Abcam, Cambridge, MA, USA) (1:2000) in 5% skim milk. Immunoreactivity is detected using the Bio-Rad Clarity western ECL (Bio-Rad). Protein bands were imaged using an ImageQuant LAS 4000 digital imaging system (GE Healthcare, UK) and the integrated optical density of the bands was analysed by the Image-J software version 1.45 s (National institutes of health, USA). The protein expressions were normalized to expression of loading controls; α-Tubulin (ab7291; Abcam, Cambridge, MA, USA) (1:5000) for whole cell proteins or cytosol Nrf2 and TATA binding protein (TBP) (ab818; Abcam, Cambridge, MA, USA) (1:2000) for nuclear Nrf2.

Quantitative real-time reverse transcriptase-polymerase chain reaction for measurement of mRNA expression

Total RNA was isolated using the illustra RNAspin Mini RNA Isolation Kit (GE Healthcare, UK). Reverse transcription was carried out with 1 μg of total RNA using the

Improm-II reverse transcriptase (Promega, Medison, USA) under the conditions described in the kit manual. Reactions were performed in triplicate for each sample in the ABI Prism 7500 Real Time PCR System (Applied Biosystems, USA) under the following amplification conditions: 95 °C for 10 min, 40 cycles of 95 °C for 15 s, 60 °C for 40 s, and 72 °C for 40 s. Real-time RT-PCR was performed in a total volume of 25 μl of reaction mixtures containing 5 μl cDNA template with FastStart universal SYBR Green Master (ROX) and 10 μM concentrations of primers. Primers for PCR were designed using the Primer Express software version 3.0 (Applied Biosystems, USA). Sequences of PCR primer sets of γ-GCL-C, γ-GCL-M, GST and GAPDH (in 5′-3′ direction) were as follows: tyrosinase sense (product sizes = 267), CATTCTTCTCCTCTTGGCAGA, and antisense, CCGCTATCCCAGTAAGTGGA; Nrf2 sense (product sizes = 161), TTCTGTTGCTCAGGTAGCCCCTCA, and antisense, GTTTGGCTTCTGGACTTGG; γ-GCLC sense (product sizes = 160 bp), GCTGTCTTGCAGGGAATGTT, and antisense, ACACACCTTCCTTCCCATTG; γ-GCLM sense (product sizes = 200 bp), TTGGAGTTGCACAGCTGGATT, and antisense, TGGTTTTACCTGTGCCCACTG; GST sense (product sizes = 72 bp), CCTGTACCAGTCCAATACCATCCT, and antisense, TCCTGCTGGTCCTTCCCATA; GST sense (product sizes = 72 bp), CCTGTACCAGTCCAATACCATCCT, and antisense, TCCTGCTGGTCCTTCCCATA; NQO1 sense (product size = 245 bp), ATGACAAAGGACCCTTCCGGAGTAA, and antisense, ATTCTCCAGGCGTTTCTTCCATCCT; GAPDH sense (product size = 150 bp), CCTCCAAAATCAAGTGGGGCGATG, antisense, CGAACATGGGGGCATCAGCAGA. The mRNA level was normalized with reference to the amount of housekeeping gene transcripts (GAPDH mRNA). The mean Ct from mRNA expression in cDNA from each

sample was compared with the mean Ct from GAPDH determinations from the same cDNA samples.

Determination of Nrf2-ARE tramscriptional activity

Transcriptional activity of Nrf2-ARE was determined using the Cignal™ Antioxidant Response Reporter (luc) Kit (SABiosciences, Qiagen, USA). B16F10 cells were transfected in 24-well plate for 16 h with an Nrf2-responsive firefly luciferase reporter plasmid and a control plasmid constitutively expressing *Renilla* luciferase (SABiosciences, Qiagen) in Lipofectamine® LTX & Plus Reagent (Invitrogen, USA) according to the manufacturer's instructions. The transfected cells were pretreated with CA, QU and AV (up to 30 μM) for 30 min before exposure to UVA (8 J/cm^2). Cells were washed, further incubated in serum-free medium and harvested at 1 h after UVA irradiation. The firefly and Renilla luciferase activities were measured using a Dual-Glo Luciferase Assay Kit (Promega, USA) in a luminometer (FLUOstar Omega, BMG labtech, Germany). Firefly luciferase activity was normalized to *Renilla* luciferase activity to account for transfection efficiency,.

8-hydroxydeoxyguanosine (8-OHdG) analysis

DNA was isolated using DNA extraction kit (Geneaid, UKAS) according to the protocol's instruction and the RNA-free DNA obtained was used to determine 8-OHdG levels using Oxiselect oxidative DNA damage ELISA kit (cell Biolabs, San Diego, CA) according to manufacturer's instructions.

Statistical Analysis

Data are expressed as means ± standard deviation of the mean (SD) of separate experiments ($n \geq 3$) performed on different days using freshly prepared reagents. The

significance of non-irradiated controls or individual treatment groups in comparison to the UVA-irradiated groups was evaluated by independent *t*-test (Student's; 2 populations) or one-way analysis of variance (ANOVA) followed by Tukey or Dunnett tests, where appropriate, using Prism (GraphPad Software Inc., San Diego, CA).

RESULTS

SiRNA knockdown of Nrf2 in HEMn and B16F10 cells enhanced melanogenesis in response to UVA irradiation

To investigate the effects of Nrf2 on melanogenesis, Nrf2 knockdown was done using a siRNA approach. To verify efficacy of siRNA against Nrf2, mRNA levels of Nrf2 and its target antioxidants and Nrf2 nuclear protein of transfected HEMn and B16F10 cells were evaluated by real-time RT-PCR and western blot, respectively, after transfection of either Nrf2-siRNA or nonsilencing negative control siRNA (siCtrl). **Fig. 1A** showed a pronounced reduction of Nrf2 mRNA by ~70% and mRNA levels of its target antioxidants including GCL and GST by ~50% as well as NQO1 by ~60% at 48 h after transfection in both HEMn and B16F10 cells compared with untransfected and siCtrl cells. Nrf2-siRNA used in this study thus efficiently depleted Nrf2 mRNA and protein levels in both HEMn and B16F10 cells. Nrf2 mRNA and its protein levels in cells transfected with siCtrl were not different from the untransfected cells.

The effects of Nrf2 on melanogenesis were examined in HEMn and B16F10 cells with and without UVA exposure by determination of melanin content as well as activity and protein expression of tyrosinase. UVA irradiation led to a significant induction of melanin content and tyrosinase activity as well as a substantial upregulation of tyrosinase protein in untransfected HEMn and B16F10 cells and siCtrl-transfected cells. Our findings indicated that Nrf2 knockdown significantly stimulated melanin content **(Fig. 1B)** in both HEMn and B16F10 cells compared to siCtrl-transfected cells in response to UVA exposure. Furthermore, enhancement of tyrosinase activity **(Fig. 1C)** and protein expression **(Fig. 1D)** was observed in UVA-irradiated siNrf2 tranfected HEMn and B16F10 cells compared to irradiated siCtrl-transfected cells. Nevertheless, levels of melanogenesis in both HEMn and

B16F10 cells treated with siNrf2 without UV irradiation were comparable to those in cells treated with untransfected and siCtrl-transfected cells.

The test phenolics inhibited UVA-induced melanin content as well as tyrosinase activity and protein expression in B16F10 cells.

Since our findings suggested that Nrf2 could play a role in melanogenesis upon UVA challenge, we then examined whether antimelanogenic mechanisms of antioxidant phenolics with different UVA blocking properties involved modulation of Nrf2-mediated antioxidant responses. Our data showed that pattern of melanogenesis in response to UVA exposure was similar between Nrf2-depleted HEMn and B16F10 cells. B16F10 cells could therefore be used for further assessment of antimelanogenic effects of test compounds in association with modulation of Nrf2. Our study evaluated inhibitory effects of phenolics without UVA absorbing properties, CA and FA, phenolics with UVA absorbing properties; QU and RU, and AV, an effectient chemical UVA filter, at non-toxic concentrations on UVA-dependent melanin content as well as tyrosinase activity and protein level in B16F10 cells. A drastic augmentation in melanin production **(Fig. 2A)**, tyrosinase activity, **(Fig. 2B)** and tyrosinase protein expression **(Fig. 2C)** was found in B16F10 cells irradiated with a UVA dose of 8 J/cm^2. Nevertheless, treatment of the cells with test phenolics before UV irradiation led to a pronounced inhibition of melanin production and tyrosinase activity. Based on the IC_{30} values, the rank order of test compounds' abilities to inhibit UVA-mediated melanin content and tyrosinase activitiy was QU > RU ≈ CA ≈ AV > FA (Table 1), suggesting that, between phenolics without and with UVA absorbing properties, CA and QU produced greater inhibitory effect than FA and RU, respectively. Thus, the antioxidant phenolics, CA and QU, as well as AV, a UVA sunscreen, were assessed in further experiments. Our findings demonstrated that all test compounds suppressd tyrosinase protein expression in UVA-

irradiated B16F10 cells compared to irradiated cells in the absence of test compounds. Moreover, QU was found to yield highest activities against increased melanogenesis mediated by UVA exposure in B16F10 cells.

All test compounds at the highest concentrations used did not substantially affect all melanogenic parameters measured in B16 cells in the absence of UVA irradiation (data not shown).

The test phenolics inhibited UVA-induced ROS formation, 8-OHdG DNA damage and GSH depletion in B16F10 cells

To examine whether antimelanogenic effects of test phenolics associated with their inhibitory actions against UVA-mediated cellular oxidative stress, we determined formation of ROS and 8-OHdG, one of the abundant oxidized DNA bases and a well-recognized oxidative damage biomarker of skin photodamage [23], as well as level of GSH, considered an indicative of cellular oxidative stress, in response to a UVA challenge. At 1 h following irradiation, UVA irradiation substantially induced ROS formation and depleted GSH level in irradiated B16F10 cells as compared to non-irradiated cells, although the presence of all test phenolics and AV abolished UVA-mediated ROS production **(Fig. 3A)** and GSH reduction **(Fig. 3C)** as compared to irradiated B16F10 cells without treatment with test compounds. Additionally, UVA irradiation was shown to augment 8-OHdG formation in B16F10 cells, although its level was suppressed by treatment with CA, QU and AV **(Fig. 3B)**. We also evaluated the protective effects of CA, QU and AV against increased 8-OHdG levels induced by H_2O_2 challenge and observed that CA and QU but not AV were able to inhibit H_2O_2-mediated 8-OHdG formation, suggesting that AV exerted photoprotective effects against oxidative DNA damage probably through UVA blocking action but not antioxidant action. In agreement with results of melanogenesis inhibition by phenolics, among all test compounds,

the greatest antioxidant activity was observed for QU because a lower concentration of QU was required to inhibit UVA-induced ROS formation, GSH depletion and 8-OHdG production.

CA, QU and AV inhibited UVA-mediated downregulation of nuclear Nrf levels and Nrf2-ARE transcriptional activity in B16F10 cells

Since the transcription factor Nrf2, which binds to the ARE present in the promoter region of several antioxidant defense genes, is crucial for regulation of antioxidant enzymes, this study thus examined whether antimelanogenic effects of test phenolics involved modulation of Nrf2 nuclear accumulation and its transcriptional activity, we assessed nuclear/cytosolic Nrf2 ratio, indicating nuclear translocation of Nrf2, by western blot analysis and ARE luciferase activity using a dual-luciferase reporter assay. As shown in **Fig. 4A**, UVA (8 J/cm^2) irradiation was found to mediate time-dependent alterations in Nrf2 nuclear accumulation. A pronounced decrease in nuclear/cytosolic Nrf2 ratio in irradiated cells was observed at 1 h following UVA exposure compared to non-irradiated cells, although a substantial recovery in the nuclear/cytosolic Nrf2 ratio was detected by 6 h in irradiated cells compared to non-irradiated control cells. Moreover, while exposure to UVA resulted in a marked decrease in Nrf2 nuclear translocation and transactivation at 1 h following irradiation, time-dependent elevation of Nrf2 mRNA levels was observed in irradiated cells from 15 min to 4 h and a decline to the basal level was found by 8 h after UVA exposure **(Fig. 4B)**.

Protective effects of CA, QU and AV on UVA-induced downregulation of Nrf2 nuclear accumulation and its transcriptional activity were further evaluated. In consistent with Nrf2 nuclear translocation data, exposure of B16F10 cells to UVA (8 J/cm^2) led to reduction of ARE luciferase activity representing Nrf2-ARE transcriptional activity at 1 h post-irradiation. Treatment of B16F10 cells with test compounds (CA, QU and AV) prior to UVA

irradiation reversed UVA-mediated downregulation of nuclear/cytosolic Nrf2 ratio **(Fig. 4C)** and ARE luciferase activity **(Fig. 4D)** as compared to irradiated B16F10 cells without compound treatment. Test phenolics at the highest concentration did not affect nuclear Nrf2 levels and Nrf2-ARE activity in B16 cells in the absence of UVA irradiation (data not shown).

CA, QU and AV inhibited UVA-mediated mRNA downregulation of γ-GCLC, γ-GCLM, GST in B16F10 cells

Since test compounds were observed to inhibit UVA-mediated the decrease in protein expression and activities of Nrf2 target antioxidants studied, we further investigated whether the their inhibitory effects involved the transcriptional modulation of Nrf2 target genes. As shown in Fig. 5, UVA caused a significant decline in mRNA expression of γ-GCLC, γ-GCLM, GST and NQO1 at 2 h post-irradiation compared to non-irradiated cells, although pretreatment of B16 cells with test compounds (CA, QU and AV) was able to reverse UVA-mediated mRNA downregulation of γ-GCLC and γ-GCLM **(Fig. 5A)**, GST **(Fig. 5B)** and NQO1 **(Fig. 5C)**.

CA, QU and AV inhibited UVA-induced decreased protein expression and activity of Nrf2 target antoxidants in B16F10 cells

We further assessed whether test compounds also have abilities to modulate Nrf2-mediated antioxidant response. In accordance with results showing time-dependent effect of UVA irradiation on nuclear accumulation of Nrf2, UVA irradiation was observed to result in time-course changes in protein expression of Nrf2 target antioxidants including GCLC, GST and NQO1 **(Fig. 6A)**. A marked reduction in protein expressions of GCLC, GST and NQO1 in UVA (8 J/cm^2)-irradiated cells was observed at 6 h post-irradiation as compared to non-

irradiated cells, although a substantial restoration in the antioxidant protein levels was detected by 12 h. To investigate whether the test compounds could restore UVA-mediated impairment of Nrf2 target antioxidants, we therefore determined whether test compounds were able to abrogate UVA (8 J/cm^2)-mediated reduction of antioxidant protein expression and activities at 4 h post-irradiation. As shown in **Fig. 6B**, while a decline in GCLC, GST and NQO1 protein expressions as well as in eznyme activites of GST and NQO1 in response to UVA exposure was observed, treament with test compounds (CA, QU and AV) prior to UVA challenge led to a concentration-dependent induction in GST **(Fig. 6C)** and NQO1 **(Fig. 6D)** activities in irradiated cells in the absence of test compounds. In addition, pretreatment with all phenolics did not affect protein expression and activities of antioxidant enzyme studied in non-irradiated cells (data not shown).

Among all compounds studied, QU was able to exert the inhibitory effects at lower doses than those of other compounds in all the experiments performed in this study, indicating that QU produced the greatest inhibition of melanogenesis and downregulation of Nrf2 target antioxidants in response to oxidative stress induced by UVA exposure.

DISCUSSION

Nrf2 is a master regulator of antioxidant and cytoprotective genes including γ-GCL, GST and NQO1 in response to oxidative stress and environmental insults including UV irradiation and hence plays a beneficial role in protection against photooxidative stress in the skin cells including melanocytes [11, 24], although whether modulation of Nrf2 by phytochemicals can protect against UVA-dependent melanogenesis has not been reported. Our findings suggested that while genetic silencing of Nrf2 using siRNA without UVA challenge did not affect melanogenesis, an immediate increase in melanin content as well as tyrosinase activity and protein expression was observed in Nrf2-depleted HEMn and B16F10 cells in response to UVA exposure, indicating that defective Nrf2 may promote melanogenesis under UVA-induced oxidative stress.

In agreement with previous reports showing a protective role of Nrf2 in melanogenesis, overexpression of Nrf2 was observed to abolish melanin synthesis and tyrosinase expression in normal human melanocytes [14]. Our study demonstrated that UVA irradiation was able to stimulate melanin production as well as activity and protein level of tyrosinase in association with oxidative stress, indicated by enhanced formation of ROS and 8-OHdG, an oxidative DNA damage, as well as GSH depletion. We further evaluated the effects of UVA challenge on Nrf2-ARE signaling and its downstream antioxidants and observed that a single dose of UVA irradiation led to time-dependent alterations of nuclear accumulation of Nrf2 and its target antioxidant proteins including GCLC, GST and NQO1 in B16F10 cells. Our findings indicated that whereas downregulation of Nrf2 was not achieved at transcriptional level, a decrease in Nrf2 nuclear translocation and its transcriptional activity occurred as early as 1 h post-irradiation. Additionally, UVA was shown to cause a pronounced downregulation of mRNA and protein expressions of its target antioxidants

(GCLC, GST and NQO1), although a recovery of nuclear Nrf2 level and protein levels of its target antioxidants was observed at later time-points. Control of Nrf2 nuclear translocation crucial for its function in Nrf2 antioxidant response pathway is complicated. Upon oxidative stress and oxidative DNA damage, interference with kinase signaling led to reduction of Nrf2 nuclear translocation and its transcriptional activity [25-27] and depletion of peroxiredoxin I, which can be induced by oxidative stimuli, could diminish Nrf2 expression, leading to increased sensitivity to UVA exposure in mouse embryonic fibroblasts (MEF) [28]. In response to ROS-mediated DNA damage, activation of p53, which played a vital role in stimulation of apoptosis, led to suppression of Nrf2-dependent transcription of antioxidant response genes [29]. Moreover, while a high dose of UVB irradiation was found to diminish nuclear translocation of Nrf2, nuclear accumulation of Nrf2 was enhanced by UVB at low dose in mouse hepatoma, human skin fibroblast and keratinocyte cells as well as by UVA in dermal fibroblasts after 2 h [30, 31]. Taken together with our findings showing that oxidative stress could either upregulate or downregulate Nrf2, oxidative insults may play a dual role in control of Nrf2 that is dependent on cell types, intensity of oxidative stimuli, time after a challenge by stress, basal Nrf2 level and Keap1 function.

This study and our previous findings suggested that a transient downregulation of nuclear Nrf2 and its down stream antioxidants could be an early response to a single UV dose and adaptative response in response to oxidative stress leads to restoration of antioxidant defenses at translational and transcriptional levels at later time points, probably, through upregulation of Nrf2 in order to maintain redox balance [7]. However, contant exposure to oxidative insults including UV can overwhelm the defense mechanisms, attemps have thus been made to investigate the roles of promising whitening compounds in protecting skin against photodamage. A number of studies suggested that phytochemicals having antioxidant activities produced benefical effects against photodamage and photocarcinogenesis of the

skin through promotion of Nrf2 [32-35]. Electrophilic compounds known as selective and potent Nrf2 activators have been widely investigated and suggested to play a role in protecting the skin against environmental stressors [36-39]. As we addressed whether antimelanogenic mechanisms of different dietary phytochemicals with and without UVA-absorbing properties involved modulation of Nrf2-regulated antioxidant defenses, CA and FA, which did not have UVA-absorbing properties, QU and RU with UVA-absorbing properties as well as AV, which possessed UVA blocking but not antioxidant properties, were chosen in this study in order to assess whether antimelanogenic actions were associated with the abilities to block UVA-induced ROS formation. Our findings indicated that all test compounds were capable of abrogating UVA-induced melanin production as well as activity and protein expression of tyrosinase in correlation with abrogation of ROS and oxidative DNA damage formation as well as GSH loss in UVA-irradiated B16F10 cells.

Since Nrf2 is a master regulator of antioxidant defense system against oxidative stress or various toxic insults, we further determined the effects of test compounds on UVA-mediated diminished downstream antioxidant enzymes through modulation of Nrf2 in B16F10 cells. Our results suggested that test compounds (CA, QU and AV) could potentially reverse downregulation of Nrf2 nuclear translocation and Nrf2-ARE activity at 1 h following UVA irradiation in B16F10 cells. Findings from this study also indicated that pretreatment with all test compounds could restore UVA-mediated reduction of Nrf2 target antioxidant genes including GCLC, GST and NQO1 and the corresponding enzyme activites in B16F10 cells. This was accompanied by substantial upregulation of GCLC, GST and NQO1 protein levels and increase in GST and NQO1 enzyme activities in UVA-irradiated cells. Previous studies using cultured skin fibroblasts, keratinocytes and reconstructed human skin model demonstrated that treatment with several electrophiles or phytochemicals for longer period (up to 4-48 h) caused upregulation and activation of Nrf2 in association with the

photoprotective actions [36, 40-42]. Nevertheless, our study demonstrated that test compounds did not provide a direct regulatory effect on Nrf2 as treatment of B16F10 cells with test compounds alone for 30 min did not significantly affect ROS formation nor Nrf2 nuclear translocation and transcriptional activity detected at later time-points in non-irradiated cells, indicating that test compounds themselves probably did not provide direct or electrophilic actions on Nrf2.

Therefore, we proposed here that antioxidant and UVA blocking compounds could potentially provide an early protection against UVA-induced oxidative stress in correlation with enhanced melanogenesis, probably, through indirect regulation of Nrf2-ARE pathway. Moreover, QU was shown to yield the inhibitory effects at lower doses than those of other compounds in all the experiments performed in this study, indicating that, among all test compounds, QU, a powerful antioxidant having UVA-obsorbing properties, may produce the strongest protective effects on UVA-mediated melanogenesis, oxidative damage and downregulation of Nrf2 and its downstream antioxidants. Hence, abilities to reverse impaired Nrf2 signaling pathway is probably associated with antioxidant potentials of photoprotective agents.

Redox regulation of pigmentation through Nrf2-regulated antioxidant responses is complex. Impaired Nrf2-ARE signaling associated with melanocyte degeneration by oxidative stress that could be implicated in depigmentation should also be taken into account [5]. Additionally, Nrf2 is tightly regulated in the cytosol by Keap-1 and further studies are thus needed concerning the effects of phytochemicals on function of Keap-1 in regulation of melanogenesis in response to UV irradiation.

In summary, depletion of Nrf2 could stimulate melanogenesis under UVA-mediated oxidative stress. In this respect, targeting Nrf2-mediated antioxidant defenses may be a potential strategy for prevention and inhibition of skin hyperpigmentation. Test phenolics

exhibited antimelanogenic effect in correlation with their antioxidant potentials against UVA-mediated downregulation of Nrf2 and its downstream antioxidants in B16F10 cells. To avoid excessive activation of Nrf2, which could harm the cells, indirect modulation of Nrf2-ARE pathway to promote redox balance by photoprotective compounds with antioxidant or sunscreen properties may provide a pharmacological insight for protection against photooxidative damage and hyperpigmentation.

CONFLICTS OF INTEREST

No conflicts of interest were declared in relation to this article.

ACKNOWLEDGEMENT

Appreciation is expressed to Thailand Research Fund (Grant No. RSA5580012), Mahidol University and the “Chalermphrakiat” Grant, Faculty of Medicine Siriraj Hospital, Mahidol University, for research funding. We are grateful to Dr. Siwanon Jirawatnotai, Department of Pharmacology, Faculty of Medicine Siriraj Hospital, Mahidol University, for technical assistance and advice.

REFERENCES

[1] Hu, Z. M.; Zhou, Q.; Lei, T. C.; Ding, S. F.; Xu, S. Z. Effects of hydroquinone and its glucoside derivatives on melanogenesis and antioxidation: Biosafety as skin whitening agents. *J Dermatol Sci* **55**:179-184; 2009.

[2] Panich, U.; Tangsupa-a-nan, V.; Onkoksoong, T.; Kongtaphan, K.; Kasetsinsombat, K.; Akarasereenont, P.; Wongkajornsilp, A. Inhibition of UVA-mediated melanogenesis by ascorbic acid through modulation of antioxidant defense and nitric oxide system. *Arch Pharm Res* **34**:811-820; 2011.

[3] Swalwell, H.; Latimer, J.; Haywood, R. M.; Birch-Machin, M. A. Investigating the role of melanin in UVA/UVB- and hydrogen peroxide-induced cellular and mitochondrial ROS production and mitochondrial DNA damage in human melanoma cells. *Free Radic Biol Med* **52**:626-634; 2012.

[4] Maddodi, N.; Setaluri, V. Role of UV in cutaneous melanoma. *Photochem Photobiol* **84**:528-536; 2008.

[5] Korac R. R.; Khambholja, K. M. Potential of herbs in skin protection from ultraviolet radiation. *Pharmacogn Rev* **5**:164-173; 2011.

[6] Nichols, J. A.; Katiyar, S. K. Skin photoprotection by natural polyphenols: anti-inflammatory, antioxidant and DNA repair mechanisms. *Arch Dermatol Res* **302**:71-83; 2010.

[7] Panich, U.; Onkoksoong, T.; Limsaengurai, S.; Akarasereenont, P.; Wongkajornsilp, A. UVA-induced melanogenesis and modulation of glutathione redox system in different melanoma cell lines: the protective effect of gallic acid. *J Photochem Photobiol B* **108**:16-22; 2012.

[8] Baldea, I.; Mocan, T. Cosgarea, R. The role of ultraviolet radiation and tyrosine stimulated melanogenesis in the induction of oxidative stress alterations in fair skin melanocytes. *Exp Oncol* **31**:200-208; 2009.

[9] Slocum, S. L.; Kensler, T. W. Nrf2: control of sensitivity to carcinogens. *Arch Toxicol* **85**:273-284; 2011.

[10] Jian, Z.; Li, K.; Song, P.; Zhu, G.; Zhu, L.; Cui, T.; Liu, B.; Tang, L.; Wang, X.; Wang, G.; Gao, T.; Li, C. Impaired activation of the Nrf2-ARE signaling pathway undermines H2O2-induced oxidative stress response: a possible mechanism for melanocyte degeneration in vitiligo. *J Invest Dermatol* **134**:2221-2230; 2014.

[11] Schafer, M.; Werner, S. Nrf2-A regulator of keratinocyte redox signaling. *Free Radic Biol Med*; 2015.

[12] Wolfle, U.; Seelinger, G.; Bauer, G.; Meinke, M. C.; Lademann, J.; Schempp, C. M. Reactive molecule species and antioxidative mechanisms in normal skin and skin aging. *Skin Pharmacol Physiol* **27**:316-332; 2014.

[13] López-Camarillo, C.; Ocampo, E. A.; Casamichana, ML.; Pérez-Plasencia, C.; Alvarez-Sánchez, E.; Marchat, L. A. Protein kinases and transcription factors activation in response to UV-radiation of skin: implications for carcinogenesis. *Int J Mol Sci* **13**:142-172; 2012.

[14] Shin, J. M.; Kim, M. Y.; Sohn, K. C.; Jung, S. Y.; Lee, H. E.; Lim, J. W.; Kim, S.; Lee, Y. H.; Im, M.; Seo, Y. J.; Kim, C. D.; Lee, J. H.; Lee, Y.; Yoon, T. J. Nrf2 negatively regulates melanogenesis by modulating PI3K/Akt signaling. *PLoS One* **9**; 2014.

[15] Thangboonjit, W.; Limsaeng-u-rai, S.; Pluemsamran, T.; Panich, U. Comparative evaluation of antityrosinase and antioxidant activities of dietary phenolics and their activities in melanoma cells exposed to uva. *Siriraj Med J* **66**; 2014

[16] Liu, D.; Hu, H.; Lin, Z.; Chen, D.; Zhu, Y.; Hou, S.; Shi, X. Quercetin deformable liposome: preparation and efficacy against ultraviolet B induced skin damages in vitro and in vivo. *J Photochem Photobiol B* **127**:8-17; 2013.

[17] Potapovich, A. I.; Lulli, D.; Fidanza, P.; Kostyuk, V. A.; Luca, C. D; Pastore, S.; Korkina, L. G. Plant polyphenols differentially modulate inflammatory responses of human keratinocytes by interfering with activation of transcription factors NFkappaB and AhR and EGFR-ERK pathway. *Toxicol Appl Pharmacol* **255**:138-149; 2011.

[18] Moyal, D.; Chardon, A.; Kollias, N. UVA protection efficacy of sunscreens can be determined by the persistent pigment darkening (PPD) method. (Part 2). *Photodermatol Photoimmunol Photomed* **16**:250-255; 2000.

[19] Pluemsamran, T.; Onkoksoong, T.; Panich, U. Caffeic acid and ferulic acid inhibit UVA-induced matrix metalloproteinase-1 through regulation of antioxidant defense system in keratinocyte HaCaT cells. *Photochem Photobiol* **88**:961-968; 2012.

[20] Panich, U.; Kongtaphan, K.; Onkoksoong, T.; Jaemsak, K.; Phadungrakwittaya, R.; Thaworn, A.; Akarasereenont, P.; Wongkajornsilp, A. Modulation of antioxidant defense by Alpinia galanga and Curcuma aromatica extracts correlates with their inhibition of UVA-induced melanogenesis. *Cell Biol Toxicol* **26**:103-116; 2010.

[21] Panich, U.; Pluemsamran, T.; Tangsupa-a-nan, V.; Wattanarangsan, J.; Phadungrakwittaya, R.; Akarasereenont, P.; Laohapand, T. Protective effect of AVS073, a polyherbal formula, against UVA-induced melanogenesis through a redox mechanism

involving glutathione-related antioxidant defense. *BMC Complement Altern Med* **13**:159-168; 2013.

[22] Siegel, D,; Kepa, J. K.; Ross, D. Biochemical and genetic analysis of NAD(P)H:quinone oxidoreductase 1 (NQO1). *Curr Protoc Toxicol*; 2007.

[23] Kato, M.; Iida, M.; Goto, Y.; Kondo, T.; Yajima, I. Sunlight exposure-mediated DNA damage in young adults. *Cancer Epidemiol Biomarkers Prev* **20**:1622-8; 2011.

[24] Jian, J.; Pelle, E.; Yang, Q.; Pernodet, N.; Maes, D.; Huang, X. Iron sensitizes keratinocytes and fibroblasts to UVA-mediated matrix metalloproteinase-1 through TNF-alpha and ERK activation. *Exp Dermatol* **20**:249-254; 2011.

[25] Rojo, A. I.; Sagarra, M. R.; Cuadrado, A. GSK-3beta down-regulates the transcription factor Nrf2 after oxidant damage: relevance to exposure of neuronal cells to oxidative stress. *J Neurochem* **105**:192-202; 2008.

[26] Sandberg, M.; Patil, J.; D'Angelo, B.; Weber, S. G.; Mallard, C. NRF2-regulation in brain health and disease: implication of cerebral inflammation. *Neuropharmacology* **79**:298-306; 2014.

[27] Piao, M. J.; Zhang, R.; Lee, N. H.; Hyun, J. W. Phloroglucinol attenuates ultraviolet B radiation-induced matrix metalloproteinase-1 production in human keratinocytes via inhibitory actions against mitogen-activated protein kinases and activator protein-1. *Photochem Photobiol* **88**:381-388; 2012.

[28] Ito, T.; Kimura, S.; Seto, K.; Warabi, E.; Kawachi, Y.; Shoda, J.; Tabuchi, K.; Yamagata, K.; Hasegawa, S.; Bukawa, H.; Ishii, T.; Yanagawa, T. Peroxiredoxin I plays a protective role against UVA irradiation through reduction of oxidative stress. *J Dermatol Sci* **74**:9-17; 2014.

[29] Faraonio, R.; Vergara, P.; Di Marzo, D.; Pierantoni, MG.; Napolitano, M.; Russo, T.; Cimino, F. p53 suppresses the Nrf2-dependent transcription of antioxidant response genes. *J Biol Chem* **281**:39776-39784; 2006.

[30] Hirota, A.; Kawachi, Y.; Itoh, K.; Nakamura, Y.; Xu, X.; Banno, T.; Takahashi, T.; Yamamoto, M.; Otsuka, F. Ultraviolet A irradiation induces NF-E2-related factor 2 activation in dermal fibroblasts: protective role in UVA-induced apoptosis. *J Invest Dermatol* **124**:825-832; 2005.

[31] Kannan, S.; Jaiswal, A. K. Low and high dose UVB regulation of transcription factor NF-E2-related factor 2. *Cancer Res* **66**:8421-8429; 2006.

[32] Chun, K. S.; Kundu, J.; Kundu, J. K.; Surh, Y. J. Targeting Nrf2-Keap1 signaling for chemoprevention of skin carcinogenesis with bioactive phytochemicals. *Toxicol Lett*; 2014.

[33] Paredes-Gonzalez, X.; Fuentes, F.; Su, Z. Y.; Kong, A. N. Apigenin reactivates Nrf2 anti-oxidative stress signaling in mouse skin epidermal JB6 P + cells through epigenetics modifications. *AAPS J* **16**:727-735; 2014.

[34] Filip, A.; Daicoviciu, D.; Clichici, S.; Mocan, T.; Muresan, A.; Postescu, I. D. Photoprotective effects of two natural products on ultraviolet B-induced oxidative stress and apoptosis in SKH-1 mouse skin. *J Med Food* **14**:761-766; 2011.

[35] Andreadi, C. K.; Howells, L. M.; Atherfold, P. A.; Manson, M. M. Involvement of Nrf2, p38, B-Raf, and nuclear factor-kappaB, but not phosphatidylinositol 3-kinase, in induction of hemeoxygenase-1 by dietary polyphenols. *Mol Pharmacol* **69**:1033-1040; 2006.

[36] Wondrak, G. T.; Cabello, C. M.; Villeneuve, N. F.; Zhang, S.; Ley, S.; Li, Y.; Sun, Z.; Zhang, D. D. Cinnamoyl-based Nrf2-activators targeting human skin cell photo-oxidative stress. *Free Radic Biol Med* **45**:385-395; 2008.

[37] Benedict, A. L.; Knatko, E. V.; Dinkova-Kostova, A. T. The indirect antioxidant sulforaphane protects against thiopurine-mediated photooxidative stress. *Carcinogenesis* **33**:2457-2466; 2012.

[38] Tao, S.; Justiniano, R.; Zhang, D. D.; Wondrak, G. T. The Nrf2-inducers tanshinone I and dihydrotanshinone protect human skin cells and reconstructed human skin against solar simulated UV. *Redox Biol* **1**:532-541; 2013.

[39] Zhao, R.; Yang, B.; Wang, L.; Xue, P.; Deng, B.; Zhang, G.; Jiang, S.; Zhang, M.; Liu, M.; Pi, J.; Guan, D. Curcumin protects human keratinocytes against inorganic arsenite-induced acute cytotoxicity through an NRF2-dependent mechanism. *Oxid Med Cell Longev*; 2013.

[40] Tao, S.; Justiniano, R.; Zhang, D. D.; Wondrak, G. T. The Nrf2-inducers tanshinone I and dihydrotanshinone protect human skin cells and reconstructed human skin against solar simulated UV. *Redox Biol* **1**:532-541; 2013.

[41] Sirerol, J. A.; Feddi, F.; Mena, S.; Rodriguez, M. L.; Sirera, P.; Aupi, M.; Perez, S.; Asensi, M.; Ortega, A.; Estrela, J. M. Topical treatment with pterostilbene, a natural phytoalexin, effectively protects hairless mice against UVB radiation-induced skin damage and carcinogenesis. *Free Radic Biol Med* **85**:1-11; 2015.

[42] Lieder ,F.; Reisen, F.; Geppert, T.; Sollberger, G.; Beer, H. D.; auf dem, Keller U.; Schafer, M.; Detmar, M.; Schneider, G.; Werner, S. Identification of UV-protective activators of nuclear factor erythroid-derived 2-related factor 2 (Nrf2) by combining a chemical library screen with computer-based virtual screening. *J Biol Chem* **287**:33001-13; 2012.

Table 1. IC_{30} values of the test compounds for inhibition of tyrosinase activity and melanin content in B16F10 cells exposed to UVA irradiation.

Test compounds	IC_{30} (μM)	
	Inhibition of melanin content	**Inhibition of tyrosinase activity**
Caffeic acid	17.54 ± 4.8**	24.1 ± 6.2***
Ferulic acid	> 30	> 30
Quercetin	7.8 ± 1.4	10.1 ± 3.1
Rutin	15.31 ± 4.7*	18.56 ± 4.2*
Avobenzone	21.94 ± 6.2***	24.25 ± 5.9***

Data are mean ± SD from at least three independent experiments. The statistical significance of differences the IC_{30} values for different compounds was evaluated by one-way ANOVA followed by Tukey's *post hoc* test. *p<0.05; **p<0.01; ***p<0.001 compared with IC_{30} values of QU

FIGURE CAPTIONS

Figure 1. Effects of Nrf2 knockdown on melanogenesis in HEMn and B16F10 cells in response to UVA irradiation. (A) HEMn and B16F10 cells were transfected with 5 nM Nrf2 siRNA (siNrf2) or non-silencing siRNA control (siCtrl) for 48 h. mRNA levels of Nrf2 and its target antioxidants (GCLC, GCLM, GST and NQO1) of HEMn and B16F10 cells transfected with siNrf2 were evaluated by real-time RT-PCR to verify efficiency of siRNA against Nrf2. ***$P < 0.001$ compared with siCtrl-transfected cells. **(B)** Melanin content and **(C)** tyrosinase activity were measured in HEMn and B16F10 cells transfected with siNrf2 or siCtrl at 1 h following UVA (8 J/cm^2) irradiation. **(D)** Tyrosinase protein expression was measured in HEMn and B16F10 cells transfected with siNrf2 or siCtrl at 24 h post-irradiation. Data was expressed as mean ± SD. The statistical significance of differences was evaluated by one-way ANOVA followed by Dunnett's test. ### $P < 0.001$ vs. untransfected cells and siCtrl-transfected cells irradiated with UVA. ***$P < 0.001$ vs. untransfected and siCtrl-transfected cells irradiated with UVA.

Figure 2. The protective effects of test compounds on UVA-induced melanogenesis in B16F10 cells. Cells were pretreated with phenolics (CA, FA, QU and RU) and AV at 7.5-30 μM prior to UVA (8 J/cm^2) exposure. **(A)** Melanin content and **(B)** tyrosinase activity were measured in B16F10 cells at 1 h after UVA irradiation by using colorimetric assay. **(C)** Tyrosinase protein level was examined by western blot analysis at 24 h after UVA irradiation. Data was represented as the means ± SD from at least three independent experiments. The statistical significant of differences between the control and irradiated cells was evaluated by Student's *t* test and between UVA-irradiated and compounds-treated cells by one-way

analysis of variance (ANOVA) with Dunnett's multiple comparison test. ### $P < 0.001$ vs. UVA-irradiated cells. $^{*}P < 0.05$; $^{**}P<0.01$; $^{***}P<0.001$ vs. untreated cells exposed to UVA.

Figure 3. The protective effects of test compounds on UVA-induced oxidative damage and GSH depletion. (A) Inhibition by test compounds (CA, FA, QU, RU and AV) at 7.5-30 μM against UVA-mediated oxidant formation was examined at 1 h after UVA irradiation (8 J/cm^2) and H_2O_2 (250 μM) treatment. Determination of DCFDA was performed by flow cytometry and data was expressed as a percentage of control (100%, non-irradiated and untreated cells). **(B)** 8-OHdG and **(C)** GSH levels were determined at 1 h after UVA irradiation. Data was expressed as mean ± SD from at least three independent experiments. The statistical significance of differences between the control and UVA or H_2O_2-treated cells was evaluated by Student's t test and between UVA or H_2O_2-treated and test compounds-treated cells by one-way ANOVA followed by Dunnett's test. ### $P < 0.001$ vs. UVA or H_2O_2-irradiated cells. $^{*}P < 0.05$; $^{**}P<0.01$; $^{***}P<0.001$ vs. untreated cells sujbected to UVA or H_2O_2 treatment.

Figure 4. The protective effects of test compounds on UVA-induced downrugulation of nuclear Nrf2 levels and Nrf2-ARE transcriptional activity. Time-dependent effects of UVA (8 J/cm^2) on Nrf2 translocation in B16F10 cells harvested at various times after UVA exposure. **(A)** Western blot analysis was performed to measure the Nrf2 translocation at 1, 3, 6 and 12 h. Level of nuclear Nrf2 was detected at 68 kDa, TATA-binding protein (TBP), the loading control for nuclear protein, at 37 kDa and and α-Tubulin, the loading control for cytosol protein, at 50 kDa. **(B)** Nrf2 mRNA was assessed at 15 min, 2, 4 and 8 h after UVA exposure. **(C)** Protection against UVA-induced suppression of Nrf2 protein translocation by test phenolics was assessed by Western blot analysis at 1 h following UVA exposure. **(D)**

Cells were transfected with ARE-luciferase reporter construct and were pretreated with test compounds (CA, QU and AV) at 7.5-30 μM prior to UVA exposure and luciferase activity was measured at 1 h post-irradiation. The data are represented as means ± SD of three independent experiments. The statistical significant of differences between the control and irradiated cells was evaluated by Student's *t* test and between UVA-irradiated and compounds-treated cells by one-way analysis of variance (ANOVA) with Dunnett's multiple comparison test. ### $P < 0.001$ vs. UVA-irradiated cells. $^{*}P < 0.05$; $^{**}P<0.01$; $^{***}P<0.001$ vs. untreated cells exposed to UVA.

Figure 5. The protective effects of test compoundss on UVA-mediated downregulation of Nrf2 target genes. (A) γ-GCL (γ-GCLC and γ-GCLM), **(B)** GST and **(C)** NQO1 mRNA expressions were assessed by real-time RT-PCR analysis at 2 h after UVA irradiation in B16F10 cells pretreated with test compounds (CA, QU and AV). The statistical significant of differences between the control and irradiated cells was evaluated by Student's *t* test and between UVA-irradiated and compounds-treated cells by one-way analysis of variance (ANOVA) with Dunnett's multiple comparison test. ### $P < 0.001$ vs. UVA-irradiated cells. $^{*}P < 0.05$; $^{**}P<0.01$; $^{***}P<0.001$ vs. untreated cells exposed to UVA.

Figure 6. The protective effects of test compounds on UVA-mediated downregulation of Nrf2 target protein and antioxidant enzyme activities. (A) Time-dependent effects of UVA (8 J/cm^2) on Nrf2 target proteins (GCLC, GST and NQO1) in B16F10 cells were determined by Western blot analysis at 3, 6 and 12 h post-irradiation. **(B)** At 6 h after UVA irradiation, Nrf2 target proteins were examined in B16F10 cells pretreated with test compounds (CA, QU and AV) at 7.5-30 μM. GCLC, GST, NQO1 and the loading control (α-Tubulin) were detected at 73, 25, 31 and 50 kDa, respectively. Enzyme activities of **(C)** GST

and **(D)** NQO1 in B16F10 cells pretreated with test compounds (CA, QU and AV) at 6 h after UVA irradiation. The statistical significant of differences between the control and irradiated cells was evaluated by Student's *t* test and between UVA-irradiated and compounds-treated cells by one-way analysis of variance (ANOVA) with Dunnett's multiple comparison test. ### $P < 0.001$ vs. UVA-irradiated cells. $^{*}P < 0.05$; $^{**}P<0.01$; $^{***}P<0.001$ vs. untreated cells exposed to UVA.

FIGURE 1:

F

F

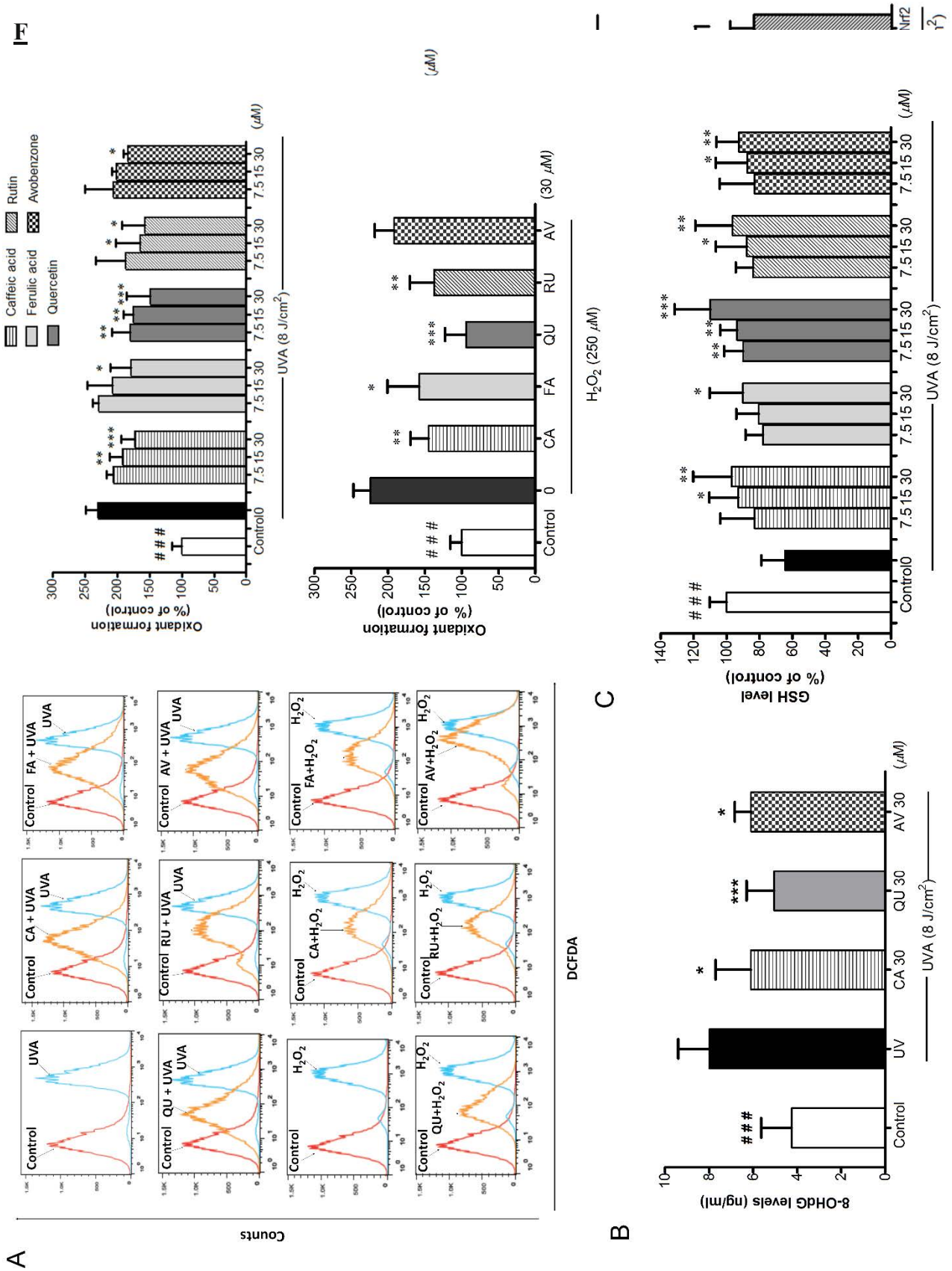
A
Counts
DCFDA
Control
UVA
CA + UVA
FA + UVA
QU + UVA
RU + UVA
AV + UVA
H2O2
CA+H2O2
FA+H2O2
QU+H2O2
RU+H2O2
AV+H2O2
Caffeic acid
Ferulic acid
Quercetin
Rutin
Avobenzone
Oxidant formation (% of control)
UVA (8 J/cm2)
H2O2 (250 μM)
B
8-OHdG levels (ng/ml)
GSH level (% of control)
C
Control
UV
CA 30
QU 30
AV 30
Control0
Nrf2

FIGURE 4:

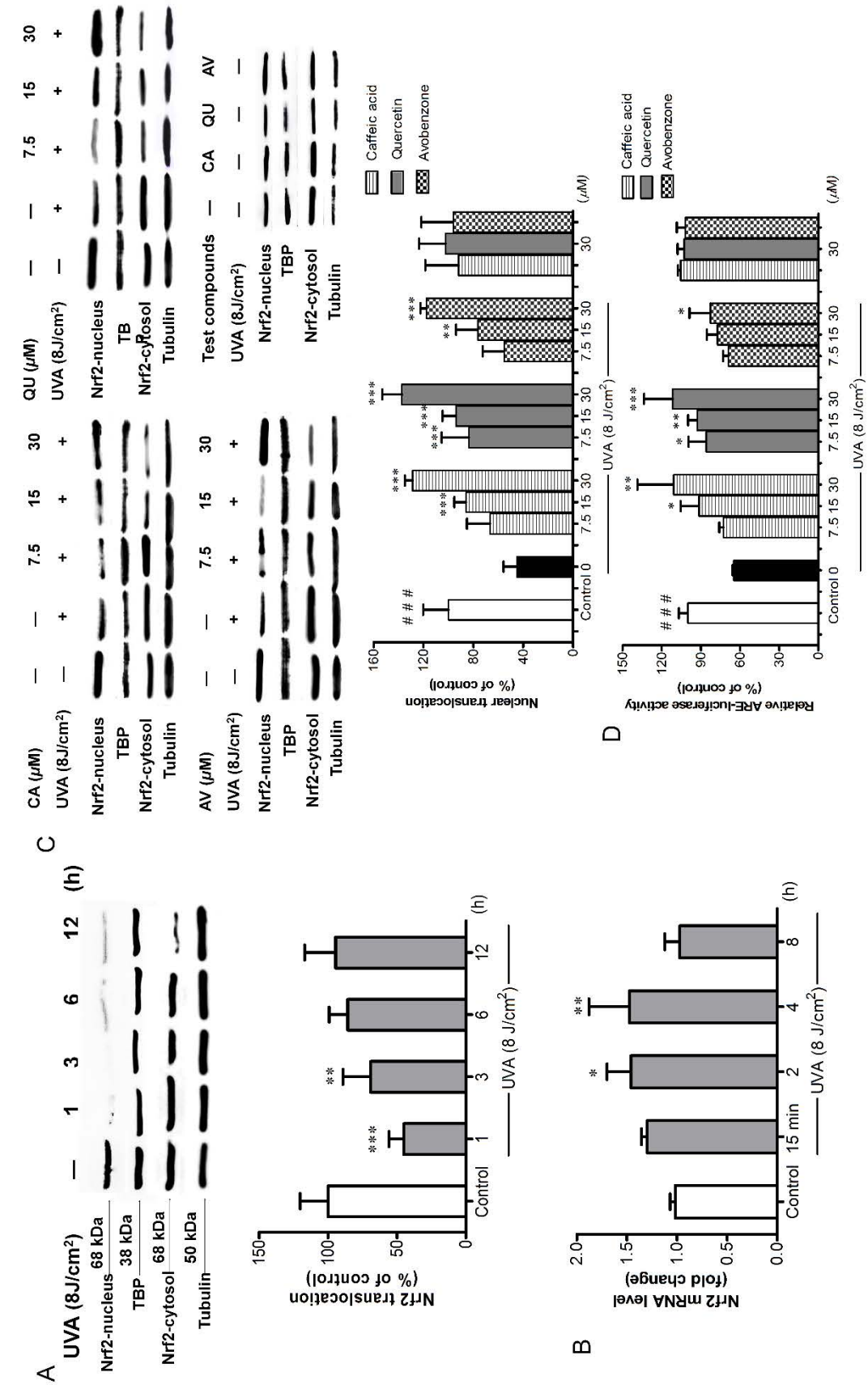
A
UVA (8J/cm²)
Nrf2-nucleus
68 kDa
TBP
38 kDa
Nrf2-cytosol
68 kDa
Tubulin
50 kDa
— 1 3 6 12 (h)
B
Nrf2 mRNA level (fold change)
Control 15 min 2 4 8 (h)
UVA (8 J/cm²)
Nrf2 translocation (% of control)
Control 1 3 6 12 (h)
UVA (8 J/cm²)
C
CA (μM) — — 7.5 15 30
UVA (8J/cm²) — + + + +
Nrf2-nucleus
TBP
Nrf2-cytosol
Tubulin
AV (μM) — — 7.5 15 30
UVA (8J/cm²) — + + + +
Nrf2-nucleus
TBP
Nrf2-cytosol
Tubulin
QU (μM) — — 7.5 15 30
UVA (8J/cm²) — + + + +
Nrf2-nucleus
TB
Nrf2-cytosol
Tubulin
Test compounds — CA QU AV
UVA (8J/cm²) — — — —
Nrf2-nucleus
TBP
Nrf2-cytosol
Tubulin
Caffeic acid
Quercetin
Avobenzone
Nuclear translocation (% of control)
Control 0 7.5 15 30 7.5 15 30 7.5 15 30 (μM)
UVA (8 J/cm²)
D
Caffeic acid
Quercetin
Avobenzone
Relative ARE-luciferase activity (% of control)
Control 0 7.5 15 30 7.5 15 30 7.5 15 30 (μM)
UVA (8 J/cm²)

FIGURE 5:

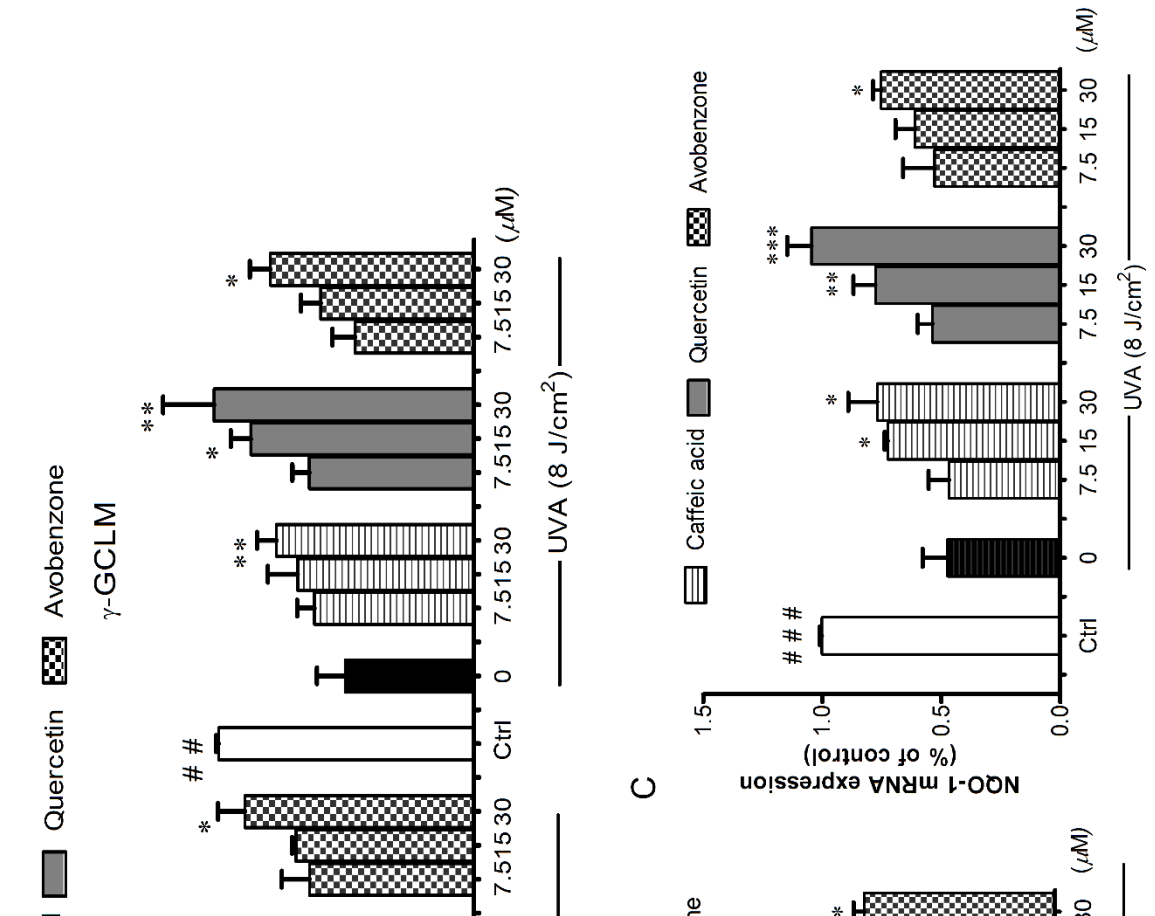
Quercetin
Avobenzone
γ-GCLM
Ctrl
0
7.5 15 30
(μM)
UVA (8 J/cm²)
C
Caffeic acid
Quercetin
Avobenzone
NQO-1 mRNA expression
(% of control)
1.5
1.0
0.5
0.0

FIGURE 6:

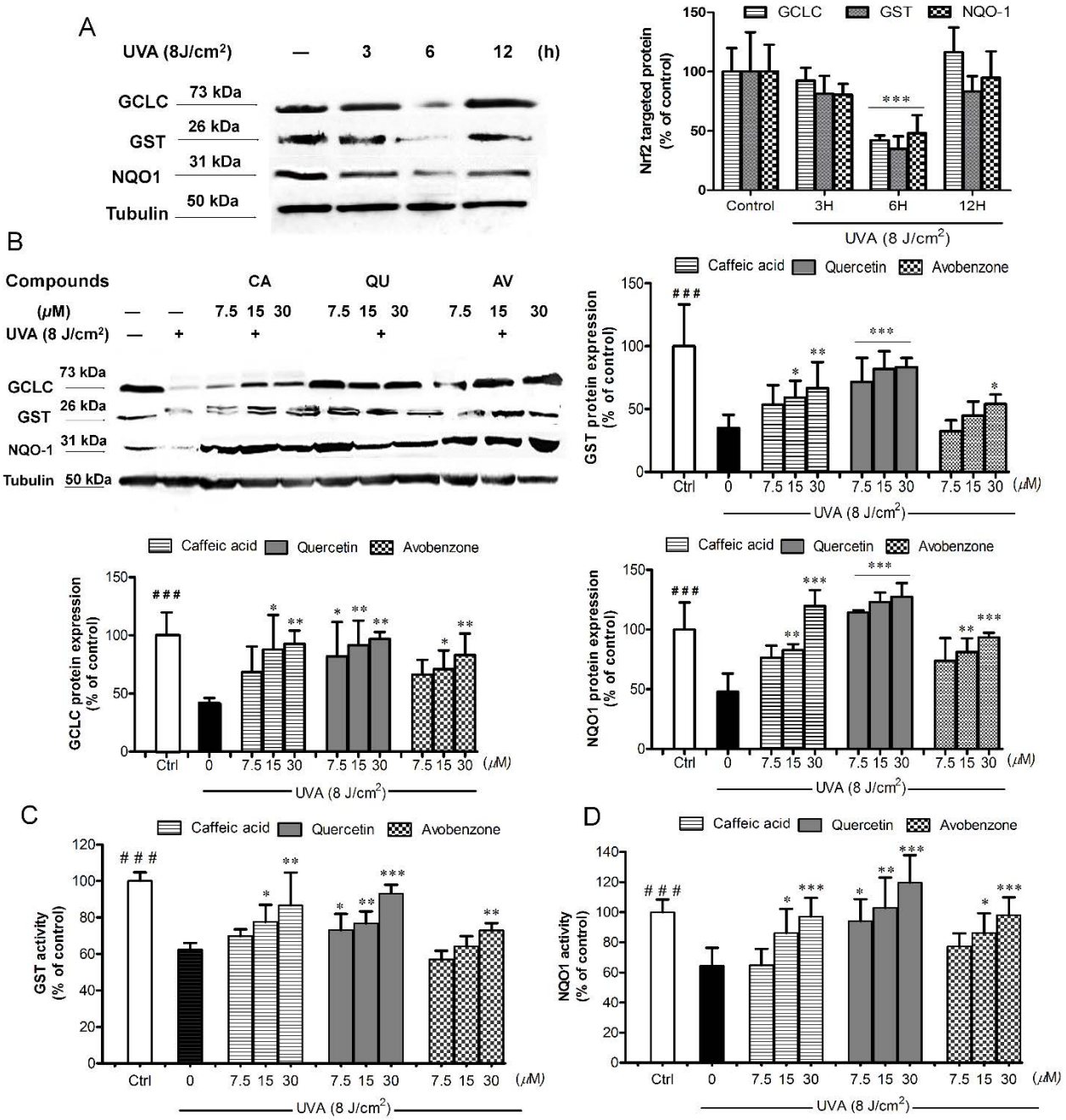
A
UVA (8J/cm²)
—
3
6
12
(h)
GCLC
73 kDa
GST
26 kDa
NQO1
31 kDa
Tubulin
50 kDa
GCLC
GST
NQO-1
Nrf2 targeted protein (% of control)
Control
3H
6H
12H
UVA (8 J/cm²)
B
Compounds
CA
QU
AV
(μM)
UVA (8 J/cm²)
GCLC
GST
NQO-1
Tubulin
Caffeic acid
Quercetin
Avobenzone
GST protein expression (% of control)
GCLC protein expression (% of control)
NQO1 protein expression (% of control)
Ctrl
0
7.5 15 30
(μM)
C
D
GST activity (% of control)
NQO1 activity (% of control)

HIGHLIGHTS

- Depletion of Nrf2 could stimulate melanogenesis under UVA-mediated oxidative stress.
- A single dose of UVA irradiation resulted in time-dependent alterations of Nrf2 nuclear accumulation and its target antioxidant proteins including GCLC, GST and NQO1 B16F10 cells.
- Antioxidant and UVA blocking compounds could effectively provide an early protection against UVA-induced melanogenesis in correlation with their antioxidant potentials through indirect regulatory effect on Nrf2-ARE pathway.
- To avoid excessive activation of Nrf2, which could harm the cells, indirect modulation of Nrf2-ARE pathway to promote redox balance by photoprotective compounds with antioxidant or sunscreen properties may provide a pharmacological insight for protection against photooxidative damage and hyperpigmentation.

Figure 1

Click here to download high resolution image

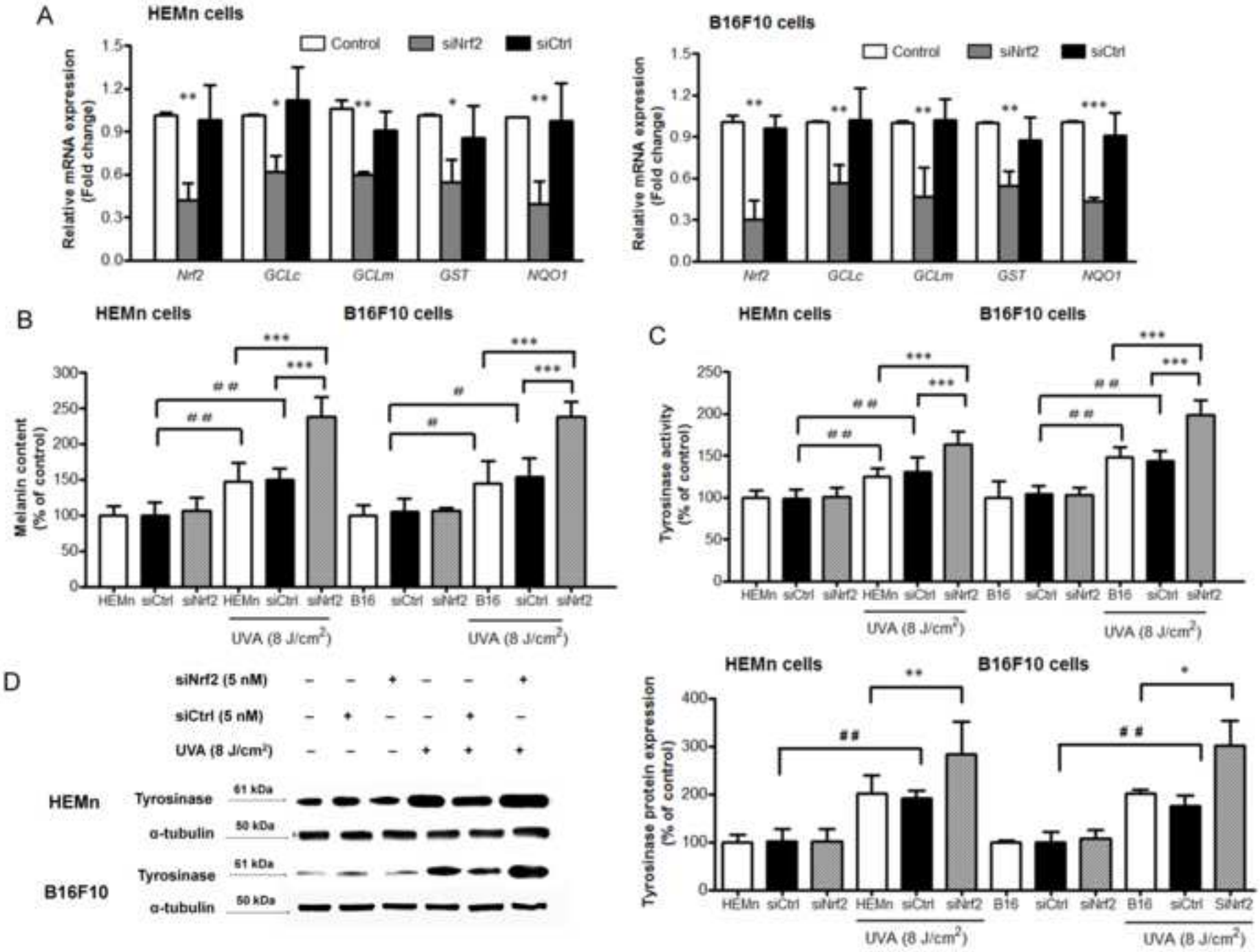

Figure 2

Click here to download high resolution image

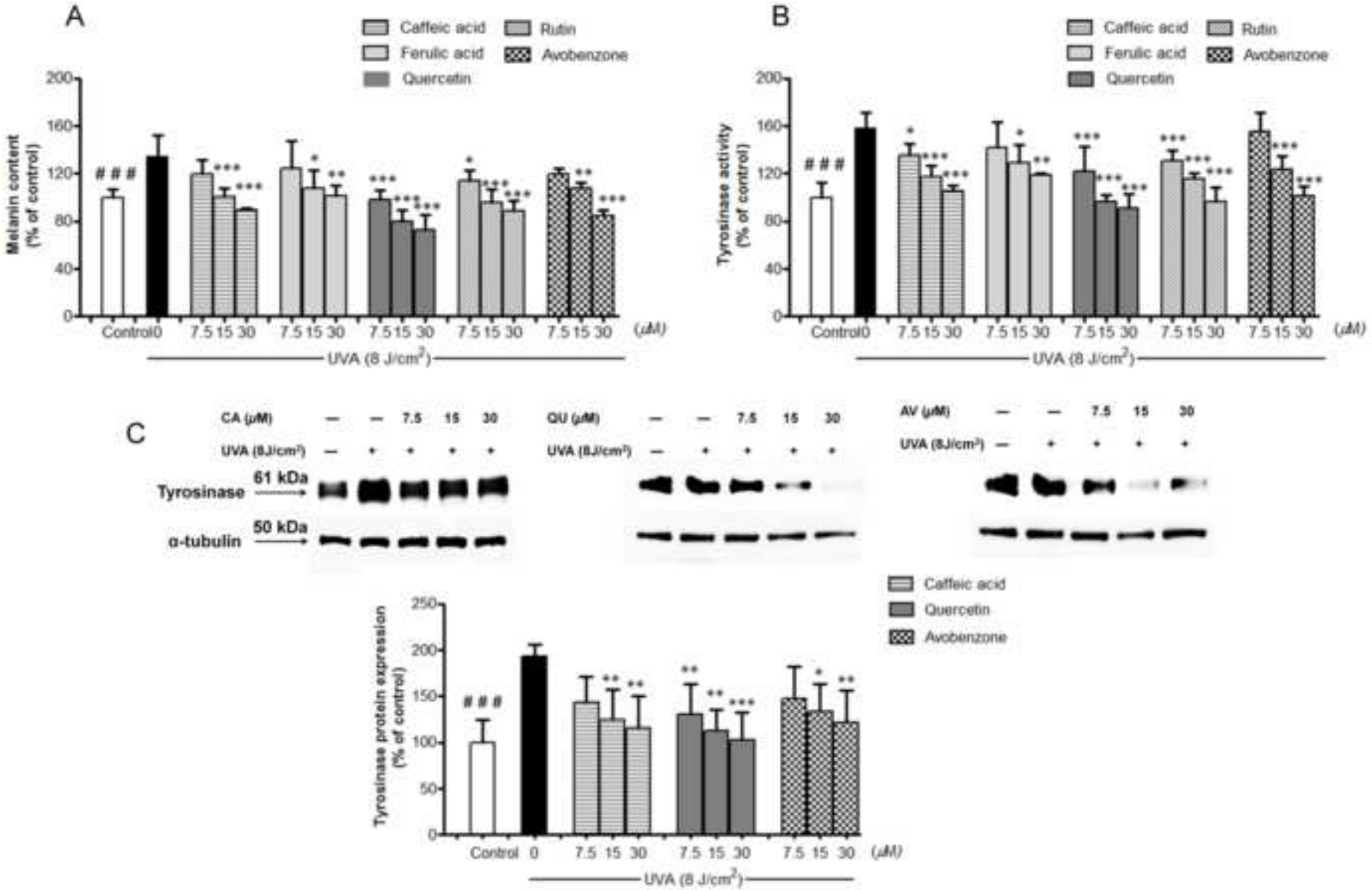

Figure 3

Click here to download high resolution image

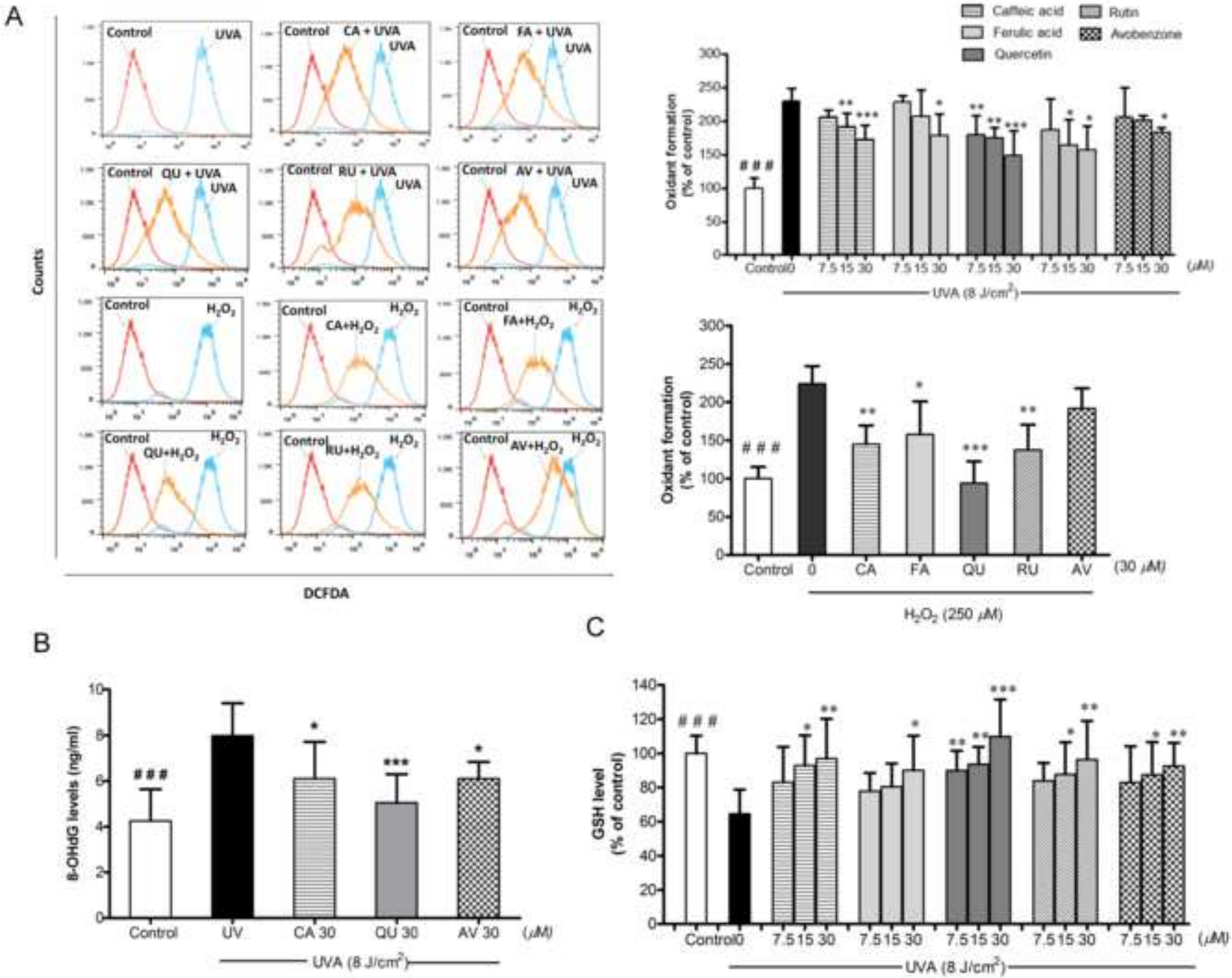

Figure 4

Click here to download high resolution image

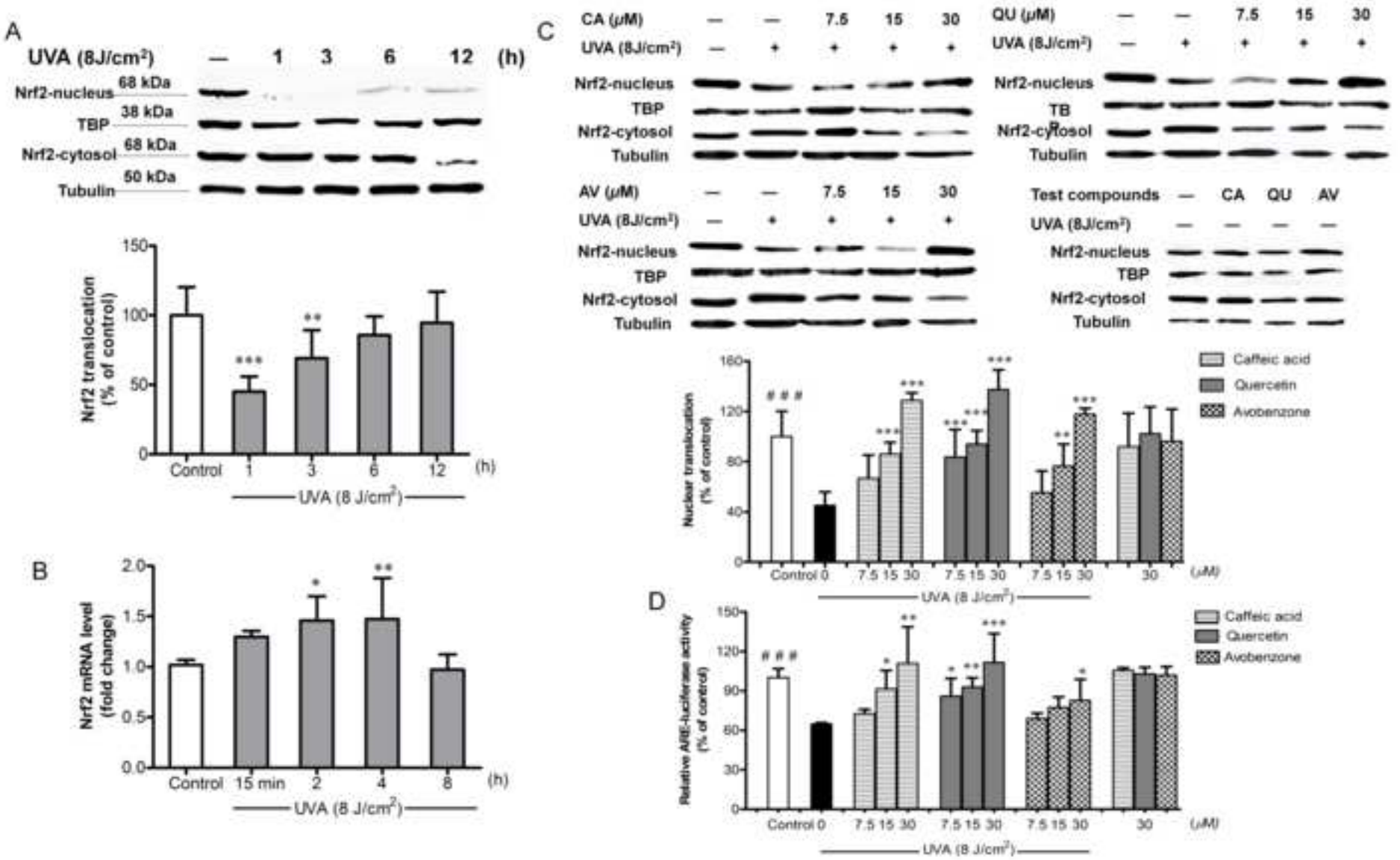

Figure 5

Click here to download high resolution image

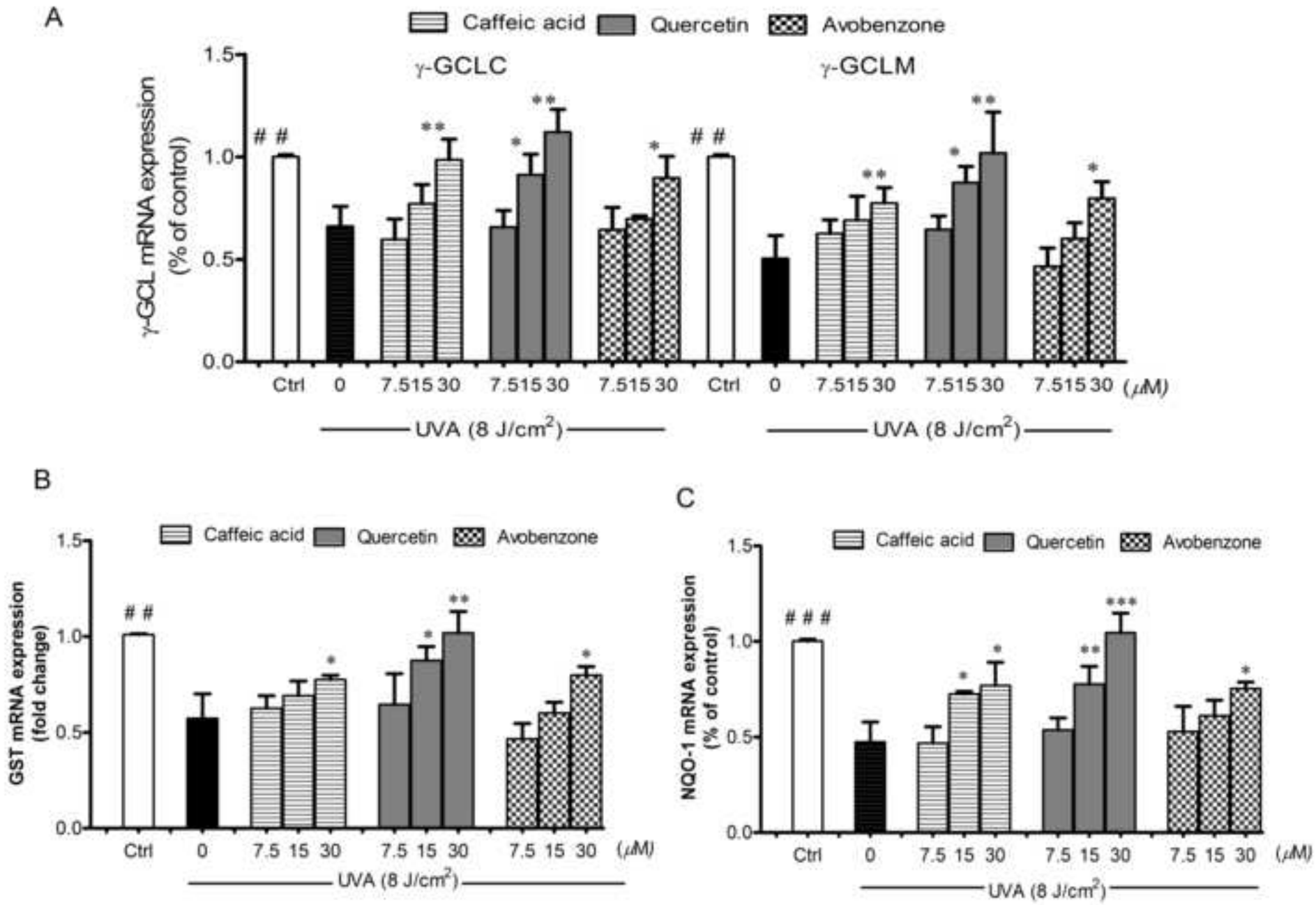

Figure 6

Click here to download high resolution image

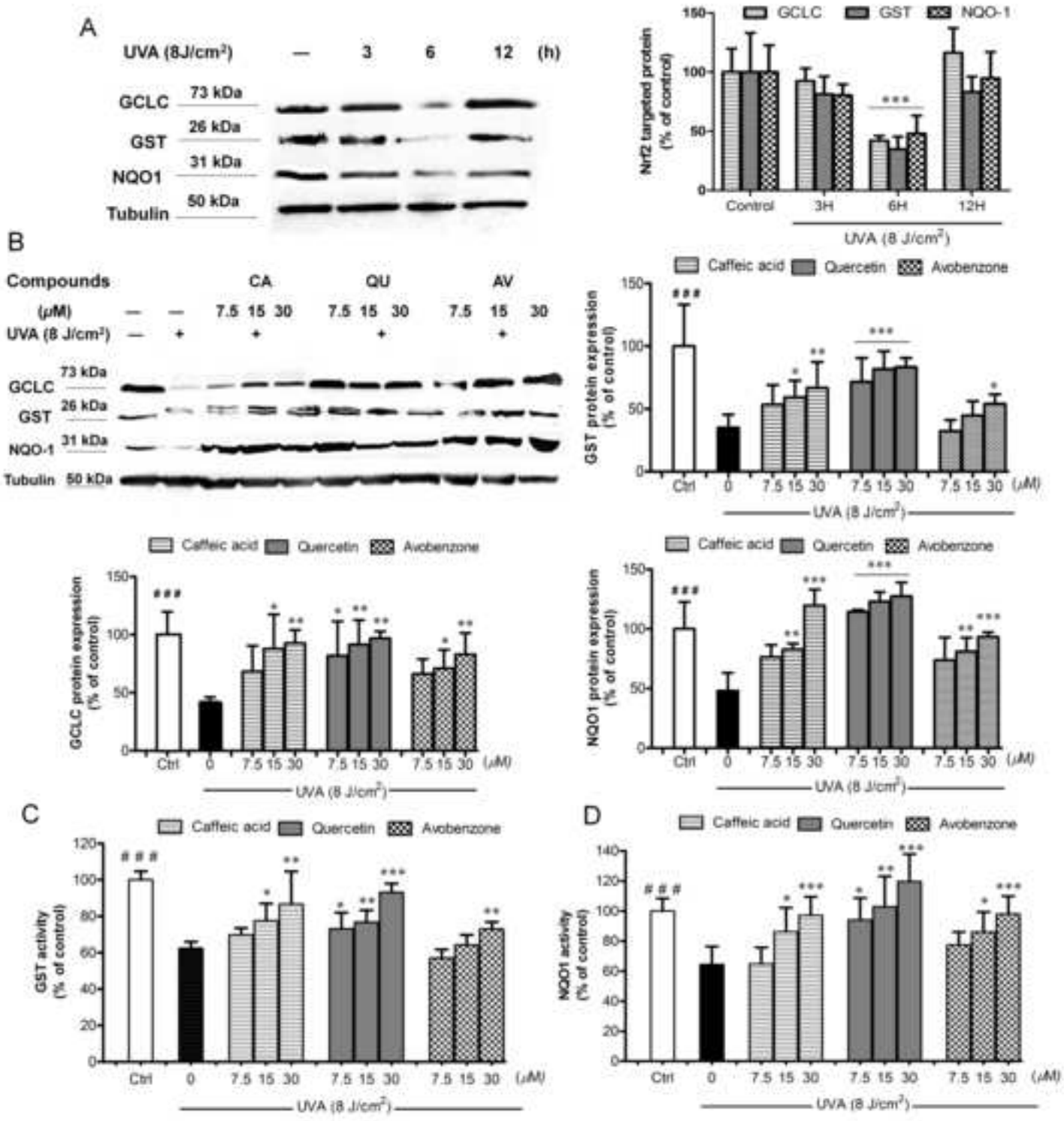

Involvement of oxidative DNA damage and alteration of antioxidant defense system in patients with basal cell carcinoma: a case-control study

Lapatsanant Chaisiriwong[1], Rungsima Wanitphakdeedecha[2], Panitta Sitthinamsuwan[3], Somponnat Sampattavanich[1], Somruedee Chatsiricharoenkul[1], Woraphong Manuskiatti[2], Uraiwan Panich[1]*

[1]Department of Pharmacology, [2]Department of Dermatology and [3]Department of Pathology, Faculty of Medicine Siriraj Hospital, Mahidol University, Bangkok 10700, Thailand

Running title: A case-control study on redox status in basal cell carcinoma

Keywords: oxidative stress, basal cell carcinoma (BCC), oxidative DNA damage, antioxidant defense

Financial support: This research project was supported by Mahidol University, Thailand Research Fund (Grant no. RSA5580012), Faculty of Medicine Siriraj Hospital, Mahidol University, Grant Number (IO) R015532039, and the "Chalermphrakiat" Grant, Faculty of Medicine Siriraj Hospital, Mahidol University.

*Corresponding author: Uraiwan Panich, M.D., Ph.D., Department of Pharmacology, Faculty of Medicine, Siriraj Hospital, Mahidol University, Bangkok 10700, Thailand. Tel.: +66 818155925; Fax: +66 24197565. E-mail: uraiwan.pan@mahidol.ac.th

Disclosure of Potential Conflicts of Interest: No potential conflicts of interest were disclosed.

Total number of figures: 3

Total number of tables: 3

Abstract

Background: Oxidative damage has been suggested to play a role in the pathogenesis of basal cell carcinoma (BCC).

Methods: This study illustrated an involvement of 8-hydroxy-2'-deoxyguanosine (8-OHdG), a biomarker of oxidative DNA damage, and changes in antioxidant defenses including catalase (CAT), glutathione peroxidase (GPx), NAD(P)H: quinone oxidoreductase 1 (NQO1), superoxide dismutase (SOD) activities and glutathione (GSH) in controls and BCC patients pre-surgery and 1-month post-surgery. 8-OHdG levels as well as protein and mRNA expressions of DNA repair enzyme hOGG1 and antioxidant defenses (CAT, glutamate-cysteine ligase (GCL), GPx, Nrf2, MnSOD) in skin tissues of control and BCC subjects were also determined.

Results: This study observed an induction in urinary 8-OHdG levels, increased 8-OHdG expression and reduced hOGG1 protein and mRNA in BCC tissues, decreased antioxidant enzyme activities but elevated SOD activities and GSH levels in BCC patients compared to controls and reduction of all antioxidant proteins and genes studied in BCC tissues. Furthermore, CAT, GPx and NQO1 activities in BCC patients were increased at 1 month and and 8-OHdG levels in BCC patients declined at 6 months post-operation compared with preoperative levels.

Conclusions: We reported for the first time that BCC patients were associated with oxidative DNA damage, defect in hOGG1 and depletion of antioxidant defenses. Surgical removal of BCC tissues correlated with improved oxidative damage.

Impact: Our case-control study identifies that oxidative DNA damage and changes in redox status were associated with BCC and may serve as oxidative stress biomarkers for prediction of BCC development and progression.

Introduction

Basal cell carcinoma (BCC) is the most common non-melanoma skin cancers (NMSC) worldwide, in particular, in fair-skinned population and its incidence has been rising over the past several years (1-3). Although BCC can be generally diagnosed and treated by surgical excision, it can be destructive and has a significance impact on patients' quality of life as the tumor removal can cause morbidity including functional disability and disfigurement. Therefore, it is of significance to understand pathogenesis of BCC in order to develop effective strategies for its detection and prevention. Photo-damage by chronic exposure to ultraviolet radiation (UVR) has been suggested to play a role in the pathogenesis of BCC, which originates from keratinocytes of the epidermal basal layer (4, 5).

Excessive reactive oxygen species (ROS) generated by UVR have been shown to contribute to malignant transformation of keratinocytes into cancerous cells including BCC probably through oxidative DNA damage, defects in DNA repair and interference with cellular signaling (6, 7). The modification of oxidative DNA base at guanine, 8-hydroxy-2'-deoxyguanosine (8-OHdG) pairs between adenine and cytosine during DNA replication, resulting in GC-TA mutations has been found to be associated with development of BCC (8). 8-OHdG has also been recognized to be the most abundant and potentially mutagenic if not substantially repaired and has thus been developed as a sensitive and stable biomarker for evaluating the degree of oxidative DNA damage. Case-control studies have previously reported that increased urinary 8-OHdG levels were detected in patients with metastatic head and neck cancer, breast cancer and lung cancer (9, 10). Furthermore, impaired DNA repair capacity was suggested to associate with enhanced susceptibility to cancer and deficiency in DNA repair enzyme, human 8-oxoguanine DNA N-glycosylase 1 (hOGG1), a key enzyme responsible for the base excision repair of 8-OHdG, may also be involved in carcinogenesis (11).

It has been proposed that promotion of antioxidant defenses including catalase (CAT), glutathione peroxidase (GPx), NAD(P)H: quinone oxidoreductase 1 (NQO1), a crucial detoxifying enzyme and superoxide dismutase (SOD) that can cope with excessive ROS formation in human body and redox regulation of nuclear factor-erythroid-2-related factor 2 (Nrf2) transcription factor may be useful to prevent ROS-mediated neoplastic transformation of various tissues including the skin (12, 13). A link between increased oxidative DNA damage/decreased antioxidant defense capacity and cancer has been proposed and oxidative/antioxidant defense status has thus been intensively investigated as promising biomarkers in cancer (14-16). However, relationship between the oxidative DNA damage/antioxidant defense parameters and BCC and whether surgical removal of tumors affects the redox status in BCC patients have not yet been reported. Here, we conducted a case-control study to investigate whether BCC was associated with the oxidative DNA damage, hOGG1 levels and antioxidant defense status and whether tumor removal affected the redox status of patients with BCC compared to control subjects with non-malignant skin diseases.

Materials and Methods

Study Population

This case-control study involving 37 Thai subjects (mean age, 66 years; range, 39-87 years, 16 males and 21 females) was approved by the ethics committee of the Siriraj Institutional Review Board (SIRB), Faculty of Medicine Siriraj Hospital, Mahidol University, and written informed consent was obtained by all participants. Case group comprising 17 patients newly diagnosed with BCC (mean age, 67 years; range, 41–87 years, 5 males and 12 females) and control group comprising 20 patients with non-malignant skin diseases (mean age, 66 years; range, 39-82 years, 11 males and 9 females) were recruited from the outpatient clinic of the Department of Dermatology, Faculty of Medicine, Siriraj Hospital from 2011 to 2014 and every diagnosis was confirmed by a pathologist. Twenty control subjects diagnosed with non-malignant skin diseases were patients with 7 dermatitis (5 males and 2 females), 2 fibroepithelial polyp (2 males), 1 melanocytic nevus (1 female), 4 normal skin (4 females), 6 seborrheic keratosis (4 males and 2 females).

Data Collection

Data were collected on demographics, clinical characteristics and lifestyle as shown in Table 1. All subjects underwent surgical intervention and the collection of blood, urine and skin tissue samples was done on surgery day prior to operation. At 1 month after surgery, blood samples were collected for evaluation of antioxidant defense parameters and the urinary 8-OHdG levels of BCC patients were determined at both 1 and 6 months after surgery.

Blood samples processing

Blood samples were collected in sodium fluoride tube, EDTA tube and lithium heparin tube for clinical chemistry and antioxidant assays. Whole blood was processed

according to standard protocols and centrifuged at 1,000 X g for 10 minutes at 4 °C and plasma samples were stored at -80 °C until testing.

Urine samples processing

Fresh urine samples were collected in urine container tube for clinical chemistry assays and for oxidative DNA damage assay. Urine samples were processed according to standard protocols and centrifuged at 3,000 X g for 10 minutes at 4 °C, and the supernatants were collected and stored at -80 °C until testing.

Tissue samples processing

The skin tissue samples were obtained from lesions of BCC and non-malignant skin diseases. Tissue samples were divided into 2 parts; the first part was fixed in formalin solution and then embedded in paraffin block for immunohistochemistry and the second part was fixed in liquid nitrogen for real-time RT-PCR until testing.

Determination of 8-OHdG levels in urine by ELISA

Urinary 8-OHdG level was quantified using a competitive enzyme immunoassay following the kit protocol (STA-320, Cell Biolabs, San Diego, CA). Briefly, urine samples or 8-OHdG standards were incubated with an 8-OHdG/BSA conjugate preabsorbed enzyme immunoassay plate and an anti-8-OHdG monoclonal antibody was then added, followed by a secondary reaction with a horseradish peroxidase-conjugated antibody. 8-OHdG levels in the urine of each subject were adjusted by urinary creatinine level and were measured as ng/g creatinine.

Determination of antioxidant defense status in plasma

Catalase (CAT) activity was determined following the kit protocol from Cayman chemical (Ann Arbor, MI). The assay was based on the reaction of methanol and the enzyme in the presence of an optimal concentration of H_2O_2. The formaldehyde produced was

measured colorimetrically at 540 nm using 4-amino-3-hydrazino-5-mercapto-1,2,4-triazole (Purpald) as the chromogen. CAT activity was expressed in unit/mg protein.

Glutathione peroxidase (GPx) activity assay was performed following manufacturer's instruction (Trevigen, Gaithersburg, MD). GPx activity was coupled to glutathione reductase (GR), which catalyzed NADPH-mediated reduction of GSSG back to GSH as previously described (17). The rate of NADPH oxidation by H_2O_2 was monitored at 340 nm and GPx activity was expressed in unit/mg protein.

NQO1 activity was evaluated spectrophotometrically as previously described (18) using 2,6-dichloroindophenol (DCPIP) as a substrate. The assay was based on the activities for NAD(P)H-dependent reduction of DCPIP at 600 nm and the reaction was specifically inhibited by dicumarol. The NQO1 activity was thus measured as the dicumarol inhibitable reduction in absorbance at 600 nm and was expressed as nmole DCPIP reduced/min/mg protein.

Assay for measurement of total superoxide dismutase (SOD) activity was modified following the method of Johns *et al*. (19, 20). and the kit protocol from Cayman chemical (Ann Arbor, MI). Superoxide anions ($O_2^{\bullet-}$) were generated by a xanthine/xanthine oxidase (XOD) system and were detected using 3'-{1-[(phenylamino)-carbonyl]-3,4-tetrazolium}-bis(4-methoxy-6-nitro)benzenesul-fonic acid (XTT) as chromogen. The SOD activity was determined by a decrease in XTT reaction rate at 470 nm as a result of superoxide produced by xanthine/XOD system. The SOD activity was calculated using the following equation: [(0.953) X ((Std.conc. 0 – blank)/(Sample – blank)) - 0.097) X Dilution factor]. Total SOD activity was expressed in unit/mg protein, where one unit of activity was the amount of protein required for a 50% decrease in the rate of XTT reduction.

GSH assay was carried out by glutathione reductase:DTNB enzymatic recycling method following the kit protocol from Sigma-Aldrich (MO, US). Determination of GSH

levels involves GSH oxidation by the sulfhydryl reagent DTNB (5,5′-dithio-bis-2-(nitrobenzoic acid) to produce the yellow TNB (5′-thio-2-nitrobenzoic acid) measured at 412 nm. The glutathione disulfide (GSSG) formed can be recycled to GSH by glutathione reductase in the presence of NADPH. The rate of TNB production is directly proportional to this recycling reaction in turn directly proportional to the concentration of GSH. The GSH level was expressed in nmol/mg protein.

Determination of protein content in plasma by Bradford assay

Protein concentration was measured using the Bio-Rad Protein Assay Kit (Bio-Rad, Munich, Germany) and bovine serum albumin (BSA) was used as protein standard.

Immunohistochemical (IHC) determination of oxidative DNA damage, antioxidant enzyme and hOGG1 expression in skin tissues

Paraffin-embedded tissues were sectioned (2 μm thickness) and placed on Super-FrostPlus glass slides fixed at 60 °C overnight. The sections were deparaffinized in xylene and rehydrated in ethanol series, then incubated in citrate Buffer, pH 6, (DaKo). Slides were incubated with 3% hydrogen peroxide and then with 2% BSA. Slides were incubated with primary antibodies against 8-OHdG (ab48508; Abcam, Cambridge, UK) (1:50), hOGG1 (NB100-106, Novus Biologicals, USA) (1:100), CAT (ab125688, Abcam, Cambridge, UK) (1:200), GCLC (ab53179; Abcam, Cambridge, UK) (1:100), GPx (ab108429, Abcam, Cambridge, UK) (1:50) and Nrf2 (ab31163, Abcam, Cambridge, UK) (1:50). The slides were then incubated with Dako REAL™ EnVision™ Detection System, Peroxidase/DAB+, Rabbit/Mouse for 30 min. Peroxidase activity was visualized with 3, 3-diamino-benzidine tetrahydrochloride (DAB) as the substrate and hematoxylin. All tissues were stained with hematoxylin-eosin (H&E) for detection of cell structure.

IHC staining of all samples was evaluated visually and scored by a pathologist twice in different days. If the IHC staining evaluated in duplicate gave different IHC scores, visual

interpretation of the IHC staining would be repeated. The semi-quantitative analysis of the stained sections was carried out by light-microscopy according to the immunoreactive score (IRS) by Kaemmerer *et al*. (21). The level of antibody staining was evaluated by IRS and calculated by multiplying the scores of staining intensity by the percentage of positive cells. Based on the IRS, antibody staining pattern was defined as IRS – classification score.

Quantitative real-time reverse transcription-polymerase chain reaction: determination of hOGG1, catalase, GCLC, GCLM, GPx, Nrf2, CuSOD, MnSOD

Improm-II™ reverse transcriptase (Promega, Medison, USA) was used to synthesize cDNA from total RNA following the manufacturer's protocol. Sequences for PCR primer sets of genes studied were designed using the Primer Express version 3.0 software (Applied Biosystems, USA). Sequences of PCR primer (in 5′-3′ direction) were as follows: hOGG1 sense (product sizes = 164), TGGAAGAACAGGGCGGGCTA, and antisense, ATGGACATCCACGGGCACAG; CAT sense (product sizes = 148), CCTTCGACCCAA GCAACATG, and antisense, CGAGCACGGTAGGGACAGTTC; GCLC sense (product sizes = 160 bp), GCTGTCTTGCAGGGAATGTT, and antisense, ACACACCTTCCTTCCCATTG; GCLM sense (product sizes = 200 bp), TTGGAGTTGCACAGCTGGATT, and antisense, TGGTTTTACCTGTGCCCACTG; GPx sense (product sizes = 94 bp), ACGATGTTGCCTGGAACTTT, and antisense, TCGATGTCAATGGTCTGGAA; Nrf2 sense (product sizes = 161 bp), TTCTGTTGCTCA GGTAGCCCCTCA, and antisense, GTTTGGCTTCTGGACTTGG; CuSOD sense (product size = 109 bp), TGCTGGTTTGCGTCGTAGTC, and antisense, ACGCACACGGCCTTCGT; MnSOD sense (product size = 141 bp), TGGCCAAGGGAGATGTTACAG, and antisense, CTTCCAGCAACTCCCCTTTG; GAPDH sense (product size = 150 bp), CCTCCAAAATCAAGTGGGGCGATG, antisense, CGAACATGGGGGCATCAGCAGA. Real-time PCR was performed using FastStart

universal SYBR Green Master with ROX (Roche diagnostic, USA) and mRNA expression was quantified by real-time PCR using ABI prism 7300 Real Time PCR System (Applied Biosystems, USA). Melt curve analysis was performed to verify specificity of the amplified product. mRNA expression was normalized to the expression of GAPDH gene. The mean Ct of each gene in each sample was compared with the mean Ct from GAPDH determinations from the same cDNA sample in order to assess mRNA expression. Ct values were then used to calculate fold change in gene expression.

Statistical Analysis

Descriptive statistics were reported as frequencies and percentage. Categorical variables were analyzed by the chi-square test and performed with SPSS 18.0 software (SPSS, Chicago, IL). Data were expressed as means ± standard deviation (SD). The results were subjected to statistical analysis using Prism 5.0 (GraphPad Software, La Jolla, CA, USA). The Shapiro-Wilk test was employed to test the normal distribution. The statistical significance between nonparametric variables was analyzed by Mann Whitney U-test or Kruskal-Wallis test and between parametric variables by unpaired student's t-test or one-way analysis of variance (ANOVA) followed by Tukey's *post hoc* test. P-values less than 0.05 were considered statistically significant. To investigate systematically similarity of biochemical profiles, we performed the principal component analysis using JMP Pro. Data were then ploted using custom MATLAB code.

Results

Demographic, lifestyle and clinical characteristics of the study subjects

Table 1 showed that there were no differences in all characteristics between BCC patients and control subjects, indicating that demographics and clinical characteristics of the study subjects did not affect all parameters of oxidative DNA damage and antioxidant defense status studied.

The urinary 8-OHdG levels and antioxidant defense status in BCC and control subjects.

The urinary 8-OHdG levels and all antioxidant defense parameters studied in BCC and control subjects were shown in Table 2. Oxidative DNA damage was significantly higher in BCC patients compared to control subjects (Fig. 1). After surgery, urinary 8-OHdG levels of BCC patients were insignificantly altered at 1 month, although they were substantially reduced at 6 months compared to preoperative levels (Fig. 1A). In addition, while preoperative values of plasma CAT, GPx and NQO1 activities were observed to be lower in BCC patients compared to control (Fig. 1B-D), plasma total SOD activities and GSH levels were substantially higher in BCC patients compared to control (Fig. 1E-F). In comparison between preoperative and postoperative levels of plasma antioxidant defense status in BCC patients, CAT, GPx and NQO1 activities were increased at 1 month postoperatively, although total SOD activities and GSH levels remained unchanged.

In control subjects, urinary 8-OHdG levels and all antioxidant defense parameters studied were not significantly different between pre- and post-surgery.

We then used the principal component analysis to systematically investigate similarity of DNA damage and antioxidant defense parameters from different groups of patients and to identify co-variation among these parameters (Fig. 1G). Although the first and second principal components explain only 38.3% and 18.1% of the observed variance, we can confirm similar parameter profile between pre-surgery and 1-month post-surgery in the

control group. Patients with BCC, however, demonstrate distinct antioxidant defense parameters between pre- and 1-month post-surgery. Interestingly, the parameters from BCC group at 1-month post-surgery begin to look more similar to the control group, although roughly half of the patients in this group still exhibit unique profiles. This finding implies the inter-patient heterogeneity of antioxidant defense response.

IHC determination of oxidative DNA damage, antioxidant enzyme and hOGG1 expressions in skin tissues of BCC and control subjects

The IHC staining was classified as negative, weak positive, mild positive and strong positive and the data were presented as average IRS scores. H&E staining identified structures of skin sections of case and control subjects as shown in Fig. 2A-C. Table 3 demonstrated that expressions of nuclear 8-OHdG (Fig. 2D,E,G) were higher and hOGG1 protein (Fig. 2H,I,K) in nucleus and cytoplasm were lower in BCC tissues than those in the epidermis of control subjects. Additionally, protein expressions of CAT (Fig. 2L,M,O), GCLC (Fig. 2P,Q,S), GPx, (Fig. 2T,U,W), Nrf2 (Fig. 2X,Y,AA) and MnSOD (Fig. 2AB,AC,AE) were observed to be lower in BCC tissues compared to the epidermis of control subjects. Furthermore, the intra-subject comparison of BCC and adjacent epidermis demonstrated a higher expression of 8-OHdG (Fig. 2E,F,G) and a lower expression of hOGG1 (Fig. 2I,J,K), CAT (Fig. 2M,N,O), GCLC (Fig. 2Q,R,S), GPx (Fig. 2U,V,W), Nrf2 (Fig. 2Y,Z,AA) and MnSOD (Fig. 2AC,AD,AE) in BCC lesions compared to adjacent normal skin. In consistent with our studies for plasma antioxidant defense status showing higher total SOD activities and GSH levels in BCC patients compared with control subjects, protein expressions of GCLC and MnSOD were higher in non-neoplastic tissues of BCC patients compared to both BCC tissues and the epidermis of control subjects.

In comparison of non-cancerous skin lesions and normal skin of control subjects, there were no significant differences in expressions of all parameters studied (data not shown).

mRNA expression of hOGG1 and antioxidant defense system in skin tissues of BCC and control subjects

In agreement with protein expression data, Fig. 3 demonstrated that mRNA expressions of hOGG1 (0.8 ± 0.1-fold decrease, $p < 0.001$), CAT (0.87 ± 0.03-fold decrease, $p < 0.001$), GCLC (0.7 ± 0.1-fold decrease, $p < 0.001$), GCLM (0.3 ± 0.2-fold decrease, $p < 0.001$), GPx (0.8 ± 0.1-fold decrease, $p < 0.001$), Nrf2 (0.6 ± 0.1-fold decrease, $p < 0.001$), CuSOD (0.5 ± 0.2-fold decrease, $p < 0.001$) and MnSOD (0.7 ± 0.1-fold decrease, $p < 0.001$) were substantially lower in BCC tissues than in skin tissues of control subjects.

Discussion

An involvement of oxidative damage in the pathogenesis of BCC has been widely discussed since several studies have shown possible mechanisms through which excessive ROS generation and antioxidant defense impairment may play a role in malignant transformation to NMSC or keratinocytic cancer including BCC (6, 22). Potential mechanisms of carcinogenesis may involve oxidative DNA damage accountable for genomic mutations because attacks on DNA by ROS result in considerable DNA lesions including strand breaks and DNA base oxidation products, in particular 8-OHdG, considered the most potentially mutagenic (23). hOGG1 is highly specific for the removal and repair of 8-OHdG from oxidatively damaged DNA. Increased 8-OHdG formation and/or loss of hOGG1's expression and function were reported to play a role in the development and progression of skin cancers including BCC (24-26). In this study, we conducted a case-control study of BCC risk in association with urinary oxidative DNA damage (8-OHdG) levels as well as expressions of 8-OHdG as well as hOGG1 protein and mRNA in the skin tissues. Our observations indicated elevation of preoperative 8-OHdG levels in urine and its expression in BCC tissues in comparison with epidermis of control subjects. At 1 month after operation, there were no significant changes in urinary 8-OHdG levels in BCC patients compared with preoperative levels, although the postoperative 8-OHdG levels in BCC patients were substantially reduced at 6 months. Hence, it is possible that greater urinary 8-OHdG in BCC patients than in control subjects could be attributed to oxidative stress in neoplastic cells. We also observed decreased protein and mRNA expressions of hOGG1 in BCC tissues in comparison with epidermis of control subjects. Furthermore, the intra-subject comparison of non-lesional and lesional BCC skin demonstrated a higher expression of 8-OHdG and a lower expression of hOGG1 in BCC tissues compared with the adjacent epidermis. Our results are consistent with those from previous case-control studies suggesting a contribution of elevated

oxidative DNA damage and impaired hOGG1 to the development of various cancers including breast, pancreatic, gastric and lung cancers (9, 27-29). Hence, augmented levels of 8-OHdG could be related to a defect in hOGG1 expression in BCC patients that may be deficient in the repair of 8-OHdG, although the mechanism by which hOGG1 impairment contributes to the development of BCC needs further investigation.

A disturbance in redox homeostasis probably contributed to development of multiple tumors including NMSC can be attributed to not only increased oxidative DNA damage but also impaired antioxidant defense capacity (6, 30). Major antioxidant defenses in the human body include GSH and enzymatic antioxidants including GPx and CAT, which neutralize H_2O_2, NQO1, which catalyzes detoxification of various electrophilic toxicants and oxidants and SOD, which dismutates the superoxide radical ($O_2^{\bullet-}$) to H_2O_2. Thus, preoperative and postoperative levels of plasma GSH levels and antioxidant enzyme (CAT, GPx, NQO1 and SOD) activities as well as expressions of related proteins (GCLC, CAT, GPx and MnSOD) and Nrf2, a well-known transcription factor that regulates expression of detoxifying enzyme genes, and levels of the corresponding genes in skin lesions were determined in BCC patients compared with control subjects. Our results indicated that while decreases in CAT, GPx and NQO1 activities in BCC patients and in protein expressions of CAT, GCLC, GPx, Nrf2 and MnSOD in BCC tissues compared to epidermis of control subjects were observed, plasma SOD activities and GSH levels were higher in BCC patients than in control subjects. In correlation with IHC findings showing diminished expressions of all antioxidant proteins in BCC tissues, mRNA levels of the corresponding genes including CAT, GCLC, GCLM, NQO1, Nrf2, CuSOD and MnSOD were also reduced in BCC tissues compared to epidermis of control subjects.

While CAT, GPx and NQO1 activities markedly declined in BCC patients compared to control subjects, elevation of SOD activities and GSH levels was observed in association

with upregulated protein expressions of GCLC, a rate-limiting enzyme in GSH synthesis, and MnSOD in the adjacent non-neoplastic tissues of BCC patients. In agreement with previous studies, lower activities of GPx and CAT as well as higher activities of SOD were observed in patients with oesophageal, gastric and cololectal cancers compared with control subjects (31, 32) and low NQO1 activity was found to be linked to increased risk of acute leukemia (33). NQO1 polymorphism, which can cause reduction of its activity, was reported to affect susceptibility to lung, bladder and colorectal cancers that could either increase or decrease cancer risks associated with ethnicity and exposure to carcinogens (34). Differential expression of antioxidant proteins was found in several cancers. Reduction of CAT and GPx protein expressions was demonstrated in neoplastic tissues of patients with esophageal, colorectal and lung cancers, although both downregulation and overexpression of MnSOD protein in lung and esophageal cancers, respectively, were reported (35-37). In addition, this study demonstrated decreased Nrf2 expression in BCC tissues compared to both adjacent non-neoplastic tissues of BCC patient and non-cancerous tissues of control subjects that was in agreement with previous reports showing down-regulation of Nrf2 and its target genes including NQO1 at mRNA and protein levels during malignant transformation and upregulation of antioxidant mRNA including CAT, GCLC, GCLM, GPx and NQO1 genes by Nrf2 overexpression was able to delay tumor growth (38). Nevertheless, the role of Nrf2 in cancer is complex as it can play a dual role in both cancer prevention and promotion depending on cellular environment (39).

Enhancement of plasma SOD activities and GSH levels in correlation to increased protein expressions of MnSOD and GCLC in the adjacent non-neoplastic tissues of BCC patients may be due to an adaptive response of normal skin cells to persistent elevation of oxidative stress and damage in cancer patients. It has been suggested that upregulation of antioxidant defenses including GSH and MnSOD may serve as the defense mechanisms for

cell survival against stress and inflammatory insults, which can take place during cancer initiation and progression (40). Further investigations are needed to clarify whether an impaired antioxidant system favors ROS accumulation leading to cancer initiation or the antioxidant system may be either downregulated or upregulated as a consequence of alterations in cellular homeostasis and anti-oxidative metabolism in tumor growth and progression. Case-control studies of genetic polymorphisms in DNA repair and antioxidant enzymes in association with BCC risk with a large number of subjects should also be done in future studies.

This study showed that patients with BCC, a locally invasive malignant skin cancer, could exhibit systemic disturbance in redox status. Acute exposure of mice skin to UVA and UVB irradiation was also reported to affect markers of oxidative damage and antioxidant defenses in plasma and non-skin tissues including erythrocytes and liver (41). Furthermore, we demonstrated that surgical intervention could influence oxidative DNA damage and antioxidant defense status only in case patients with BCC but not control subjects with non-malignant skin diseases as tumor removal was observed to be related to improvement of redox status by reducing 8-OHdG levels at 6 months postoperatively and enhancing plasma antioxidant defenses including CAT, GPx and NQO1 activities at 1 month postoperatively.

In conclusion**,** patients with BCC may be under oxidative stress associated with induction of oxidative DNA damage, defects in DNA repair hOGG1 at protein and mRNA levels and reduction of plasma CAT, GPx and NQO1 activities and of all antioxidant proteins and genes studied in the BCC tissues. Surgical removal of BCC tissues correlated with improved redox status. An elevation of plasma total SOD activities and GSH levels as well as protein expressions of MnSOD and GCLC in non-neoplastic tissues of BCC patients may indicate an adaptive response to oxidative stress. Whether oxidative DNA damage and

antioxidant defense parameters can serve as biomarkers of oxidative stress to predict development and progression of BCC needs further studies.

Conflicts of interest

No conflicts of interest were declared in relation to this article.

Acknowledgments

This research project was supported by Mahidol University, Thailand Research Fund (Grant no. RSA5580012), Faculty of Medicine Siriraj Hospital, Mahidol University, Grant Number (IO) R015532039 and the "Chalermphrakiat" Grant, Faculty of Medicine Siriraj Hospital, Mahidol University. We are grateful to Clinical Instructor Sasima Eimpunth, Department of Dermatology, Faculty of Medicine Siriraj Hospital, Mahidol University, for precious advice and support on subject recruitment. Negative and positive control tissues for IHC study were kindly provided by Asst. Prof. Sorawuth Cho-ongsakol and Prof. Ponchai O-Chareonrat, Department of Surgery, Faculty of Medicine Siriraj Hospital, Mahidol University. We are grateful to Miss Kanittar Srisook and Mrs. Ameon Amesombun, Department of pathology, Faculty of Medicine Siriraj Hospital, Mahidol University, for IHC technique, advice and support. We also wish to thank Ms. Phassara Klamsawat and Ms. Phonsuk Yamlexnoi for their assistance in recruiting subjects and managing the database.

References

1. Christenson LJ, Borrowman TA, Vachon CM, Tollefson MM, Otley CC, Weaver AL, et al. Incidence of basal cell and squamous cell carcinomas in a population younger than 40 years. Jama. 2005;294(6):681-90.

2. Flohil SC, Seubring I, van Rossum MM, Coebergh JW, de Vries E, Nijsten T. Trends in Basal cell carcinoma incidence rates: a 37-year Dutch observational study. The Journal of investigative dermatology. 2013;133(4):913-8.

3. Lomas A, Leonardi-Bee J, Bath-Hextall F. A systematic review of worldwide incidence of nonmelanoma skin cancer. Br J Dermatol. 2012;166(5):1069-80.

4. Iannacone MR, Wang W, Stockwell HG, O'Rourke K, Giuliano AR, Sondak VK, et al. Patterns and timing of sunlight exposure and risk of basal cell and squamous cell carcinomas of the skin--a case-control study. BMC cancer. 2012;12:417.

5. Xiang F, Lucas R, Hales S, Neale R. Incidence of nonmelanoma skin cancer in relation to ambient UV radiation in white populations, 1978-2012: empirical relationships. JAMA dermatology. 2014;150(10):1063-71.

6. Sander CS, Hamm F, Elsner P, Thiele JJ. Oxidative stress in malignant melanoma and non-melanoma skin cancer. Br J Dermatol. 2003;148(5):913-22.

7. Tilli CM, Van Steensel MA, Krekels GA, Neumann HA, Ramaekers FC. Molecular aetiology and pathogenesis of basal cell carcinoma. Br J Dermatol. 2005;152(6):1108-24.

8. Kunisada M, Yogianti F, Sakumi K, Ono R, Nakabeppu Y, Nishigori C. Increased expression of versican in the inflammatory response to UVB- and reactive oxygen species-induced skin tumorigenesis. The American journal of pathology. 2011;179(6):3056-65.

9. Rozalski R, Gackowski D, Roszkowski K, Foksinski M, Olinski R. The level of 8-hydroxyguanine, a possible repair product of oxidative DNA damage, is higher in urine of cancer patients than in control subjects. Cancer epidemiology, biomarkers & prevention : a publication of the American Association for Cancer Research, cosponsored by the American Society of Preventive Oncology. 2002;11(10 Pt 1):1072-5.

10. Kuo HW, Chou SY, Hu TW, Wu FY, Chen DJ. Urinary 8-hydroxy-2'-deoxyguanosine (8-OHdG) and genetic polymorphisms in breast cancer patients. Mutation research. 2007;631(1):62-8.

11. Shinmura K, Yokota J. The OGG1 gene encodes a repair enzyme for oxidatively damaged DNA and is involved in human carcinogenesis. Antioxidants & redox signaling. 2001;3(4):597-609.

12. Acharya A, Das I, Chandhok D, Saha T. Redox regulation in cancer: a double-edged sword with therapeutic potential. Oxidative medicine and cellular longevity. 2010;3(1):23-34.

13. Bickers DR, Athar M. Oxidative stress in the pathogenesis of skin disease. The Journal of investigative dermatology. 2006;126(12):2565-75.

14. Knasmuller S, Nersesyan A, Misik M, Gerner C, Mikulits W, Ehrlich V, et al. Use of conventional and -omics based methods for health claims of dietary antioxidants: a critical overview. The British journal of nutrition. 2008;99 E Suppl 1:ES3-52.

15. Koedrith P, Seo YR. Advances in carcinogenic metal toxicity and potential molecular markers. International journal of molecular sciences. 2011;12(12):9576-95.

16. Loft S, Danielsen P, Lohr M, Jantzen K, Hemmingsen JG, Roursgaard M, et al. Urinary excretion of 8-oxo-7,8-dihydroguanine as biomarker of oxidative damage to DNA. Archives of biochemistry and biophysics. 2012;518(2):142-50.

17. Pluemsamran T, Onkoksoong T, Panich U. Caffeic acid and ferulic acid inhibit UVA-induced matrix metalloproteinase-1 through regulation of antioxidant defense system in keratinocyte HaCaT cells. Photochemistry and photobiology. 2012;88(4):961-8.

18. Siegel D, Kepa JK, Ross D. Biochemical and genetic analysis of NAD(P)H:quinone oxidoreductase 1 (NQO1). Current protocols in toxicology / editorial board, Mahin D Maines. 2007;Chapter 4:Unit4 22.

19. Johns EJ, O'Shaughnessy B, O'Neill S, Lane B, Healy V. Impact of elevated dietary sodium intake on NAD(P)H oxidase and SOD in the cortex and medulla of the rat kidney. American journal of physiology Regulatory, integrative and comparative physiology. 2010;299(1):R234-40.

20. Monk LS, Fagerstedt KV, Crawford RM. Superoxide Dismutase as an Anaerobic Polypeptide : A Key Factor in Recovery from Oxygen Deprivation in Iris pseudacorus? Plant physiology. 1987;85(4):1016-20.

21. Kaemmerer D, Peter L, Lupp A, Schulz S, Sanger J, Baum RP, et al. Comparing of IRS and Her2 as immunohistochemical scoring schemes in gastroenteropancreatic neuroendocrine tumors. International journal of clinical and experimental pathology. 2012;5(3):187-94.

22. Rizzato C, Canzian F, Rudnai P, Gurzau E, Stein A, Koppova K, et al. Interaction between functional polymorphic variants in cytokine genes, established risk factors and susceptibility to basal cell carcinoma of skin. Carcinogenesis. 2011;32(12):1849-54.

23. Kryston TB, Georgiev AB, Pissis P, Georgakilas AG. Role of oxidative stress and DNA damage in human carcinogenesis. Mutation research. 2011;711(1-2):193-201.

24. Huang XX, Scolyer RA, Abubakar A, Halliday GM. Human 8-oxoguanine-DNA glycosylase-1 is downregulated in human basal cell carcinoma. Molecular genetics and metabolism. 2012;106(1):127-30.

25. Kunisada M, Sakumi K, Tominaga Y, Budiyanto A, Ueda M, Ichihashi M, et al. 8-Oxoguanine formation induced by chronic UVB exposure makes Ogg1 knockout mice susceptible to skin carcinogenesis. Cancer research. 2005;65(14):6006-10.

26. Murtas D, Piras F, Minerba L, Ugalde J, Floris C, Maxia C, et al. Nuclear 8-hydroxy-2'-deoxyguanosine as survival biomarker in patients with cutaneous melanoma. Oncology reports. 2010;23(2):329-35.

27. Chang CH, Hsiao CF, Chang GC, Tsai YH, Chen YM, Huang MS, et al. Interactive effect of cigarette smoking with human 8-oxoguanine DNA N-glycosylase 1 (hOGG1) polymorphisms on the risk of lung cancer: a case-control study in Taiwan. American journal of epidemiology. 2009;170(6):695-702.

28. Hocevar BA, Kamendulis LM, Pu X, Perkins SM, Wang ZY, Johnston EL, et al. Contribution of environment and genetics to pancreatic cancer susceptibility. PloS one. 2014;9(3):e90052.

29. Ma Y, Zhang L, Rong S, Qu H, Zhang Y, Chang D, et al. Relation between gastric cancer and protein oxidation, DNA damage, and lipid peroxidation. Oxidative medicine and cellular longevity. 2013;2013:543760.

30. Trachootham D, Lu W, Ogasawara MA, Nilsa RD, Huang P. Redox regulation of cell survival. Antioxidants & redox signaling. 2008;10(8):1343-74.

31. Dursun H, Bilici M, Uyanik A, Okcu N, Akyuz M. Antioxidant enzyme activities and lipid peroxidation levels in erythrocytes of patients with oesophageal and gastric cancer. The Journal of international medical research. 2006;34(2):193-9.

32. Maffei F, Angeloni C, Malaguti M, Moraga JM, Pasqui F, Poli C, et al. Plasma antioxidant enzymes and clastogenic factors as possible biomarkers of colorectal cancer risk. Mutation research. 2011;714(1-2):88-92.

33. Smith MT, Wang Y, Kane E, Rollinson S, Wiemels JL, Roman E, et al. Low NAD(P)H:quinone oxidoreductase 1 activity is associated with increased risk of acute leukemia in adults. Blood. 2001;97(5):1422-6.

34. Chao C, Zhang ZF, Berthiller J, Boffetta P, Hashibe M. NAD(P)H:quinone oxidoreductase 1 (NQO1) Pro187Ser polymorphism and the risk of lung, bladder, and colorectal cancers: a meta-analysis. Cancer epidemiology, biomarkers & prevention : a

publication of the American Association for Cancer Research, cosponsored by the American Society of Preventive Oncology. 2006;15(5):979-87.

35. Chung-man Ho J, Zheng S, Comhair SA, Farver C, Erzurum SC. Differential expression of manganese superoxide dismutase and catalase in lung cancer. Cancer research. 2001;61(23):8578-85.

36. Murawaki Y, Tsuchiya H, Kanbe T, Harada K, Yashima K, Nozaka K, et al. Aberrant expression of selenoproteins in the progression of colorectal cancer. Cancer letters. 2008;259(2):218-30.

37. Zhang J, Wang K, Zhang J, Liu SS, Dai L, Zhang JY. Using proteomic approach to identify tumor-associated proteins as biomarkers in human esophageal squamous cell carcinoma. Journal of proteome research. 2011;10(6):2863-72.

38. Funes JM, Henderson S, Kaufman R, Flanagan JM, Robson M, Pedley B, et al. Oncogenic transformation of mesenchymal stem cells decreases Nrf2 expression favoring in vivo tumor growth and poorer survival. Molecular cancer. 2014;13:20.

39. Moon EJ, Giaccia A. Dual roles of NRF2 in tumor prevention and progression: possible implications in cancer treatment. Free radical biology & medicine. 2015;79:292-9.

40. Reuter S, Gupta SC, Chaturvedi MM, Aggarwal BB. Oxidative stress, inflammation, and cancer: how are they linked? Free radical biology & medicine. 2010;49(11):1603-16.

41. Svobodova AR, Galandakova A, Sianska J, Dolezal D, Ulrichova J, Vostalova J. Acute exposure to solar simulated ultraviolet radiation affects oxidative stress-related biomarkers in skin, liver and blood of hairless mice. Biological & pharmaceutical bulletin. 2011;34(4):471-9.

Table

Table 1. Demographics and clinical characteristics of controls subjects and BCC patients.

Characteristics	Control (n=20)	Cases (n=17)	*p*-value
Demographic			
Age (years)	65.65 ± 11.24	66.82 ± 12.71	0.714[b]
Gender, n (%)			
Male	11(55.00)	5(29.40)	0.117[a]
Female	9(45.00)	12(70.60)	
BMI (kg/ m^2)	23.62 ± 2.53	22.98 ± 3.63	0.217[b]
Clinical characteristics			
Glucose (mg/dl)	96.90 ± 13.00	101.60 ±15.46	0.317[c]
BUN (mg/dl)	13.78 ± 4.06	14.32 ± 5.59	0.891[b]
Creatinine (mg/dl)	1.06 ± 0.25	1.05 ± 0.28	0.949[c]
Cholesterol (mg/dl)	191.20 ± 38.70	201.8 ± 37.52	0.407[c]
Triglyceride (mg/dl)	135.20 ± 66.10	109.8 ± 47.55	0.156[b]
HDL-Chol (mg/dl)	59.55 ± 20.09	63.59 ± 18.95	0.402[b]
LDL-Cal (mg/dl)	104.60 ± 33.28	116.2 ± 34.08	0.110[b]
AST (U/L)	28.30 ± 12.76	26.82 ± 14.81	0.359[b]
ALT (U/L)	21.50 ± 9.90	21.29 ± 13.91	0.593[b]
eGFR (mL/min/1.73 m^2)	66.55 ± 20.65	65.24 ± 20.77	0.849[c]
CBC			
Hemoglobin (g/dl)	13.37 ± 1.87	12.84 ± 1.38	0.200[b]
Rbc count (X 10^6/ul)	4.65 ± 0.65	4.49 ± 0.53	0.404[c]
Wbc count (X 10^3/ul)	7.05 ± 1.76	7.63 ± 1.63	0.195[b]
Lifestyle			
Smoking, n (%)			
Non-Smoker	14(70.0)	14(82.5)	1.265[a]
Ex-Smoker	5(25.0)	3(16.7)	
Current Smoker	1(5.0)	0(0)	
Drinking alcohol, n (%)			
Non-Drinker	15(75.0)	14(82.4)	0.940[a]
Ex-Drinker	4(20.0)	3(17.6)	
Current Drinker	1(5.0)	0(0)	

Abbreviations: BMI = Body Mass Index, BUN = Blood Urea Nitrogen, HDL-Chol = High Density Lipoprotein-Cholesterol, LDL-Cal = Calculated Low Density Lipoprotein Cholesterol, AST = Aspartate aminotransferase, ALT = Alanine aminotransferase, eGFR = estimated glomerular filtration rate, CBC = Complete Blood Count, RBC = Red Blood Cell, Wbc = White blood cell. Data are presented as the mean ± SD. The statistical significance of differences in categorical variables data was evaluated by chi-square test (a), nonparametric variables was analysed by the Mann-Whitney U test (b) and parametric variables by unpaired student's t-test (c).

Table 2. Comparison of urinary oxidative DNA damage levels and plasma antioxidant defense status between control subjects and BCC patients.

Parameters	Controls (n = 20)		Cases (n = 17)		
	Before surgery	1 month after surgery	Before surgery	1 month after surgery	6 months after surgery
8-OHdG (ng/g creatinine)	63.68 ± 15.57	75.36 ± 17.97	105.79 ± 30.52***	102.91 ± 27.33***	66.86±20.19$^{\#\#\#}$
CAT (unit/mg protein)	4.21 ± 0.77	3.82 ± 0.63	2.62 ± 0.45***	4.01 ± 1.15$^{\#\#\#}$	
GPx (unit/mg protein)	0.73 ± 0.20	0.73 ± 0.20	0.45 ± 0.14***	0.73 ± 0.11$^{\#\#\#}$	
NQO1 (μmole DCPIP reduced/min/mg protein)	888.33 ± 198.64	968.97 ± 165.71	710.71 ± 134.46**	1009.64 ± 306.05$^{\#\#\#}$	
Total SOD (unit/mg protein)	0.02 ± 0.01	0.02 ± 0.00	0.03 ± 0.01***	0.04 ± 0.01***	
GSH (μmol/mg protein)	161.29 ± 42.35	164.40 ± 40.27	223.43 ± 42.29***	206.69 ± 51.88*	

Results were expressed as mean ± standard deviation (SD).

$^{*}P < 0.05$, $^{**}P < 0.01$, $^{***}P < 0.001$ compared to control, before surgery.

$^{\#}P < 0.05$, $^{\#\#}P < 0.01$, $^{\#\#\#}P < 0.001$ compared to case, before surgery.

Table 3. Expressions of oxidative DNA damage, DNA repair enzyme and antioxidant proteins in skin tissues of control subjects and BCC patients by IRS score.

Parameters	Controls (n = 20)	Cases (n = 17)	
	Epidermis	BCC	Adjacent epidermis
8-OHdG	2.35 ± 0.67	2.88 ± 0.33*	2.13 ± 0.74$^{\#}$
hOGG1	2.60 ± 0.50	1.76 ± 0.44***	2.59 ± 0.51$^{\#\#\#}$
CAT	2.10 ± 0.64	1.00 ± 0.35***	2.00 ± 0.54$^{\#\#\#}$
GCLC	2.30 ± 0.47	1.56 ± 0.62*	2.88 ± 0.33$^{*,\#\#\#}$
GPx	2.05 ± 0.39	1.06 ± 0.24***	1.73 ± 0.46$^{\#\#\#}$
Nrf2	2.45 ± 0.61	1.53 ± 0.51***	2.31 ± 0.48$^{\#\#}$
MnSOD	2.00 ± 0.56	1.24 ± 0.66*	2.66 ± 0.49$^{*,\#\#\#}$

Results were expressed as mean ± standard deviation (SD).

$^{*}P < 0.05$, $^{***}P < 0.001$ compared to epidermis of control.

$^{\#}P < 0.05$, $^{\#\#}P < 0.01$, $^{\#\#\#}P < 0.001$ compared to BCC lesion.

Figure legends

Figure 1. The urinary 8-OHdG levels (A) and plasma antioxidant defense status [CAT (B), GPx (C), NQO1 (D) and total SOD (E) activities and GSH levels (F)] in control subjects and BCC patients before and after surgery. Values given are mean ± SD. The statistical significance of differences between the control and case was evaluated by one-way ANOVA followed by Tukey's *post hoc* test. * $P < 0.05$, ** $P < 0.01$, ***$P < 0.001$ compared to preoperative values in control subjects prior to surgery, $^{###}P < 0.001$ compared to preoperative values in BCC patients prior to surgery. Principal component analysis was performed to systematically investigate similarity of DNA damage and antioxidant defense parameters from different groups of patients (G). Factor analysis is overlaid on top of the patient scores, both for pre-surgery (case: triangle; control: square) and 1-month post-surgery (case: circle; control: plus). The dashed and dotted ovals delineate the approximated distribution of each group with 95% confidence intervals.

Figure 2. The H&E staining (A-C) and IHC staining for oxidative DNA damage, 8-OHdG (D-G), DNA repair enzyme, hOGG1 (H-K), and antioxidant proteins, CAT (L-O), GCLC (P-S), GPx (T-W), Nrf2 (X-AA) and MnSOD (AB-AE), in control subjects and tumor and non-tumor lesions of BCC patients. Values given are mean ± SD. The statistical significance of differences between the control and case was evaluated by nonparametric variables with Kruskal-Wallis test followed by Dunnett's *post hoc* test. *$P < 0.05$, **$P < 0.01$, ***$P < 0.001$ compared to control, $^{#}P < 0.05$, $^{##}P < 0.01$, $^{###}P < 0.001$ compared to tumor lesions of BCC patients.

Figure 3. DNA repair and antioxidant gene expression in non-malignant skin tissues of control subjects and BCC tissues. Gene expression was evaluated by real-time PCR with the $2^{-\Delta\Delta Ct}$ method. The data are presented as the fold change in gene expression normalized to GAPDH. Values given are mean ± SD. The statistical significance of differences between the

control and case was evaluated by nonparametric variables with Mann Whitney U-test. ***$P < 0.001$ compared to control.

Figure 1

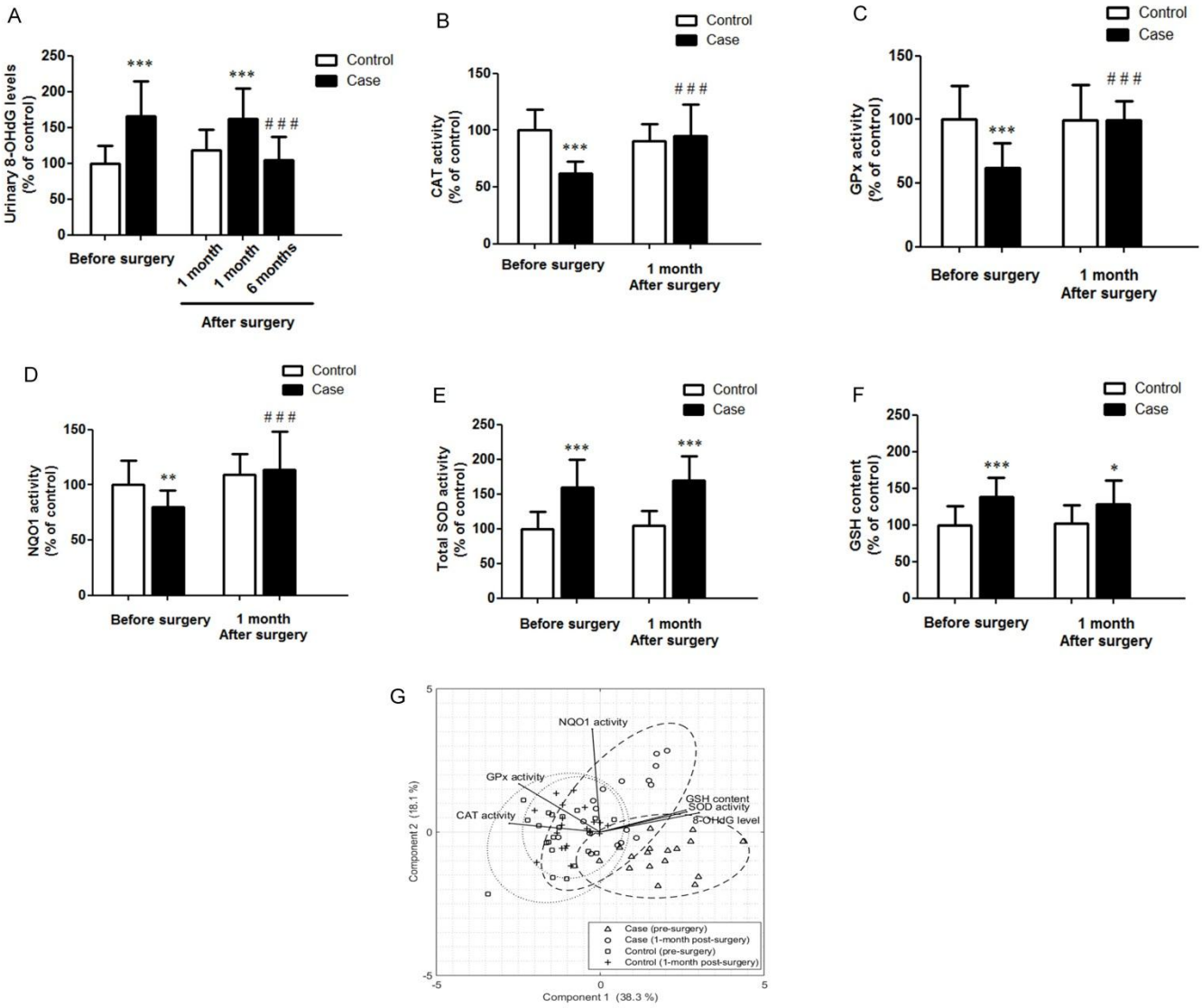
A
Urinary 8-OHdG levels (% of control)
Control
Case
***
***
###
Before surgery
1 month
1 month
6 months
After surgery
B
CAT activity (% of control)
Control
Case
***
###
Before surgery
1 month
After surgery
C
GPx activity (% of control)
Control
Case
***
###
Before surgery
1 month
After surgery
D
NQO1 activity (% of control)
Control
Case
**
###
Before surgery
1 month
After surgery
E
Total SOD activity (% of control)
Control
Case
***
***
Before surgery
1 month
After surgery
F
GSH content (% of control)
Control
Case
***
*
Before surgery
1 month
After surgery
G
NQO1 activity
GPx activity
CAT activity
GSH content
SOD activity
8-OHdG level
Component 2 (18.1 %)
Component 1 (38.3 %)
Case (pre-surgery)
Case (1-month post-surgery)
Control (pre-surgery)
Control (1-month post-surgery)

Figure 2

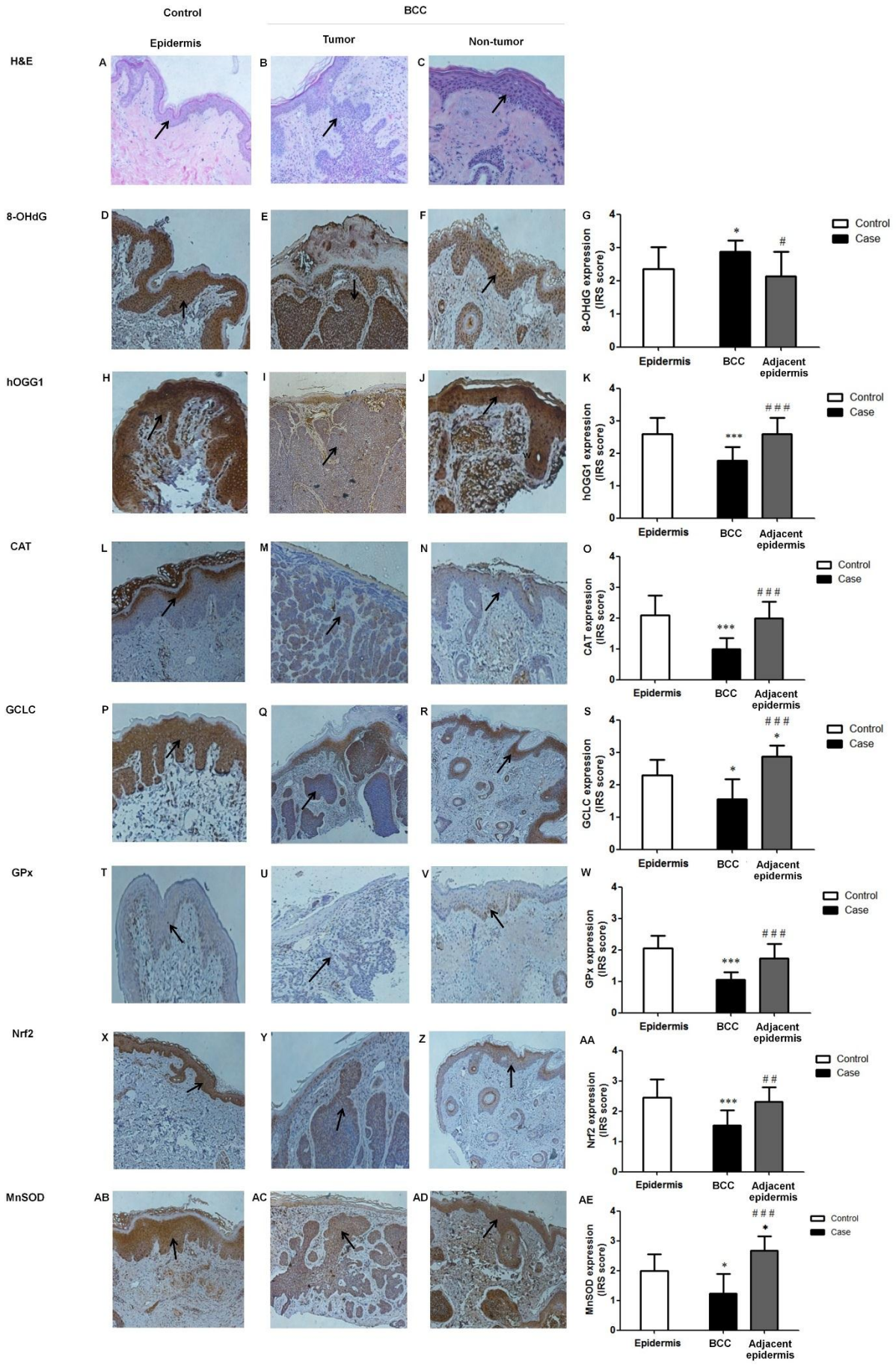
Control
BCC
Epidermis
Tumor
Non-tumor
H&E
A
B
C
8-OHdG
D
E
F
G
8-OHdG expression (IRS score)
Control
Case
Epidermis
BCC
Adjacent epidermis
hOGG1
H
I
J
K
hOGG1 expression (IRS score)
CAT
L
M
N
O
CAT expression (IRS score)
GCLC
P
Q
R
S
GCLC expression (IRS score)
GPx
T
U
V
W
GPx expression (IRS score)
Nrf2
X
Y
Z
AA
Nrf2 expression (IRS score)
MnSOD
AB
AC
AD
AE
MnSOD expression (IRS score)

Figure 3

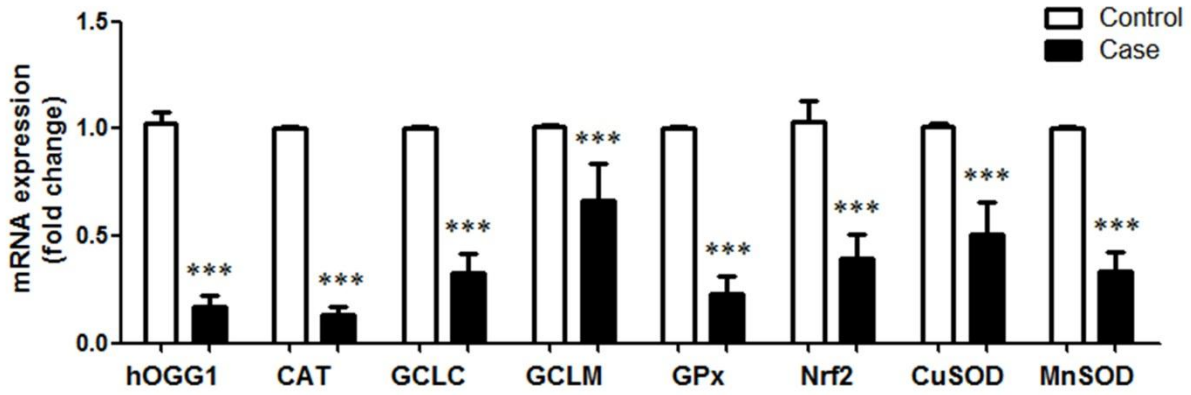
Control
Case
mRNA expression (fold change)
1.5
1.0
0.5
0.0
***
hOGG1
CAT
GCLC
GCLM
GPx
Nrf2
CuSOD
MnSOD